

LASER SCANNING AS A METHODOLOGY FOR THE 3-D DIGITIZATION OF
ARCHAEOLOGICAL SHIP TIMBERS: A CASE STUDY USING THE WORLD
TRADE CENTER SHIPWRECK

A Dissertation

by

CHRISTOPHER MATTHEW DOSTAL

Submitted to the Office of Graduate and Professional Studies of
Texas A&M University
in partial fulfillment of the requirements for the degree of

DOCTOR OF PHILOSOPHY

Chair of Committee,	Donny L. Hamilton
Committee Members,	Kevin J. Crisman
	Luis Filipe Vieira de Castro
	Ergun Akleman
Head of Department,	Cynthia Werner

May 2017

Major Subject: Anthropology

Copyright 2017 Christopher Matthew Dostal

ABSTRACT

Accurate documentation of cultural heritage material is essential to its study and interpretation by archaeologists. In order to continually refine the documentation process, technological advances are incorporated into traditional methodologies. This study demonstrates the utility of high-definition laser scanning for the documentation of disarticulated timbers from the ship remains found during the excavation of the former site of the World Trade Center in New York City. Laser scanned models of the timbers were used to virtually re-assemble the ship, produce traditional scaled drawings for standard documentation, loft a series of ship lines for reconstruction modeling, and to produce a scaled 3-D printed model of the ship.

DEDICATION

For Carolyn

ACKNOWLEDGEMENTS

I would like to acknowledge a fraction of the incredible people in my life that have helped me along the way on this journey of academia. This has been the singularly most rewarding time of my life so far, and having the opportunity to learn from, work alongside, and befriend such an incredible group of people is something I am more grateful for than I could ever express.

First and foremost, I could never begin to exhaust my gratitude to the legendary Donny Hamilton. There has never been anyone in my adult life that I have learned so much from and admire so much, both personally and professionally. Donny has given me more opportunities of a lifetime than I could have ever imagined. It never occurred to me to say ‘no’ to anything he asked of me, because every single thing led to something incredible. The word ‘mentor’ describes Donny the same way the word ‘big’ describes the Grand Canyon; it’s technically correct, but doesn’t really convey the magnitude very well. Donny, thank you. Thank you for your trust, your support, your advice, and your friendship. It really does mean the world to me.

The entire concept of this project would have never occurred to me if it were not for Filipe Castro graciously inviting me to participate on the *Belhino I* shipwreck project in Esposende, Portugal. So, apart from spawning this project, and along with being an invaluable resource of information about shipbuilding and archaeology, Filipe has been an unstoppable force of support, mentorship, and friendship, and I am incredibly grateful

to have had the opportunity to learn from and be influenced by such a brilliant and thoughtful person.

To Kevin Crisman, whose insight and ideas were foundational to my understanding of the WTC ship and its construction, and whose high standards of academic excellence have inspired me and driven me these past years. Thank you for being on yet another committee for a weird project I managed to dream up.

Peter Fix, the PI for the conservation of the WTC ship project, has been extremely generous with his time and has supported and demanded a great deal from me, both of which have helped me grow into the scholar I am. Thank you for being willing to talk about esoteric conservation techniques, for your advice, for your encouragement, and your friendship.

I owe a great deal to the incredible Jim Jobling, who coordinated and facilitated every step of this project, and who would often casually mention a brilliant way to overcome a vexing problem. Appreciation is hardly the word, but Jim's incredible insight and knowledge, his ability to help solve every conceivable problem, and his unflagging support to everyone around him are something that I admire and respect, and I very much cherish his friendship.

I am forever grateful to Wayne Smith, who introduced me to whole world of laser scanning and computer graphics. More than just that, I am thankful that he always stopped by, offered valuable advice, and took the time to intelligently answer my left-field questions about conservation and computer graphics whenever they popped into my head.

A huge thanks to John Hamilton and the crew working at the CRL for the hundreds of times they had to stop what they were doing to help me move timbers in and out of the scanning area, and for having to listen to my impassioned arguments about how Nicolas Cage is indeed the greatest actor of all time.

I could easily double the length of this document if I tried to set out to try and express how grateful I am to the brilliant Carolyn Kennedy for her unwavering love, support, and encouragement. So how about this: you are the best partner anyone could ever hope for. Thank you.

CONTRIBUTERS AND FUNDING SOURCES

Contributors

This work was supported by a dissertation committee consisting of Professor Donny Hamilton, Professor Kevin Crisman, and Professor Filipe Castro of the Department of Anthropology, and Professor Ergun Akelman of the Department of Visualization.

Rebecca Mattson, Dorothy Rowland, and Meredith Stoops, graduate students in the Department of Anthropology aided in the scanning of the timbers for this project as volunteers. Dr. Peter Fix of the Conservation Research Laboratory at Texas A&M University helped define the requirements for the timber drawings in Chapter V.

All other work for this dissertation was completed by the student independently.

Funding Sources

Graduate Study was supported by Graduate Assistant Teaching and Graduate Assistant Research positions provided by the Department of Anthropology at Texas A&M University. Additional funding was provided by the Conservation Research Laboratory at Texas A&M University, and the Center for Maritime Studies and Conservation at Texas A&M University.

TABLE OF CONTENTS

	Page
ABSTRACT	ii
DEDICATION	iii
ACKNOWLEDGEMENTS	iv
CONTRIBUTERS AND FUNDING SOURCES	vii
TABLE OF CONTENTS	viii
LIST OF FIGURES	x
LIST OF TABLES	xvii
CHAPTER I INTRODUCTION	1
The Importance of Documentation	1
Types of <i>Ex Situ</i> Documentation	7
Workflow Overview	10
CHAPTER II BACKGROUND	13
Literature Review	13
The World Trade Center Ship Remains	17
Construction Sequence	21
CHAPTER III SCANNING METHODOLOGY	29
Preparing the Wood for Scanning	29
Configuring the Settings of the LLP	39
Scanning Procedure	46
File Organization	54
Post-Processing	56
Accuracy Verification	73
Complications and Lessons Learned	77
CHAPTER IV VIRTUAL RECONSTRUCTION	85
Mechanics	85

Arrangement Methodology	88
Calculating a Lines Drawing.....	102
CHAPTER V MESH MODELS TO TIMBER CATALOG.....	110
CHAPTER VI 3-D PRINTING AND PHYSICAL RECONSTRUCTION	131
Preparing the Models for Printing	133
Modifying Oversized .stl Files in <i>Rhinoceros 5</i> for Printing	142
Printing	144
Cleaning and Labelling the Prints	146
Assembly	147
CHAPTER VII ALTERNATIVE METHODS OF 3-D DIGITIZATION.....	156
Computer Vision Photogrammetry	156
Contact Probe Digitization	166
Large-Area Survey Laser Scanning	171
CHAPTER VIII ETHICAL AND PHILOSOPHICAL CONSIDERATIONS WITH DIGITAL HERITAGE.....	175
What is an Accurate 3-D Model?	175
The Diminishing Returns of Resolution.....	178
Realism as a Ruse.....	182
Misrepresentation of Data	186
Who Owns the Past?	191
CHAPTER IX DISSEMINATION OF DATA	194
Online Distribution of Interactive Models	195
Offline Distribution of Interactive Models.....	197
Non-Interactive Distribution: Animating the Model.....	198
Curation.....	199
CHAPTER X ASSESSMENT AND CONCLUSION.....	201
REFERENCES	207
APPENDIX I.....	216
APPENDIX II	218
APPENDIX III	220

LIST OF FIGURES

	Page
Figure 1: A Set of Ships Lines	10
Figure 2: View Aft of the Six Aftmost Floor Timbers (Left).	11
Figure 3: Example of a Timber Drawing Produced for the Newport Ship Project With CMM Arm Contact Probing.....	15
Figure 4: The Composite Model of the CSS <i>Hunley</i>	16
Figure 5: Site Plan of the WTC Ship Site.	18
Figure 6: Frames 10, 14, 18, And 23 Are Notched at the Ends of the Timbers, While the Rest of the Frames are Squared.	22
Figure 7: X-Ray Radiographs for the First Futtock From Port Side of Frame 20 (Left) and Frame 23 (Right).	23
Figure 8: Estimated Location of Battens Based on the Locations of Fasteners on the Outboard of the Master Frames.	25
Figure 9: Measuring the Distance Between Frames on the Virtual Model Once Placed on the Keel According to Fastener Location.	27
Figure 10: The Main Storage Vat for the WTC Timbers. Note the Grass Clippings Floating on the Surface.	29
Figure 11: Floor Timber FN FS 9-0 Loaded Onto a Stainless Steel Cart to Be Cleaned And Transported to the Scanning Area.	31
Figure 12: A Paper Tag From the Excavation that is No Longer Readable.....	33
Figure 13: Secondary Storage Tank For Scanned Timbers.....	34
Figure 14: A Volunteer Graduate Student Scanning With the V2 LLP on the Steel Table in the CRL Loading Bay	35

Figure 15: The Second Scanning Arm, The Faro Edge CMM Arm With V5 HD LLP, Relocated To a New Room With a New Scanning Table In November of 2016.....	36
Figure 16: The Distance Between the Points in the Point Cloud for CN 4-4 Vary from Point to Point.	40
Figure 17: Gaps in the Scan Data Caused By Moving the LLP too Quickly for the Maximum Edge Length Setting.	43
Figure 18: <i>Design X</i> Scanning Interface.	46
Figure 19: Reference Encoder.....	47
Figure 20: The LLP Struggled to Scan the <i>Teredo Navalis</i> Damage on the Stern Post (ST 1), Resulting In Gaps (Left).	57
Figure 21: The First Stage of Processing Utilizes The Mesh Buildup Wizard, Found In The <i>Points</i> Tab.....	59
Figure 22: Using the 'Find Floor' Selection Tool, the Plane of the Scanning Surface was Automatically Selected.	60
Figure 23: The Differences When Using the 'Visible Only' Option When Selection Portions of the Mesh.	61
Figure 24: Noisy Cluster Selection (the Light Blue Areas Were Noisy Clusters).	62
Figure 25: Mesh Buildup Wizard Data Merging Settings Used In <i>Design X</i>	63
Figure 26: The Unaltered Point Cloud (Top), Compared to the UHD Version of Mesh with No Noise Reduction And No Gap Filling (Bottom Left) Vs HD Version With Moderate Noise Reduction And Gap Filling (Bottom Right).	65
Figure 27: Under The Polygons Tab, Select Mesh Buildup Wizard To Align Two Mesh Halves.	66
Figure 28: Arranging The Two Scans For Alignment.	67
Figure 29: As Pins Are Dropped On the Same Point in the Overlapped Section of Each Scan, The Software Will Begin to Align The two Meshes.	68

Figure 30: Manually Aligned Model Before Best-Fit Alignment (Top) and After (Bottom).	69
Figure 31: Global Remeshing ST 1, the Sternpost.	71
Figure 32: The Mesh For ST 2, the Disarticulated Portion of the Sternpost After Being Analyzed By the Healing Wizard.	72
Figure 33: FN 15-0.1 Measured Physically and Virtually.	74
Figure 34: Verifying Accuracy By Scanning a Pair of Calipers Set to 10 mm (Left) and an Etched Steel Ruler (Right).	76
Figure 35: A Guide to Aligning a Plank that Requires Six Separate Scans.	78
Figure 36: Crazy Ant Infestation of the Faro Arm Circuitry Housing.	81
Figure 37: Damaged Ends of the Keel.	88
Figure 38: Aligning the Keel Pieces.	89
Figure 39: Aligning the Stern Knee.	90
Figure 40: Positioning ST 1, The Lower Portion of The Stern Post To The Stern Knee By Aligning The Fasteners.	91
Figure 41: Positioning The Disarticulated Portion of the Sternpost	92
Figure 42: Five Foot Draft Marking on the Sternpost.	92
Figure 43: Rectangular Prisms Were Placed Along The Keel at the Fastener to Aid in Placing the Floors.	93
Figure 44: Balancing and Mirroring a Copy of Incomplete Floors.	94
Figure 45: Positioning FN FS 9-0 on the Stern Knee.	95
Figure 46: Placing the Floors on the Keel.	96
Figure 47: Aligning the Master Frames to the Futtocks Was Done By Aligning the Fastener Locations, as Notated by the Arrow.	98
Figure 48: Repairing a Timber in <i>Rhinoceros 5</i>	99

Figure 49: Lines of the French Light Frigate <i>La Belle</i>	102
Figure 50: A Series of Guidelines Were Drawn to Aid in the Position of the Points Along the Bottom of the Structural Timbers.....	103
Figure 51: After the Points Are Placed On the Outboard of the Frames, They Need To Be Aligned In the Left Or Right View So That They Have the Same Y-Value.....	105
Figure 52: Each Curve Produced Was Faired Using the 'Fair' Command.	107
Figure 53: Horizontal Waterlines Were Drawn, Then a Point Placed Where Each Waterline Intersected With The Body Plan Curve To Produce The Curves For The Half-Breadth Plan.....	108
Figure 54: Half-Breadth Lines Representing The Remains of The Ship.	108
Figure 55: Body Plan Lines From the WTC Ship Overlying a Set of Lines From For a Beamy Hudson River Sloop.	109
Figure 56: Cad Timber Drawing From <i>La Belle</i> , Used As a Template For the Design of the WTC Timber Drawings.	111
Figure 57: Timber Catalog Entry For the Stern Knee.	112
Figure 58: A Timber Catalog Entry Generated With a Converted Cad Body In Solidworks.....	113
Figure 59: A Mesh Of the Bolt (Left) Vs. a Solid Model of the Bolt (Center).....	114
Figure 60: The Mesh For FN FS 10-0 (Left) And the Resultant Error In the Solid Model.	116
Figure 61: Fn Fs 10-0 Being Prepared For a Timber Drawing.	117
Figure 62: Creating a New Layout For the Timber Drawing Using the 'Drafting' Tab.....	119
Figure 63: New Blank Layout Page, After a Border Has Been Drawn And An Information Box Drawn In On the Bottom Right.	120
Figure 64: The Four Larger Viewports Being Added To the Timber Drawing Sheet. ...	121
Figure 65: Standardized Timber Drawing Layout For the WTC Project.....	123

Figure 66: Using the Section Tool, a Cross Section Can Be Extracted From the Mesh Model.....	124
Figure 67: Moving the Cross Section (In Yellow) Away From the Mesh To Prevent It From Being Visible In the Other Views.	125
Figure 68: The Faro Scan of USS <i>Westfield</i> Artifact 121-52 C69.	127
Figure 69: The Scale Bar For The Timber Drawing Is a 100 cm X 5 cm Black Plane With 10 cm X 5 cm White Planes Atop It.....	129
Figure 70: The Digital Model Reconstructed And the 3-D Printed Structural Timbers for the WTC Ship Project Prior To Reconstruction.	131
Figure 71: Orientation of BF 3 In <i>Z-Suite</i>	132
Figure 72: Customization Options In <i>Z-Suite</i>	133
Figure 73: The Effects of Orientation On Print Quality.....	135
Figure 74: Different Levels of Infill.....	137
Figure 75: Preparing the Gateway Arch (Left) For Printing Requires Supporting Any Area of the Print That Is Not Overlapping a Previous Layer By 20°.....	139
Figure 76: Slicing Maps the Route For the Extruder To Take During Each Layer of the Print.	140
Figure 77: Cutting a Timber Model In <i>Rhinoceros 5</i> So That It Will Fit On the 3-D Print Bed.....	142
Figure 78: The Reassembled Keel With the Stern Knee And Stern Post Attached.	148
Figure 79: The First Attempt At Assembling the Printed Timber Models.	149
Figure 80: Several Early Stanchion Design Attempts.....	152
Figure 81: The First Step In Creating a Stanchion That Can Be Printed Out And Used To Balance the Physical Model On the Floor Timbers On the Keel Is To Create a Solid Object Between the Floor And the Timber.....	153
Figure 82: The Stanchions Are First Cut With the Boolean Difference Between the Block And the Timber Mesh (Left).....	154

Figure 83: Assembling the Physical Model.	155
Figure 84: Early Stereoscope Image of the Cuyahoga River In Cleveland, OH.	157
Figure 85: Stages of Photogrammetry.....	160
Figure 86: Computer Vision Photogrammetry Model of Timber Bf 2 Generated With Agisoft <i>Photoscan</i>	161
Figure 87: Each Photograph Of BF-2 Was Edited In Photoshop And a Mask Was Produced, So That <i>Photoscan</i> Would Not Process the Background of the Image.....	162
Figure 88: Comparison Between High-Definition Laser Scanning (Top) And Computer Vision Photogrammetry (Bottom).	165
Figure 89: Mesh Model of the Number Zero (Top Left) Vs. a Nurbs Model of the Number Zero (Top Right).	167
Figure 90: An Example of How a Series of Data Points Can Be Interpreted In Different Ways.	168
Figure 91: Toby Jones Using Contact Probe Digitization To Trace a Timber From the Newport Ship Project.	169
Figure 92: Large-Area Laser Scan of the WTC Ship During the Excavation.....	172
Figure 93: Mesh of the Mid-Excavation Large-Area Laser Scan.	173
Figure 94: World Trade Center Ship Outer Plank From the Sixth Strake, Starboard Side.....	175
Figure 95: The Full Resolution Point Cloud For An Outer Plank With Visible Wood Grain.	179
Figure 96: A Purposefully Misaligned Plank.....	182
Figure 97: A Photogrammetry Model of the CRL With Obvious Errors.....	183
Figure 98: Digital Sculpture Project: Caligula.....	189
Figure 99: Replica of the Human-Headed Winged Bull From Nimrud, Iraq On Display in the Colosseum In Rome.....	192

Figure 100: Screenshot of the Smithsonian X 3D Website, With a Fully Interactive Model of Benedict Arnold's Gunboat *Philadelphia*. 196

LIST OF TABLES

Page

Table 1: Distance Between Individual Frames and the Average26

CHAPTER I

INTRODUCTION

The Importance of Documentation

In 2012, during the construction of One World Trade Center in New York City, a ship was found under the former location of the World Trade Center towers that had been destroyed in the September 11th, 2001 terrorist attacks. The ship, an 18th-century wooden sailing vessel (known as the World Trade Center ship, or WTC ship), was excavated by an archaeological team and the disarticulated timbers were shipped first to the Maryland Archaeological Conservation Laboratory, and then later to the Conservation Research Laboratory (CRL) at Texas A&M University. They were kept in wet storage until 2016 while the funds were raised for conservation treatment. Prior to treatment, it is the policy of the CRL to document each timber in the greatest detail possible, allowing for scholarship of the vessel while the timbers undergo a lengthy conservation treatment, and for accurate evaluation of the efficacy of the treatment. The purpose of this project is to provide an overview and evaluation of the first ship to be archaeologically documented entirely in 3-D with high-definition laser scanning.

The ability to accurately gather data is foundational to any scientifically-informed pursuit. The accuracy of data gathering is something that is under constant revision, and as data gathering techniques improve and are refined, the understanding of the subject being studied should ostensibly improve along with them. Imagine the impossibility of understanding biology without microscopes capable of imaging cellular

structure, or sending a man to the moon without the aid telescopes to tell us how far away it is. As instrumentation improves, so does our ability to comprehend the world, and as our comprehension of the world grows, so does our ability to accurately tell the story of humanity.

A fundamental premise that underlies this study is the assumption that maximizing data acquisition is desired when it comes to archaeological documentation. More data is not necessarily better data; there are instances when the presentation of excessive data can be confusing and overwhelming, but that is an issue of poor dissemination, not poor data acquisition. The goal of this project was to document the WTC ship timbers with the highest resolution and accuracy as could be achieved by the equipment available at the CRL. Given that this was an experimental study, each timber was photographed and conventionally measured in addition to the high-definition laser scanning, and each digital model produced from the laser scan was used to produce an annotated 2D drawing.

Mr. Richard Steffy, a pioneer in the field of nautical archaeology and the founder of the Ship Reconstruction Laboratory at Texas A&M University, wrote that “the parameters of research and reconstruction are defined by the quantity and quality of recorded information from which they are conceived” (Steffy 1994, 191). Given the importance placed on documentation in nautical archaeology, there are a variety of methods used to capture an array of important details. Deciding which details are recorded and the methods by which they are documented directly impacts the quality of

the future interpretations. Variations in this decision mean that different archaeologists can come to different conclusions when trying to understand the same source material.

Ideally, a standard set of details would be recorded that would allow for easy comparison between sites, but the reality is that the personnel available, the time, the location of the site, the state of artifact preservation, and the equipment available for excavation and documentation varies widely between projects. Because of this, there is a constant drive to expand the arsenal of tools available for achieving the best documentation possible in the shortest amount of time for the least amount of money. The achievement of all three of these ideals is rarely achieved, but the drive towards one or two of them has consistently moved the technologies used for documentation in the field forward.

Considering the nascence of the field of nautical archaeology and the pace of technological innovation, it is not surprising that a plethora of documentation techniques have been tried over the years. Each new technique is evaluated on its ease of use, cost, and the accuracy of the results. Additionally, it is useful to evaluate new methods based on the standards set out by the United States' Secretary of the Interior for the documentation of heritage materials. Standard I states that documentation should adequately explicate and illustrate what is significant or valuable about the object being documented. Standard II states that the documentation should be prepared accurately from reliable sources with the limitations clearly delineated, allowing for independent verification. Standard III states that documentation should be prepared on materials that are readily reproducible, durable, and adhere to the appropriate standards. Finally,

section IV states that documentation should be clearly and concisely produced (Interior 1990, 4-8). When a method achieves a desirable blend of those characteristics, it gradually becomes adopted as one of the standard methods of documentation. These standard methods have not changed much over the years: hand drawings, photographs, measurements, and detailed notes remain the backbone of archaeological recording since the inception of the modern field of nautical archaeology by Dr. George Bass and his colleagues in the 1960s. These methods continue to be used to this day, though they have undergone evolutionary changes, like the shift from film photography to digital photography.

No matter the means of documentation of any cultural heritage material, the desired end result remains the same: to capture as much information as accurately and precisely as possible. In the case of ship timbers, apart from the *in situ* location and orientation, this means that the sided and molded dimensions, the shape of the timber, the location and angles of all fasteners, and tool marks and markings. Looking through any archaeological report or paper, it becomes quickly apparent that the gold standard for the documentation of ship timbers is the scaled drawing. The scale of the drawing should be such that all useful details mentioned above can be recorded. Discarding information because it is too small to be seen at the scale being used is unacceptable, and is a clear indicator that the scale needs to be corrected.

Though there are a number of unique methods for creating accurately-scaled drawings or other images of the timbers, they all rely on the skill and intuition of the archaeologist to accurately capture the salient features of the timber. This can be

problematic for projects with few experienced personnel, a large number of timbers, or a pressing deadline. When resources are stretched thin, the recording of timbers can fall to those without the experience necessary to understand which details are necessary to record and to what level of detail. This can in turn lead to misinterpretation of the vessel and the site later, when the only access to the materials is through their records. (Note: there is not a specific example of erroneous recording being referenced here, merely hypothetical musings based on the author's experiences.)

Given how commonplace it is for archaeological excavations to double as field schools for students, the ideal goal when developing any new method of documentation is to devise a method that minimizes the artistic and technical skill and experience necessary to obtain acceptable records. A method in which the same quality results could be obtained by seasoned veterans and first-year volunteer students would be a welcome addition to the methodological tool chest. If this ideal is not entirely possible, then a means by which documentation done by novices could be quickly and easily checked for accuracy and corrected with limited supervisory resources would at least minimize the risk of erroneous records.

In the last decade or so, there has been a push towards using 3-D digitization to supplement and even replace the standard methods for documenting sites and artifacts (an overview of these techniques can be found in Chapter VII). Broadly, 3-D digitization is the recording of data in a format that can be digitally manipulated to show more than two dimensions. An accurate 3-D model of an object can deliver the information conveyed with drawings and measurements in a more comprehensive and

understandable way than a hand-drawn plan. For this project, the WTC ship timbers were digitized using a FARO brand high-definition laser line probe (LLP) attached to a coordinate measuring machine (CMM) arm. This is not a new approach to documenting archaeological materials, but its utility in documenting ship timbers was dismissed early on for two reasons: it demanded excessive post-processing time to convert the scan data to usable models, and the data that were gathered lacked interpretation (Nayling and Jones 2014, 244).

Access to powerful computers and streamlining the post-processing procedure all but eliminated the inconvenience of processing the scan data, and the speed of scanning with the LLP was so rapid that the time spent processing was negligible in the overall work flow compared to other methods. The lack of interpretation in the data gathered was viewed not as a drawback, but instead as one of the most positive aspects to this method of documentation. All methods of documentation come coupled with some degree of error and interpretation by the person or persons doing the recording. With drawings, the talent of the artist plays a significant role in the quality of the data. For photography, the technical ability of the photographer and the quality of the equipment can be the difference between insightful photos that help with the interpretation of the material or unfocused, poorly-framed pictures that do not contribute any meaningful data. Measurements can change from person to person depending on the accuracy of the tools and the consistency of the placement of the points being measured. Observations made in field notes depend largely on the experience of the note taker and often can suffer because of the fragility of imperfect memories.

The goal when developing the technique for high-definition laser scanning used in the WTC ship project was to obtain fast, accurate, and logically-organized data that could be gathered reliably regardless of the conceptual understanding of the object being scanned. As a result, many of the 3-D models featured in the reconstruction of the WTC ship were created by first-semester graduate students in the nautical archaeology program at Texas A&M University, well before they understood ship construction or timber recording methodology. Once scanned and processed, the data accurately conveys a manageable and comprehensive collection of the relevant data that can be used to interpret the material at the leisure of the principle investigator.

Types of Ex Situ Documentation

There are two phases of archaeological timber recording: *in situ* and *ex situ*, meaning either in their original location, or removed from it. For many wrecks studied by nautical archaeologists, the resources are simply not available to excavate and conserve the wreck, and therefore *in situ* documentation is the only option. If a ship is to be excavated, it is always recorded *in situ* prior to and during the excavation. *In situ* documentation techniques are not entirely dissimilar to the techniques discussed in this section, but the focus here will be for ships that are fully excavated. In these cases, the detailed *ex situ* documentation is best done at a conservation facility, where the pressures of field deadlines are mitigated and tools and equipment are on hand in a controlled environment. For *ex situ* documentation, there is not much use in proposing a new methodology that does not retain the strengths of other methods while reducing their

shortcomings, and therefore it is impossible to assess a new method without understanding the other methods that are currently used.

For the documentation of the timbers themselves, there are three methods that should be compared to high-definition laser scanning: 1:1 tracings, scaled drawings, and 3-D modeling. For 1:1 tracings, the goal is to create life-sized representation of each timber. Typically the timber is placed either above or below a transparent surface, and then the outline is traced onto a transparent writing surface, the relevant details, like fastening patterns, marking, or anything the artist deems worth noting are filled in (Fix, *Archaeological Watercraft: A Review and Critical Analysis of the Practice* (Doctoral Dissertation) 2015, 134). Though this method has been used hundreds of times with great success, there are a number of potential problems worth noting. For one, when tracing something that is not entirely flat on each side, it becomes the prerogative of the artist to decide at which point on an angled surface will be the extent of the outline. This point can vary from artist to artist and day to day, and so there may be subtle variations in the way that the timbers are recorded. In that same vein, there is the issue of parallax. If the writing surface that the tracing is being done on is rigid, and a timber is not entirely flat, there will be variations in the distance between the surface of the wood and the writing surface at various points along the timber. Wherever these variations occur, human depth perception causes the size of the timber to vary from the actual measurements. Another issue with 1:1 tracings is something that is a problem with scaled drawings as well: the decision of what to include in the drawing is being made by the artist, and these

decisions can vary from artist to artist, depending on training, experience, and personal preference.

For other scales of drawings, a series of linear measurements, angles, and triangulation of points may be used to accurately depict the timber. One effective method is to place the artifact to be recorded over a flat surface with an imprinted grid with standard dimensions. A skilled artist can convey the detail of an artifact more succinctly than a photograph can, by highlighting the salient features and minimizing the extraneous ones. The potential problems with scaled drawings are the same as the 1:1 tracing listed above, as well as the potential for misinterpreting measurements or other data. Measurements of an object are almost always slightly different depending on who does the measuring, and so a heavy reliance on data with known variability can lead to errors in both the recording and interpretation of scaled drawings. At the time of this writing, 3-D digital documentation of ship timbers is principally achieved with either computer vision photogrammetry, CMM arm contact probing, or large-area survey scanners. All three of these methods are discussed at length in Chapter VII and will not be discussed here.

In contrast to these three methods of recording ship timbers, the WTC ship timbers were documented using a FARO ScanArm, which is a CMM arm with an attached LLP. The FARO LLP works via laser triangulation. The probe consists of a laser and an optical sensor. The distance between the laser and the sensor is known, and the angle between them is known. The sensor detects the laser when it is reflected off of the object being scanned, and using trigonometric triangulation, the distance between the

object and the sensor is calculated (3D Systems, Inc. n.d.). When this distance is calculated, a point is placed in 3-D space, and as other points are gathered, they are accurately placed in relation to the other points. Like the individual pixels that make up a digital photograph, when enough data points are gathered, the resultant point cloud forms a representation of the object that was scanned.

Workflow Overview

Whatever the method used to record the timbers of a ship, the ultimate goal is to develop a set of plans that lets the archaeologist understand the form and function of the ship, and to use that knowledge to further understand the people who used it. The first

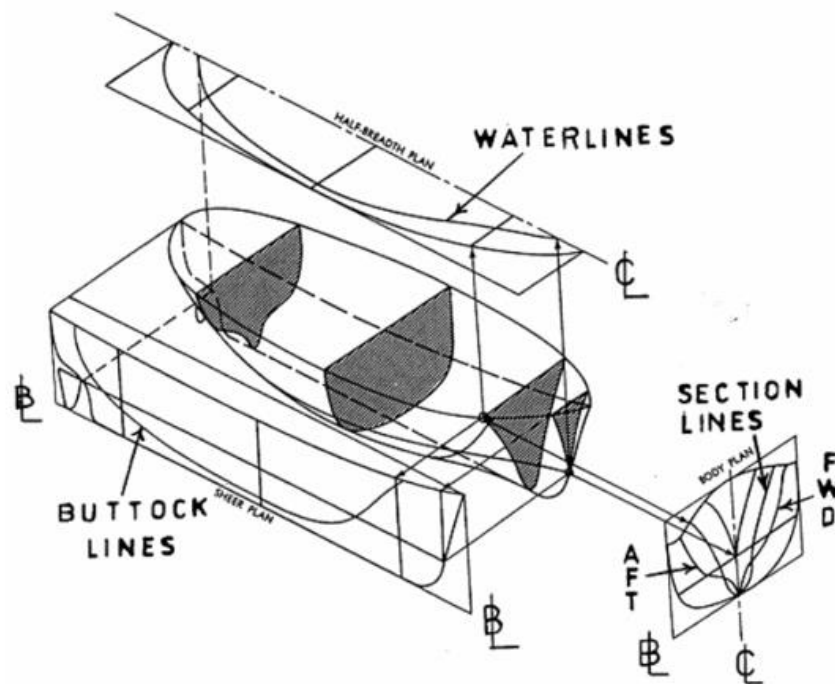


Figure 1: A set of ships lines. To develop lines from timbers, the exterior surfaces of the structural timbers are traced, and then overlain atop one another to developed the shape of the hull. Reprinted from MarineWiki 2007.

step in achieving this goal is to convert the data acquired from the physical timber into the type of plans that would have been used by naval architects and shipwrights when they were conceiving and constructing the ship: a set of lines drawings (Crisman, *An Archaeological Approach* 1993, 314). Lines drawings are a 2D projection of the 3-D form of the ship on paper. They are projected from the side (the sheer plan), the top (the half-breadth or breadth plan), and the cross section view (the body plan). When timbers are recorded, the structural timbers (frames, knees, etc) can be copied to semitransparent paper and the outlines can be traced. The outlines of the frames of the ship placed atop one another will yield a set of ships lines (Figure 1), which is typically the ultimate goal of the reconstruction process. A set of ships lines are the blueprint for its design, and all theoretical reconstructions are based on them.

Figure 2 shows the aftmost six floors of the WTC wreck, digitally rendered in *Rhinoceros 5*, a computer graphics program. Tracing the outline of these timbers yielded

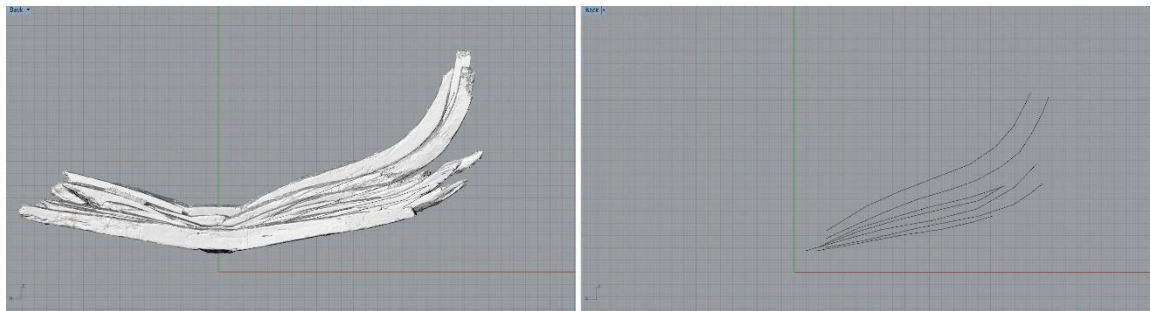


Figure 2: View aft of the six aftmost floor timbers (left). Tracing the outline of these timbers yields a rudimentary set of lines drawings for this portion of the hull (right). Image by author.

rough estimate of what a small portion of the lines of this ship might look like. Compare the right side of Figure 2 to the body plan of Figure 1 for an example of how lines are developed. As long as each timber is properly aligned based on the evidence of the fasteners and a solid understanding of ship construction techniques, and the lines are extracted very precisely, an archaeologically-informed set of ship lines can be drawn. Methods for reconstructing ships with lines drawings are exhaustively covered elsewhere (see Anderson 1988, 4.2.7, Dillion 1993, 223), and as such the method for extracting lines is the salient part of the process for this dissertation, not the way that the lines are used nor the reconstruction of the ship. See Chapter V for a more comprehensive procedure for extracting lines from a 3-D model.

After a comparative pilot study comparing CMM contact probe tracing, computer vision photogrammetry, and high-definition laser scanning with the FARO ScanArm, the ScanArm produced the most reliably accurate 3-D models of the ship timbers for the WTC ship. Building upon the success of the exceptional work being done recording ship timbers around the world, this dissertation outlines the methodology, advantages and disadvantages, and the results of laser triangulation scanning the structural timbers of the WTC ship, as well as the digital and physical reconstruction of the ship using this data.

CHAPTER II BACKGROUND

Literature Review

The documentation of the World Trade Center (WTC) ship has three main stages of work: collecting the data for the individual timbers, determining how those timbers were arranged to reconstruct the shape of the ship, and then to use that reconstruction to create a set of lines drawings that convey the design of the ship in the way that it was conceived and built. This process is distinct from the documentation of an articulated vessel, and though there are areas where the methodologies may overlap, the processes outlined here are meant for disarticulated timber recording. All three stages of work follow a long tradition of scholarship in the archaeological community, and to properly assess the methodology used, it must be compared to the examples that inspired it.

The most common method for recording archaeological ship timbers is the 1:1 tracing method mentioned in Chapter I. As a rule, if ship timbers are excavated, they are recorded using this method. A very short perfunctory list of projects that utilized 1:1-scale drawings to document timbers are the eight Yenikapi Byzantine shipwrecks excavated by Cemal Pulak in Turkey, the 16th-century Arade 1 Shipwreck excavated by Filipe Castro, the 17th-century French shipwreck *La Belle*, excavated by the Texas Historical Commission, and the focus of this project, the WTC ship, excavated by Warren Riess in Manhattan (Castro 2005, Castro 2006; Pulak, Ingram, & Jones, 2014; Loureiro & Alves, 2008, p. 274; Grieco, 2003, p. 4; AKRF Inc. , 2013, pp. 2-12

The principal utility of a set of 1:1-scale timber drawings is to produce a set of lines to reconstruct the ship. Because the locations of diagnostic information like fasteners and tool marks are included in the drawings, the drawings of the structural timbers can be superimposed over one another and aligned, and then the exterior of each structural timber traced can then be translated into a set of ship's lines, which in turn can be used to reconstruct the vessel. The benefit of 1:1-scale tracing is that the ship is well documented through the lens of a skilled archaeologist, and a life-size copy of the timbers is available for study. The major drawback to relying on tracing is that quality of the recording is linked directly to the skill and experience of the archaeologist drawing an artifact. Ideally, significant variability in the quality of documentation would be minimized for all archaeological projects. To do this, human perception can be bolstered with the use of modern imaging tools like cameras and 3-D modeling. This increases the reliability of the measurements being taken, and also allows for a more dynamic visualization of the data obtained.

Dozens of major 3-D digitization projects in nautical archaeology have been undertaken since the turn of the millennium, and each project has nudged the field forward. In 2001, Anne Sorensen, Vibeke Bischoff and Kenn Jensen created a groundbreaking 3-D model of the Danish *Ladby* ship by triangulating the positions of nail and rivet positions (Sørensen 2001). In 2004, Toby Jones and Nigel Nayling began the massive undertaking of the 3-D digitization of the Newport Medieval ship using CMM point probing and *Rhinoceros 5* to model every timber and reconstruct the ship with unprecedented accuracy (Nayling and Jones 2014) (Figure 3). Christopher Watters

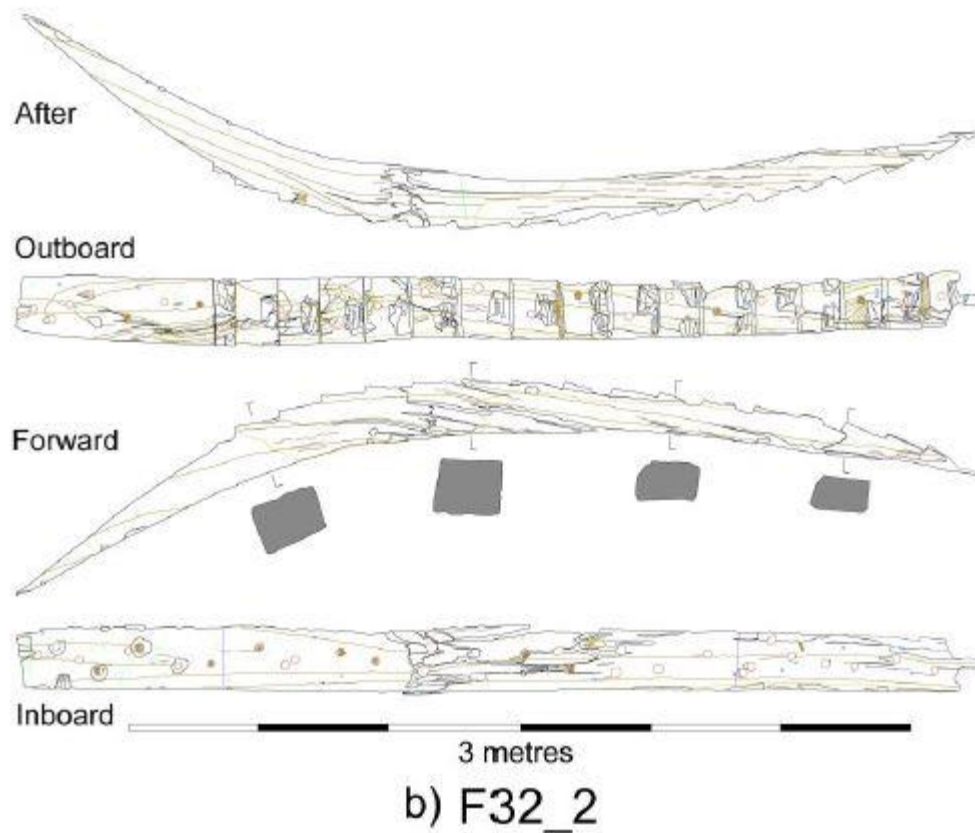


Figure 3: Example of a timber drawing produced for the Newport Ship Project with CMM arm contact probing. Reprinted from Toby Jones, from Nayling and Jones 2014, 257.

and the team working on the conservation of the Confederate submarine *CSS Hunley* used a combination of laser scanning, structured light scanning, and a 3-D point cloud system known as the Vulcan 3-D point cloud to create a highly detailed, textured model (Watters, et al. n.d.). This provided a unique challenge due to the inability to disarticulate the individual components of the ship, thus over 1500 scans were completed and stitched together to create the composite model (Figure 4).

Since around 2010, computer vision photogrammetry has become nearly ubiquitous for the documentation of archaeological projects due to its relative ease of use and lack of required expensive equipment. Photogrammetry uses overlapping photographs to make a 3-D model, and is covered in detail in Chapter VIII. Kotaro



Figure 4: The composite model of the CSS *Hunley*. Photo by the Warren Lasch Conservation Center. Reprinted from Church 2012.

Yamafune used photogrammetry to document the *Gnalic* shipwreck in Croatia, as well as the Lake Champlain steamboat *Phoenix II* with great results. Computer vision photogrammetry may well be the future of archaeological documentation, although it is not without its own set of flaws and concerns.

Building on the success of the pioneers of 3-D documentation in this field, and thanks to improvements in the scanner technology, the processing software, and computer power, using high-definition laser scanning to document ship timbers was a logical next step. Even with the known drawbacks, the long tradition of documenting ship timbers with a 1:1-scale drawing means that a set of these drawings is fully expected to accompany the publication of the archaeological remains of a ship, and as such it was important to find a way to incorporate a version of this traditional

methodology into the design for this project. It was theorized that the resolution of a high-definition laser scan could be used in lieu of 1:1 tracing, and that using the scan to produce a comparable document would create a drawing with more precision and less human error. This was indeed accomplished, and is covered in detail in Chapter V.

The World Trade Center Ship Remains

On September 11th, 2001, terrorists hijacked two commercial airplanes and flew them into the iconic World Trade towers in New York City, killing 2,977 people and injuring over 6,000 more (National 9/11 Memorial 2016). Apart from the impact the attacks had on the national psyche, they dramatically changed the skyline of Manhattan. Five years after the attacks, construction of a new tower and a memorial center began on the same site. During the foundation excavation for the new tower in the summer of 2010, construction workers uncovered what appeared to be the remains of a wooden ship (AKRF Inc. 2013, S-1).¹ Work on the foundation was halted and a New York City based cultural resource management (CRM) firm, AKRF Inc., was brought in to assess the situation under the supervision of Dr. Warren Reiss. The CRM firm identified the timbers as the remains of a historical ship, and in order to preserve this important historical resource AKRF Inc. excavated the ship and sent the timbers to the Maryland Archaeological Conservation Laboratory in July of 2010, and then shipped to the Conservation Research Laboratory (CRL) at Texas A&M University in April of 2011 for

¹ Note: In this text the physical remains of the ship are referred to as the WTC *shipwreck*. This is done intentionally because of its common use in describing archaeological examples of ships, despite the evidence indicating that the ship was not involved in an actual wrecking event.

conservation and study. In August of 2011, remains of the bow of the ship were discovered and shipped directly to the CRL (Fix, Personal Correspondence 2017).

It might seem strange to find a ship buried under solid ground in New York City, but a quick glimpse of a historical map of the city shows that in the 17th and 18th centuries the geography of the city was radically different than it is today. In the post-Revolutionary War economic boom, the city grew and developed rapidly, and the demand for real-estate far outstripped the land available for development. Developers on the coast established land-fill projects in the 1790s to extend the dry land of the island into the Hudson River. Based on the historical research done by AKRF, the area where

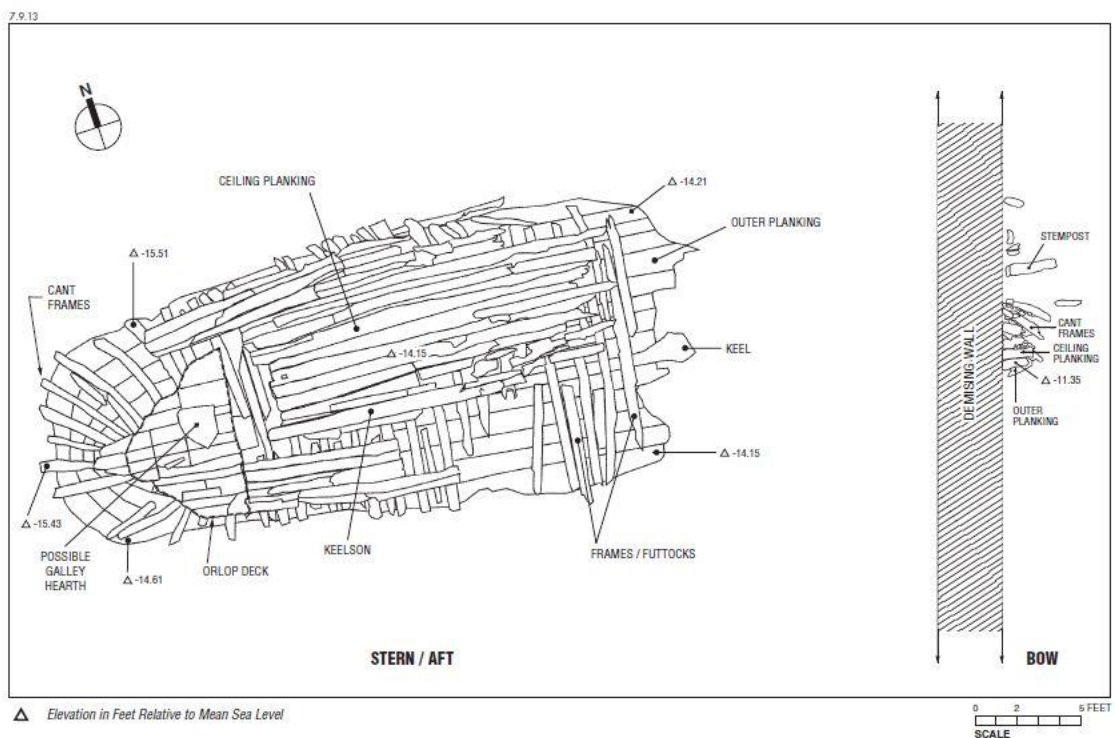


Figure 5: Site plan of the WTC ship site. Reprinted from AKRF Inc. 2013, Figure 6-1

the WTC ship was found was filled and developed by 1818 (AKRF Inc. 2013, 3-5) .

The evidence outlined in AKRF's final report to New York City indicated that the WTC ship was used as fill for this development project. Their archival research indicated that the fill project was complete by 1818, and if the construction date can be ascertained, so can an estimate of the working life for this vessel. The archaeological evidence does not include the name or the owner of the vessel, but dendrochronological samples of the hull show that the timbers for the ship were initially cut down in 1773 from a forest near Philadelphia (AKRF Inc. 2013, 6-21). If we assume that the timbers were seasoned for two to three years, the ship was likely built in the late 1770s or early 1780s. Though there are many variables that could be at play that would shift this date in either direction, the ship likely had a working life of 10-20 years before it was used as fill for the 1790s expansion project. Oyster shells on the hull indicated that the vessel was stationary at this location for the estimated two to three years, given their size; oysters tend not to survive moving from one port to the next because they are sensitive to minor changes in salinity (AKRF Inc. 2013, 8-2).

Hundreds of timbers were recovered during the excavation, including ceiling planking, outer planking, the keel, floors, futtocks, the stern knee, and sternpost. Twenty-three frames were recovered, all of them abaft of midships. No maststep was found, and the keelson did not survive beyond frame 18, well-aft of the likely location of the maststep, which was not recovered. The structural timbers point to a vessel designed to navigate the shallow, shoal-filled waters of the Hudson River, prioritizing cargo capacity over speed (Fontenoy 1994, 93) The midship frame, which is the frame at the

widest portion of the ship, (which is either frame 23 or one just forward of it that was not recovered), is broad and flat. The shape of the ship resembles that of a Hudson River sloop: a beamy, single-masted heavily-rigged ship type that was popular for trade between Albany and New York City in the mid-late 18th century (Fontenoy 1994).

The fasteners were mostly iron spikes and nails, with only three wood treenails found. Given the cost of nails and the fact that they are not terribly well suited for vessels used in a brackish river system, this was an odd choice for the shipyard to make. This may have been the result of some of the design experimentation that was happening at the time in the area, and this ship seems to represent a very fascinating transition in ship design (Fontenoy 1994, 27-44).

Because of the need to navigate the shallow, rocky waters of the Hudson River, ship builders in the mid-18th century began altering hull designs to overcome these obstacles (AKRF Inc. 2013, S-1) . What they ended up with was a fairly unique ship type, characterized by its size and shape, typically around 15 m long, very beamy and a shallow draft, with heavy timbers that could take the abuse of the rocks. They had a large aft cabin that took up one quarter of the deck area, the mast was heavily raked, and despite being heavily rigged, they were not particularly fast. The typical cargo capacity of a Hudson Bay sloop was around 60-80 tons, compared to the 20-30 tons typical of coastal traders (Fontenoy 1994, 43).

Because of the shape of the WTC ship, it does not appear to be an ideal ship for sailing on the open ocean, but analysis of the *teredo navalis* infestation evident in the stem and several planks show that the ship made at least one voyage to warmer waters

down south, most likely to the Caribbean (AKRF Inc. 2013, 6-18). It will take a precise reconstruction of the ship to be sure of the body type, but based on its location and shape, it is reasonable to suggest the WTC ship is an example of the Hudson River sloops at the pinnacle of their popularity in the late 18th and early 19th centuries, before they were made obsolete by the introduction of steam boats to the area.

It is not nor has it ever been the goal of this dissertation to reconstruct the WTC ship as it would have been. This will be done by Texas A&M University's nautical archaeology program ship model builder Glenn Grieco in order to create a reconstructed version of the ship as a wooden model. Instead, the goal here was to develop a methodology for each step of the documentation and reconstruction process, from scan, to arranged digital model, to partial lines drawing, to physical 3-D model.

Construction Sequence

The virtual reconstruction methodology will be discussed in the next section, but before that it is useful to discuss the extent of remains and the probable construction sequence of the World Trade Center (WTC) ship. As found in 2010, the hull was found with the stern of sloping down, buried 6-10 m below the modern street level (AKRF Inc. 2013, S-1). Analysis of the site plan and the virtual reconstruction suggest that despite the ship remains being mostly articulated, the shape was deformed, most likely due to the weight of the city block built atop of them. Along with the deformation, the ship was partially destroyed during the construction of the original World Trade Center towers, with a foundational wall built right through the ship, close to the area where the maststep

would have been. On the other side of the wall, portions of the bow were found, giving an overall length of approximately 15 m to 18 m. The main dimensions and scantlings of the WTC ship are indicated in Table 1 below. Analysis of the ship timbers and their construction sequence hints that the WTC ship was assembled in a manner similar to other archaeological examples of wooden ships built in northeastern North America at this time: the 1789 schooner *Nancy*, the 1759 sloop *Boscawen*, and the 1814 steamboat *Ticonderoga* (Crisman 2014, 264; Sabick 2014, 81; Steffy 1994, 170).

The first step in the construction of the WTC ship was to lay down the keel, as the ‘backbone’ of the ship, and attach the stem and sternpost. The surviving length of the keel was an approximately 8 m-long solid piece of hickory (*carya*), but the original keel would have run the length of the ship, around 15 to 18 m (AKRF Inc. 2013, S-2). Next,

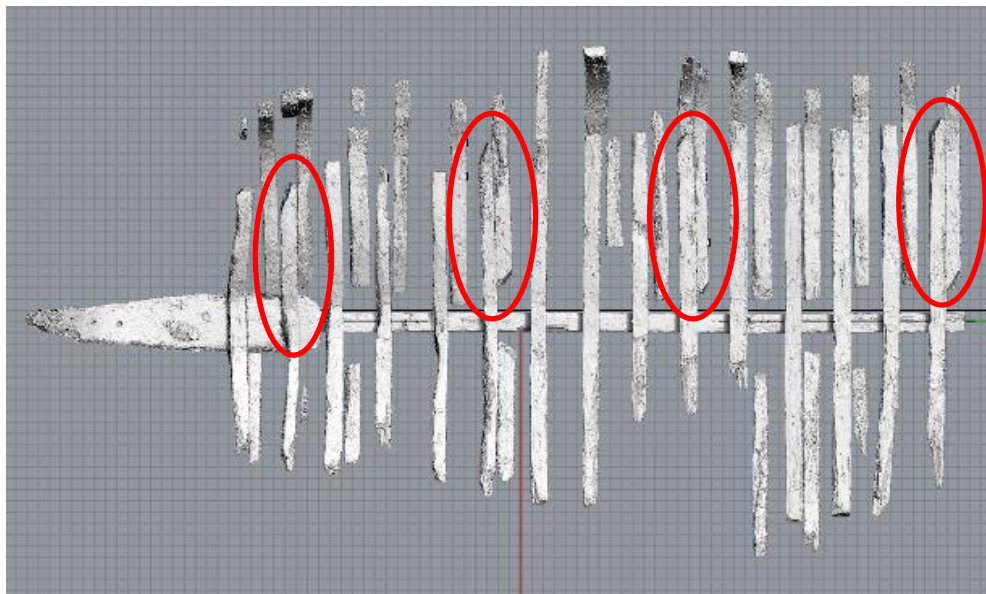


Figure 6: Frames 10, 14, 18, and 23 are notched at the ends of the timbers, while the rest of the frames are squared. Image by author.

the shipwrights reinforced the stern with a solid stern knee, bolted to both the keel and the sternpost. The stern knee was 2.1 m long at the base, 0.5 m wide, and weighed nearly 300 kg. Several pre-assembled frames (frames that were already fastened to their first futtocks) were then bolted to the keel, to act as a guide for the remaining floors and futtocks.

In the report generated by AKRF, the authors speculated that frames 10, 14, and 20, (frames were numbered in ascending order starting from the stern), were the only surviving made frames based on the fact that these were the only frames that had the futtock flush against floor when the ceiling planking was removed during the excavation.

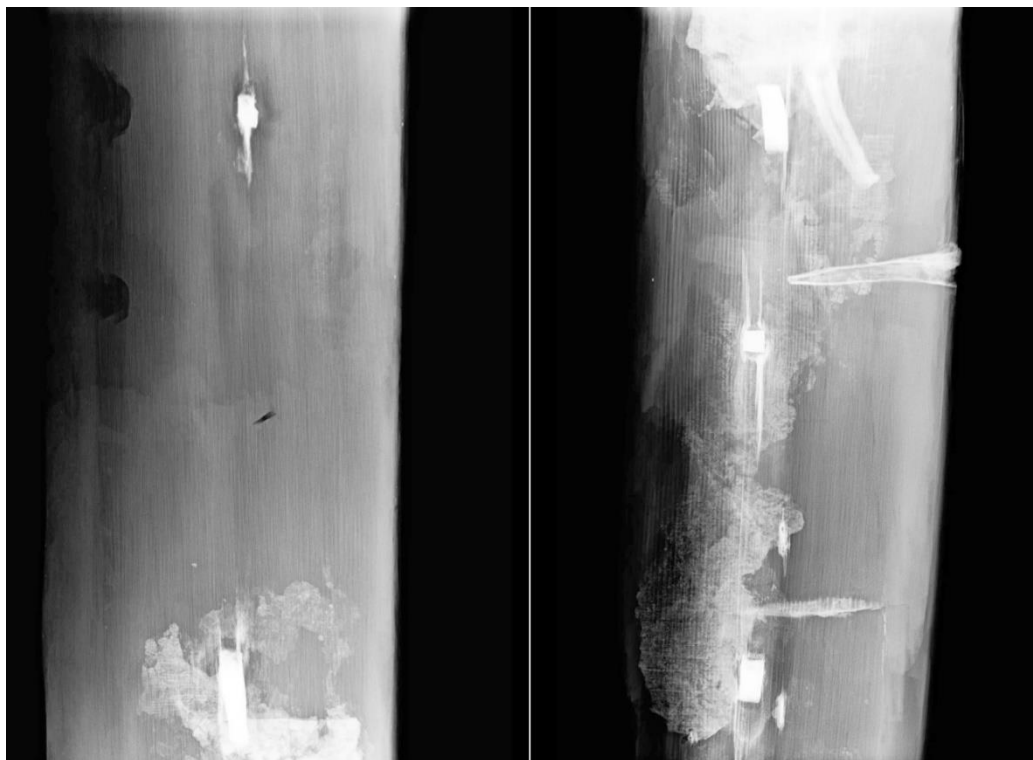


Figure 7: X-ray radiographs for the first futtock from port side of frame 20 (left) and frame 23 (right). Note that frame 23 has transverse fasteners where the floors were nailed to the futtock, while 20 does not. Image by the author.

Frames 10 and 14 had visible spike marks where the first futtocks were fastened to the floors, and 20 was speculated to have been a made frame as well. X-ray radiography of the first futtock for frame 20 taken at the CRL showed that this was not the case. The discovery of which frames were made frames and which were not occurred when studying the 1:10 scaled 3-D printed timber models with Kevin Crisman. As soon as the scanned floors and futtock models were 3-D printed, it was noted that some were squared at the ends, and some tapered (Figure 6). Once the 1:10 model began to be assembled, Crisman noted that the floors and futtocks with tapered ends were spaced evenly, and likely represented made frames, as the tapered end would have been easier to drive a spike through. X-ray radiography of the associated floors and futtocks revealed transverse fasteners, confirming that frames 10, 14, 18, and 23 were the made frames (Figure 7). Made frames 10, 14, and 18 were separated by three frames each, and frame 23 was separated from 18 by four frames. This is likely an indication that frame 23 is either the midship frame, or very near it. Starting with the aftmost made frame, frame 10, made frames were bolted to the keel approximately every 2 m.

Once all of the made frames were bolted in place along the keel, the shipwrights ran wooden battens along the exterior of these frames in a number of places to fair the lines of the ship. The location of the battens can be seen on the remains of the made frames in the digital model, determined by matching up the spike marks on the exterior of the timbers (Figure 8). The made frames and battens acted as molds for the insertion of the remaining unassembled floors futtocks. The precise positions of the floors on the keel were ascertained from the physical evidence of the corrosion stains on both the floor and the keel, as well as the actual fastener positions. The corrosion stains were removed in the process of conserving the wood, which is why the laser scanning of the timbers was done prior to conservation. The corrosion stains allowed for precise timber positioning on the virtual model, more than would have been possible using just the

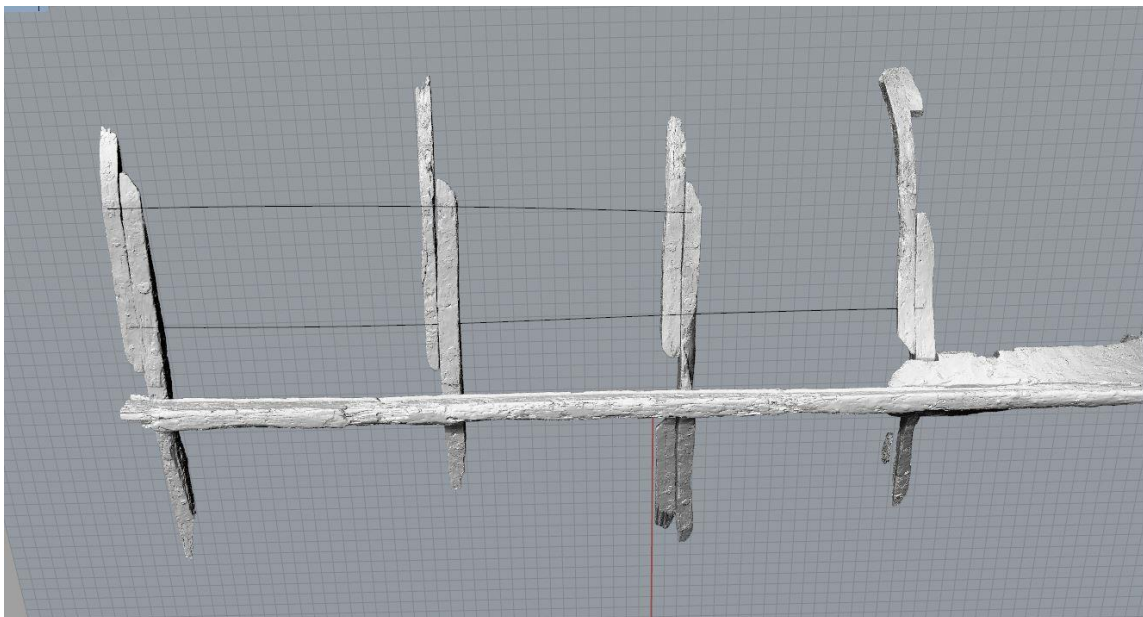


Figure 8: Estimated location of battens based on the locations of fasteners on the outboard of the master frames. Image by the author.

fastener markings as guides. The fastener markings on the keel show that, the floors were placed approximately 45 cm apart from spike to spike (Figure 9). Table 1 shows the spacing distances and their averages.

Frame to Frame	Spike to Spike	Forward Face to forward face
23-22	41.27 cm	41.83 cm
22-21	45.46 cm	42.76 cm
21-20	42.60 cm	43.26 cm
20-19	49.00 cm	48.11 cm
19-18	45.02 cm	44.84 cm
18-17	42.38 cm	44.19 cm
17-16	43.92 cm	42.23 cm
16-15	47.89 cm	47.89 cm
15-14	43.46 cm	43.10 cm
14-13	44.80 cm	44.19 cm
13-12	49.88 cm	48.87 cm
12-11	44.80 cm	44.41 cm
11-10	37.74 cm	39.07 cm
10-9	50.88 cm	47.24 cm
Average on keel	45.04 cm	44.64 cm
Average on Stern knee	44.31 cm	43.16 cm
Total Average	44.93 cm	44.43 cm

Table 1: Distance between individual frames and the average

The next step in the construction process was to begin planking both sides of the vessel from the keel outward. The floors and futtocks of the made frames acted as molds, or templates, for the remaining futtocks. The lack of transverse fasteners between the futtocks and floors of the non-made frames show that the shipwrights attached the outer planking to the made frames. After the outer planking strakes reached the tops of the first futtocks on the made frames, the remaining first futtocks were dropped into place and fastened to the outer planking. An abbreviated scantling list is available in Appendix III.

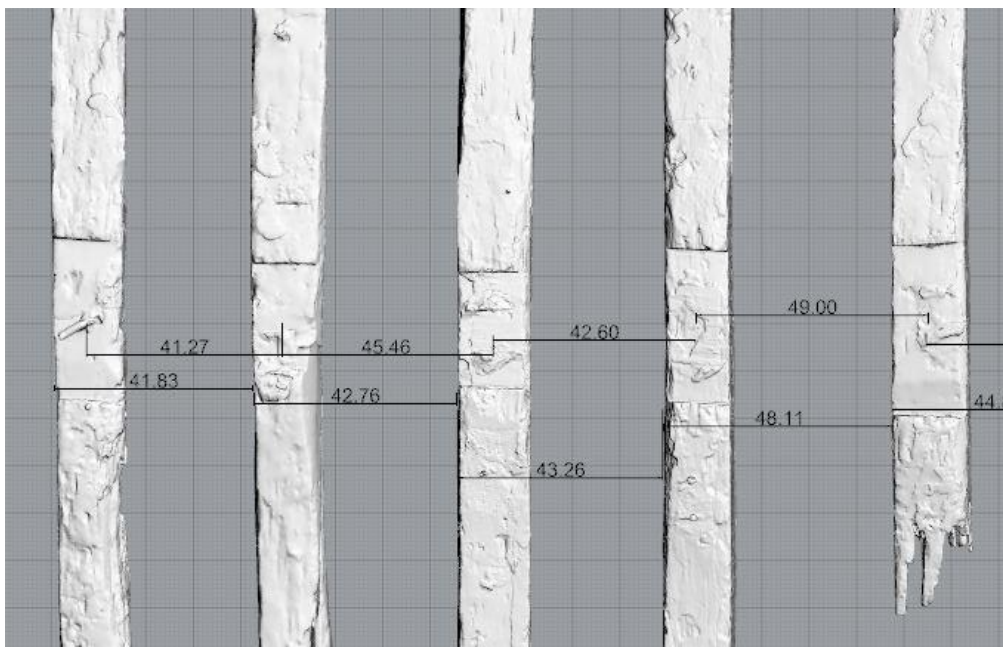


Figure 9: Measuring the distance between frames on the virtual model once placed on the keel according to fastener location. Image by the author.

The construction sequence outlined above was followed closely for assembling the 3-D printed timbers for the physical model, but frankly was unnecessary in assembling the virtual model. The virtual model does not simulate gravity, and therefore

does not need any kind of support to keep the timbers in place. This allowed for the theoretical placement of the futtocks without having to wait for the planking to be scanned, which allowed for lines to be drawn, faired, refined, and redrawn a number of times until the timbers were all in the most logical place that they should go. This helped direct the placement of the 3-D printed timbers, allowing for a more accurate reconstruction than was otherwise possible.

CHAPTER III

SCANNING METHODOLOGY

Preparing the Wood for Scanning

The World Trade Center (WTC) ship remains were disarticulated during the excavation and sent to the CRL. The ship was buried in a fine clay sediment, which prevented aerobic bacterial decomposition, and was perpetually wet due to its location below the water table. The anaerobic, waterlogged environment prevented the timbers from decomposing (AKRF Inc. 2013, 2-9). Waterlogged wood, like the timbers of this ship, must be kept submerged in water until stabilized with conservation treatment to prevent the wood from warping, cracking, or losing its structural integrity (Hamilton 1996, 25). Because it is neither practical nor safe to transport timbers submerged in water, the Maryland Archaeological Conservation Laboratory wrapped each timber in



Figure 10: The main storage vat for the WTC timbers. Note the grass clippings floating on the surface. Image by the author.

plastic for shipment to Texas. When they arrived at the CRL, they were offloaded into one large concrete fresh water vat with a plastic lining.

A large pool of fresh water in the Texas sun proved to be a very productive growth medium for insects and algae, a fact that was exacerbated by the habit of the landscaping crew to blow their lawn clippings into the vats. To combat the ill effects that bacterial growth can have on the timbers, the storage tank was periodically dosed with a biocide to prevent biological growth. The WTC ship timbers sat in storage for several years while the necessary funds were allocated for their conservation, and so even with the biocides that were added and the periodic exchange of water, over the years some of the hardier forms of algae managed to get a foothold in the tank and grow along the exterior of the timbers. As a result, when the timbers were removed to be scanned, the majority of them had some kind of growth on at least one face. In order to accurately record the wood surfaces, the timbers had to be thoroughly cleaned with tap water and scrubbed with a soft paint brush to remove the growth.

The storage vats were approximately 15 m from the area where the scanner was set up. The weight and fragility of the timbers meant that it was both difficult and unwise to carry the timbers all the way to the scanning area, so the timbers selected for scanning were loaded onto a stainless steel cart, cleaned, and then rolled to the scanning area (Figure 11). The procedure for handling the timbers differed slightly between small timbers and the larger timbers such as the stern knee or the frame floors. Smaller timbers were taken from the vat in batches, set onto the stainless steel cart, and washed all at once. All of the timbers were brought into the area where the scanning took place, and

the timbers that were not being scanned were draped with towels and thoroughly soaked to prevent any uncontrolled drying and subsequent cellular collapse in the wood



Figure 11: Floor timber FN FS 9-0 loaded onto a stainless steel cart to be cleaned and transported to the scanning area. Image by the author.

(Pearson 1987, 59). Larger timbers were brought in one at a time, and any exposed areas not being scanned were draped in wet towels as well.

When handling degraded timbers, it is important to consider how the stress of movement can affect the wood. Many of the floors and futtocks were split and splintered from the expansion of ferric corrosion around the areas where the iron fasteners were, and these areas were especially weak and prone to breakage. All potentially-weak areas

had to be identified before moving the timbers, and special care was taken to ensure they were supported when moving them to prevent further damage. The majority of the structural timbers (floors and futtocks, etc) were intact enough that there was no real threat of damage when moving them. This was not the case with the planks; even when they were structurally sound, too much weight along the wrong plane would cause them to snap. When moving planks, it is always best to carry the planks vertically, so that the weight is spread across the entire width of the plank and not just the thickness. Any wood with *teredo navalis* damage can be very fragile to the touch, but damage can be minimized by focusing on the areas with the most integrity and by limiting movement as much as possible. When washing the timbers, it was important to use a gentle spray of water so as to prevent the flaking of the surface of the wood, and to avoid spraying at too oblique of an angle, for the same reason.

It is vital to the success of any reconstruction project to ensure that the identification of each piece of the wreck is maintained throughout the entire documentation and conservation process. The timbers for this project were initially tagged with paper tags in the field, which were fixed to the wood with stainless steel staples. These tags had to be removed prior to scanning, otherwise the part of the surface that they obscured would not be recorded. The majority of the timbers were issued replacement timber tags when they were initially inventoried by the personnel at the CRL, because paper tags fade rather quickly when stored in water, especially when the water is exposed to the sun (Figure 12). The replacement tags were made from embossed plastic strips, and tied around the timbers with fishing line. Once the

individual timbers were scanned, replacement tags were embossed if necessary, and the field tags were discarded. When the scanning was complete, the timbers were re-



Figure 12: A paper tag from the excavation that is no longer readable. Image by the author.

submerged in one of several smaller vats to keep the scanned timbers separate from those that still needed to be scanned (Figure 13).

Instead of grabbing random timbers to scan out of the vat, it was determined that the most productive order would be to start with ten small structural timbers and five small planks. The reason for this was to establish an efficient procedure for scanning and processing the individual scans. Dozens of scanning projects had been completed by the author prior to the WTC ship project, including scanning water-logged timbers. However, those projects did not match the scope of work of the WTC ship project;



Figure 13: Secondary storage tank for scanned timbers. Image by the author.

instead of tens of items to scan, the WTC ship project presented hundreds. It was therefore important to establish the most efficient workflow possible, as a small inefficiency repeated hundreds of times could result in a substantial amount of wasted time and resources. It is recommended that extra time be taken at the beginning of a project to perfect the procedure before jumping in and starting work. Once the workflow was refined for this project and a standard procedure was established, the scanning began in earnest. Organizationally, the structural timbers were scanned first, and the planks last. By having the structural timbers scanned first, it was possible to proceed with the virtual reconstruction in a similar sequence to how the shipwrights would have constructed the vessel, and complete the portion of the project necessary for this dissertation in a timely manner.

There were two scanning arms used for this project. The first, used for the vast majority of the structural timbers, was a FARO brand Fusion coordinate measuring machine (CMM) arm with the V2 laser line probe (LLP). This arm was mounted on a 6ft (1.8m) by 3ft (0.9m) heavy duty steel table in one of the loading bays of the CRL (Figure 14). The table was heavy enough to remain stable if bumped, which is important when scanning to prevent unwanted movement of the object being scanned. Because many of the timbers were considerably larger than the size of a table, a second table on



Figure 14: A volunteer graduate student scanning with the V2 LLP on the steel table in the CRL loading bay. Image by the author.

castors was used to support any overhang if necessary. To prevent the second table from moving, it was clamped to the main table, and the wheels were secured with wedges.

Both tables were topped with white chloroplast sheets, to allow the wet timbers to easily slide along the surface and to prevent the wood from being damaged by the rough surface of the table. The white color of the chloroplast was chosen to minimize the efficacy of the scanner for picking up that surface, as the settings for the sensor were calibrated to focus on the dark color of the wood (this will be covered in detail in the next section of this chapter).

The second scanning arm was acquired in November of 2016 as a replacement for the damaged arm. This was a FARO Edge CMM arm with a V5 HD LLP. Because of



Figure 15: The second scanning arm, the FARO Edge CMM arm with V5 HD LLP, relocated to a new room with a new scanning table in November of 2016. Image by the author.

the high traffic location of the loading bay where the older arm had been used, as well as the lack of climate control, the new arm was relocated to a classroom location adjacent to the loading bay, and fixed to a heavy slate table that was much sturdier than the steel table (Figure 15). This slate table, which had been used extensively over the years as a surface for epoxy casting for artifact duplication had a rough surface. It was sanded and painted with a heavy duty outdoor paint to provide an acceptable scanning surface, and the chloroplast was no longer necessary because of the smoothness of the painted surface.

Regardless of which scanning arm was used, the scanning procedure was the same. Only five of the six faces of a timber can be scanned at once, as one side is always resting on the table. To record complete scans, it was necessary to scan each timber at least twice, and then align the two scans later to develop a complete model (see the *Post-Processing* section of this chapter). To align the two or more scans needed to capture the entire timber, the separate scans needed to have sufficient overlap with each other in order to identify identical locations that could be used to tie the scans together. If there was an area that the scanner could not reach in any of the separate scans, that area would be an empty void in the completed model, which was not acceptable. If the timber was arranged too closely to the FARO Arm on the scanning table, the LLP would not be able to articulate to reach the part of the timber closest to the base of the arm. To achieve sufficient overlap between scans, the closest edge of the timber needed to be kept at least 45 cm away from the base of the arm.

Whenever waterlogged wood is not submerged in water prior to conservation, it is necessary to keep the surface damp at all times to prevent warping and cracking (Hamilton 1996, 23). Scanning with a LLP is relatively fast compared to other scanning methods, but even so, the scanning takes enough time that the wood is out of the water long enough that drying is a concern. The scanning of the structural timbers of the WTC ship with the first scanning arm was done in the summer of 2016 in a non-air conditioned building in central Texas. The heat and humidity, as well as the use of fans to keep the LLP within its temperature limits meant that the timbers would rapidly dry out if not constantly re-wetted. To keep the wood wet, a large spray bottle with tap water was used to spray down the wood regularly, and the sections of larger timbers that were out of the reach of the LLP were kept covered with damp towels.

The need to keep the surface of the timbers damp provided a unique challenge for a process that relies on visible light for data collection. Water refracts light differently than air, and if the surface of the wood was too wet, the data was plagued by random ‘noise’, or points that occurred due to interference and did not represent accurate points that existed in reality. If the scanning had been done without understanding the effects that standing water would have and mitigating these effects in the post-processing phase, the surface of the completed model would not be representative of the actual timber. To minimize the noise caused by the refractive properties of the water, damp towels were used to pat away excessive moisture between sprayings, and the settings for the LLP were tuned to prevent excessive noise.

Configuring the Settings of the LLP

Prior to scanning, the LLP was configured to account for the color, reflectivity, and the absorption of light on the object being scanned. The LLP is, at its core, a digital camera that photographs laser light and derives the depth based on the reflection return angle and time. The LLP consists of a pulsing laser emitter that projects a line of laser light, and a charge-coupled device (CCD) sensor, which is a grid of pixels that convert photons of light into electrical charges that are then interpreted as digital images (FARO 2012, 10). The CCD measures the reflection of the laser photons emitted from the probe, and much like a camera, the settings need to account for all of the things that can affect the way that the photons will reflect back to the sensor. There are two groups of configuration settings that need to be set before scanning. The first set deals with the data acquisition in the software, which is akin to adjusting the resolution and white balance of a digital camera, while the second group of settings deals with the physical way the sensor collects that data, which is like changing a camera's shutter speed and aperture setting.

For the data acquisition settings, the goal is to tell the software how much data should be gathered and which data should be discarded. The concept of resolution is more complex for a 3-D model than it is for a 2D image. When considering the resolution of a 2D digital photograph, the more pixels in a given area, the higher the resolution of the picture. The resolution is fixed across the photo, and therefore easy to convey. With a 3-D model, the resolution is not fixed across the model; areas with greater curvature will have a higher point density and areas that are flatter will have a

lower point density. As seen in Figure 16, there is no fixed distance between points. The points have an average distance between them that is determined by the user in the settings, but because of these variations, the concept of resolution is not as easy to convey for 3-D models. Instead, the settings that determine how the collected data are managed is used to convey the concept of resolution. Of the data acquisition settings,

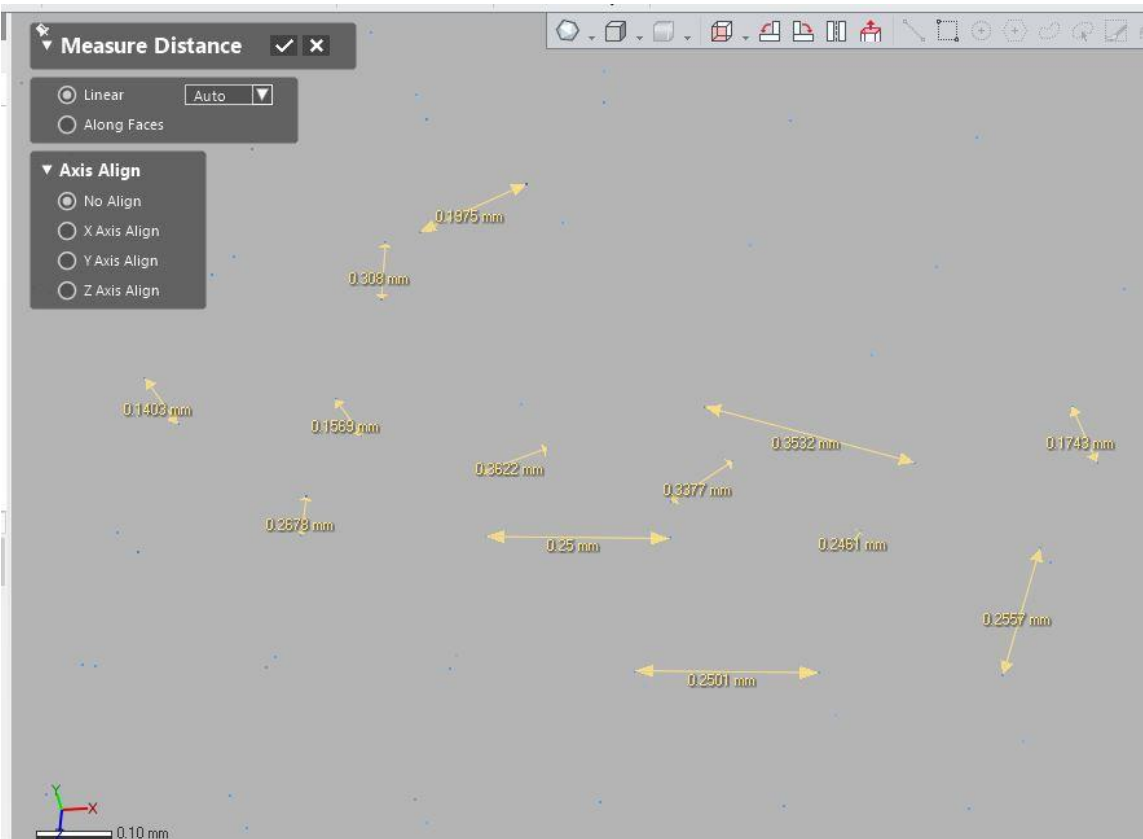


Figure 16: The distance between the points in the point cloud for CN 4-4 vary from point to point. Image by the author.

there are three main variables that convey resolution: the grid size, the maximum point distance and the maximum deviation.

The grid size setting is used to determine the average distance between points. As the laser line passes across the surface of the material being scanned, the sensor picks up more points than are necessary to create an accurate model. Conceptually, if the scanner CCD picks up 1,000 points for a given area and the user configures the settings so that in that given area, only 10 points are desired to convey the shape, it creates a grid of 10 squares over the thousand points and averages out 100 points in each grid square to generate a single point (Geomagic Support 2016). However, specifying the number of points is not a realistic way to specify resolution, because point count is dependent of the size of an object. Instead of specifying the number of points, the size of the grids are specified. If a small, detailed object was scanned and a small grid size of 0.075mm was specified, it would mean that all of the points collected in every 0.075mm grid square would be averaged into a single point.

The grid size does not necessarily specify the distances between the individual data points. Within a particular grid square, the average point is not always in the direct center of the grid. Because of this, the distances between the points can vary depending on where in their grid they are placed. Figure 16 shows the distances between points in the point cloud for plank CN 4-4. They are all roughly 0.35mm apart, because that was the grid size specified in the settings, but they vary within that average. Because of the computing resources and memory needed to manipulate the point clouds, a small grid size is not yet feasible for a large object like a ship timber. That said, even if there were no concerns about processing power, the amount of additional data collected would be negligible (for more on this, see *The Diminishing Returns of Resolution* in Chapter VIII).

For the WTC ship timbers, several grid sizes were experimented with before settling on 0.35mm. This size allowed for the capture of extremely nuanced detail, but still allowed for file sizes that were able to be easily handled by the computers available.

The maximum edge length setting determines the distance between adjacent laser stripes that will give continuous data. The LLP collects data at a fixed rate, and if the probe is moved too quickly, there will be gaps between the acquired data. Imagine using a camera to take several photos per second to create a panorama; if the camera is moved too quickly, there will be insufficient overlap between the pictures to create the panorama. The maximum edge length determines how much overlap between the scan lines are acceptable. A small maximum edge length means that if the probe is moved too fast and the overlap is not sufficient, the strips of data that are acquired will be discarded. A larger maximum edge length means that less overlap is necessary to preserve the data, and if there are gaps, they will be filled automatically. This makes the scanning easier, but it also means that the areas where no data points are collected will be filled in with estimated data points, which diminishes the accuracy of the model.

Figure 17 shows what a scan looks like when the scanner is moved too fast, causing gaps between the laser lines. The maximum edge length used for this project was 3.5mm. This distance was determined through a series of trial and error scans to be the largest edge length that could be employed without losing significant data on a small timber.

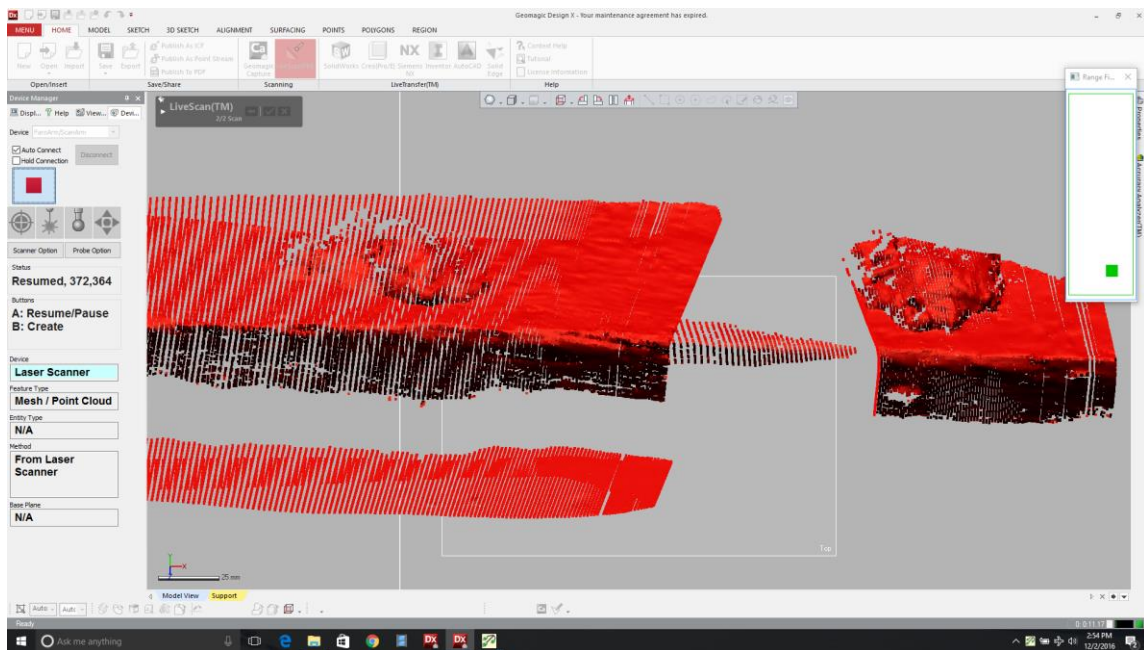


Figure 17: Gaps in the scan data caused by moving the LLP too quickly for the maximum edge length setting. Image by the author.

The maximum deviation setting is a noise reduction tool. Because the CCD sensor works by registering the location of reflected laser light, sometimes photons with the same energy signature as the laser being emitted from the LLP enter the CCD sensor and register as data points. This ‘noise’ is unavoidable, but it is undesired and therefore it must be accounted for and eliminated if a scan is to meet archaeological standards of accuracy. An analogous problem with digital cameras is lens flare in a digital

photograph. It is technically representative of photons entering the lens and hitting the sensor, but they are photons that are not representative of the scene being photographed. One way to mitigate this is by telling the software that if a data point comes in that deviates from the rest of the data points being collected by a certain distance, it will be discarded as noise. This setting is called the maximum deviation distance, and for the scanning of the WTC ship timbers for this project, a maximum deviation of 0.05mm was used.

The second group of settings deal with the way the sensor actually acquires the data. There are four basic settings that can be adjusted: noise threshold, exposure, scan rate, and scan density. Of the four, only two are commonly adjusted to account for the different color and reflectivity of an object: exposure and noise threshold. Both of these can be automatically obtained by the software, much in the way that automatic settings calculate exposure and the lens aperture for a camera. The noise threshold setting configures the sensitivity of the CCD to the returned photons; the electrical charge of each pixel is measured on a scale of 0-255, and any value below the noise threshold will be discarded (FARO 2012, 10). For the WTC timbers, the standard FARO-recommended set point of 15 was used.

The exposure setting for the LLP controls the amount of time that the sensor collects light per laser pulse, similar to how the exposure setting controls the length of time for the shutter to be open on a digital camera. The exposure is measured on a scale of 1-80, which corresponds to an exposure time in milliseconds. For lighter-colored objects, a lower exposure setting is needed, and for darker objects, a higher one. If a

light object is scanned with too high an exposure, the resulting scan will contain significant noise. If a dark object is scanned with too low an exposure, the electrical charge for each pixel on the CCD will be too low and will be discarded. Because the wood is fairly dark, an exposure setting of 70 was used, which corresponded to 4.375 milliseconds. After the second scanner was purchased in November, setting the exposure became unnecessary, thanks to refinements in the software for the auto-exposure option.

Finally, the last two settings are the scan rate and the scan density. These settings control how much information is obtained per laser pulse. The scan rate controls the number of scan lines captured per second, with a maximum of 30 for the V2 LLP and a maximum of 280 for the V5 LLP. The scan density controls the number of points captured per line, with a maximum of 640 for the V2 LLP and 2,000 for the V5 LLP (FARO 2017). This means that the overall capture rate for the V2 LLP was 19,200 points per second, and 560,000 points per second for the V5. Lowering the scan density allows the LLP to be moved faster, but lowers the resolution of the data being gathered. Initially the maximum scan rate and scan density was used with the V2 LLP, but when the scanner was upgraded, the scan density and the scan rate were lowered to the maximum levels of the V2 LLP for consistency. The lower settings on the newer hardware resulted in substantially faster scanning.

Scanning Procedure

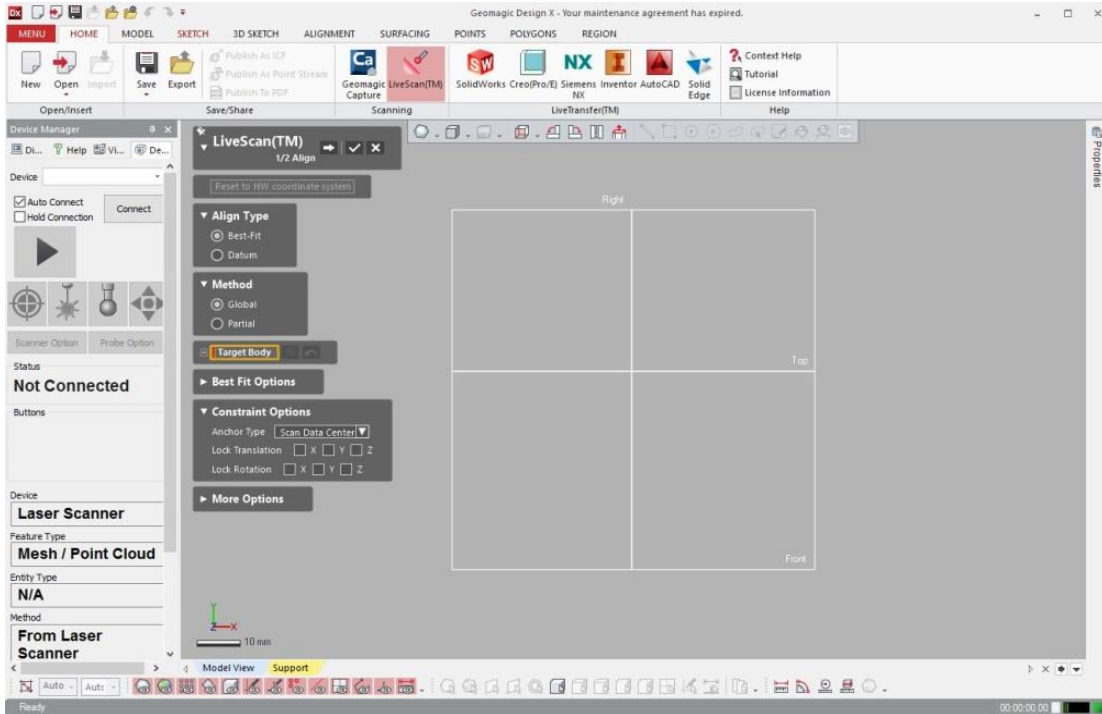


Figure 18: *Design X* Scanning Interface. Image by the author.

The actual scanning of the timbers was done using a third-party software package from 3-D Systems, Geomagic *Design X*. *Design X* is a reverse engineering software package based on Rapidform *XOR* and Geomagic *Studio* after both Geomagic and Rapidform were acquired by 3-D Systems in 2012 and 2013, respectively (Taggart 2013, Rapidform 2012). *Design X* is set up to work with a number of laser scanners, and the program works with the FARO LLP without requiring any additional plug-ins. The steps described in this section are specific to *Design X*, but the general steps of the workflow are the same with all 3-D scanners and software packages.

To begin, on the 'Home' tab of *Design X*, the 'LiveScan™' icon was clicked. This launches the LiveScan™ scanning protocol directly to an alignment stage, allowing the settings outlined in the previous section to be changed. Figure 18 shows the LiveScan™ interface. The first time the FARO Arm was connected to the computer for the day, it needed to be walked through a process of referencing the encoders located in each of the articulated joints. This process is straight forward; a dialog box with a picture of the arm is displayed on the screen with a red arrow showing the joint which needs to be referenced, at which point the user simply moves the joint until the red arrow clears, indicating that the encoder has been satisfactorily referenced. Once all encoders are

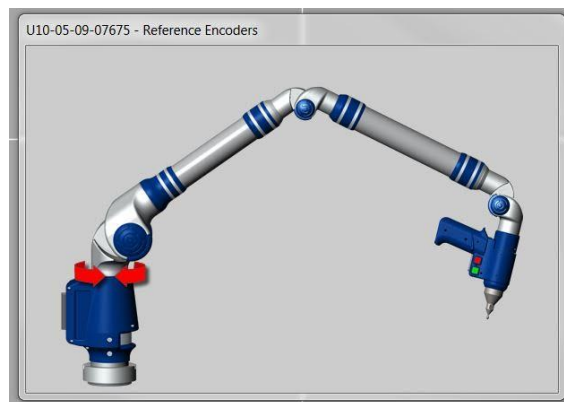


Figure 19: Reference Encoder. Image by the author. referenced and the red arrows are cleared, the dialog box disappears and the scanner is ready.

The workflow as outlined in the help file for the program is as follows:

1. Select the device (FAROArm/ScanArm).
2. Connect the device.

3. Click the forward arrow to progress from the alignment stage to the scanning stage.
4. Click the green arrow.
5. Scan the object using the buttons on the scan arm; green for start and pause, and red for stop.
6. When the scanning is completed, click the stop button.

During the scanning process, the laser probe has to be kept at a certain distance from the object being scanned. If the probe is too close, the laser cannot return to the sensor window, and likewise if it is too far away. There is a range of distances that work depending on the object being scanned. The LLP has a rangefinder on it to show when the scanner is at the correct distance from the object, and the computer screen will show whether or not data is being collected in real time. Because of the narrow range of distances at which data collection takes place, it is especially important to pay close attention to the screen when scanning the edges of the timbers at an angle perpendicular to the edge. If the LLP is too far from the edge, the tip of the edge can be in range but the faces not, or if the LLP is held too close, the faces of the timber can be in range but the edge not.

Since data acquisition is a product of the laser line return to the sensor, it was necessary to scan from a variety of angles to minimize shadow areas where the laser line return was obstructed. The most productive data acquisition occurs when the LLP is held perpendicular to the face being scanned, but there are almost always areas that require a

more oblique angle to capture. A good way to envision the angle at which the laser line is directed at the object being scanned is to think of a flashlight shining on a rough surface in the dark. If you shine perpendicular to the object, you will light most of it up. If you come down at an oblique angle, there will be shadows from the rough edges. Any shadow that you might have is an area that the light is not hitting, and therefore would represent an area within which the LLP could not collect data.

As mentioned in the scanning steps, the scanning arm has two buttons. The green button, which starts and pauses the scanning, does not need to be held to scan or pause, just tapped once. During the scanning process, it is helpful to pause and restart the scan often. If a scan was done too quickly or the data does not meet the limits of the noise thresholds set prior to scanning, scanned data will be discarded. The data is not discarded on the fly though, it is discarded after the scanning is either paused or stopped. Pausing allows the user to see which parts of the scan are being kept and which parts are being discarded. It is also a good idea to pause the scan prior to repositioning the LLP; if the scanner is still trying to collect data while the LLP is moved, it can scan something not intended to be scanned, or collect noisy data.

Depending on the settings and the size and texture of the object being scanned, the number of points collected can easily exceed tens of millions. Like any work that involves computers, it is prudent to save the work often to prevent data loss due to a crash or error. The LiveScan™ work flow was designed to have a scan completed prior to saving, but it was found that too-large point clouds tended to crash the software if not stopped and saved periodically. The laptop computer used to run *Design X* for the

scanning was bought with its purpose in mind and had high-end specifications for a laptop at the time of purchase (see Appendix I: Hardware configurations), but even so, it was found that if more than four million points were gathered without completing the workflow and saving, *Design X* would either freeze or crash, and the data would be lost. If the process was stopped and the LiveScan™ protocol completed, the file could be saved, and as long as the timber being scanned was not moved during the save, the scanning process could be resumed and the newly collected data would be added to the saved scan data.

The stability of the timber to prevent movement during the scanning process was vital for an accurate scan. If the timber moved even a millimeter, all of the data that was collected after the movement will no longer accurately align with the previous parts of the scan. Though technically it is possible to go back and realign these scan section, the movement is often very difficult to discern and the time and energy needed to re-align was much greater than simply re-scanning without moving the timber. Unintentional movement of timbers was inevitable, and happened for one of three reasons: the table was bumped, the wood was bumped with the probe tip of the FARO Arm if the distance between the LLP and the wood was not maintained, or the wood was balanced precariously and fell or shifted mid-scan.

As mentioned in the *Preparing the Wood for Scanning* section of this chapter, during the use of the V2 LLP, the base of the FARO Arm was fixed to a heavy duty steel table for this project. The heavy table was used in this case so that incidental contact from other members of the CRL conservation team would not result in data loss. It is not

always a table that is used to mount a CMM arm, often a sturdy tripod is used if scanning in the field. If using a tripod, it is important to not bump the table *or* the tripod; any shift in relation to one another would throw off the scan. Given the extra work created by an accidental bump, it is useful to designate an area to scan with low traffic, or set up a boundary area around the scanner and table to minimize the risk of contact. Preventing any nudging of the object being scanned with the tip of the probe is merely a matter of practice. It most commonly happens when the LLP is oriented directly over the top of the wood, with the tip pointing towards the timber. The weight of the arm will tend to cause the user to start to droop towards the wood without realizing it, and this can cause the tip to bump protrusions on the surface. The arm is counter-balanced with a spring in the joints to prevent fatigue in the user, but even so, the weight of the arm and the LLP becomes strenuous after a period of scanning, especially for new users.

As far as ensuring the timbers will not move due to the instability of their position on the table, small Plexiglas squares of various thicknesses were used to prop up uneven sections to prevent unwanted movement. Plexiglas was chosen because of its transparency; it was much less likely to reflect the laser back to the LLP sensor than opaque materials. If a transparent material is not available, support material should have a noticeably distinct texture from that of the object being scanned; this will allow for easier identification of the support material when it needs to be deleted in post-processing. Using a support with a much brighter or much darker color than the object being scanned can help as well, as long as the settings outlined in the previous section are correctly configured for the color of the object being scanned.

While scanning, it is important to conceptually understand the post-processing procedure to ensure that all of the data that needs to be acquired to achieve an acceptable model is obtained for each scan. All timbers have to be scanned at least twice to capture all sides. The length of the FARO ScanArms used for this project (see Appendix I: Hardware Specifications), meant that the timbers from this project required anywhere from two to six scans to cover the entire timber. For the timbers that only required two scans, it was important to ensure that the areas scanned on the sides had enough overlap with the other scan to ensure accurate alignment between scans. This was doubly important for the larger timbers requiring four or six scans. There needed to be enough overlap between all four sides for alignment. For this project, the amount of overlap was decided before scanning so as to provide clear guidelines for the scanning process and to prevent problems. It also meant that particular attention was paid to the small details in the overlap zones, as these small details were the ideal points to choose between the overlapping scans to tell the software how to align them.

It was determined that when scanning frame pieces, it was best to stop the scan 2-3 cm above the surface of the table for both sides, as long as there was 4-6 cm of possible overlap. This precluded the need to edit out the table, and it also helped prevent some of the alignment errors discussed in the *Post-Processing* section later in this chapter. For the planks, the majority of them were 4 cm thick, which obviously does not leave the required 4-6 cm of overlap, so the entire sides had to be scanned, table and all.

With the capture rate of the V2 LLP, each timber took anywhere from 45 minutes to 7 hours to scan. The average floor timbers took four scans to cover, with each one

taking 1-2 hours. None of the futtocks took more than two scans, and would typically take the same amount of time per scan. The largest timber, the stern knee, required four scans, and close to 9 hours to complete. The vast majority of the 134 timbers that were scanned prior to the purchase of the new scanning arm were done between June and October of 2016. Though the time it takes to scan a timber with the LLP is considerably shorter than other methods of 3-D recording, it was still long enough to require the CMM arm and LLP to be run for the better part of an 8:00 am to 5:00 pm work day. Because of the way the CRL is set up, this meant that the arm would be operating in a non- air-conditioned environment in the Texas summer during the hottest parts of the day. Temperatures at the lab during the summer of 2016 routinely soared above 37°C, and the relative humidity was typically between 90-100% (Weather Underground 2016).

The temperature and humidity meant that the LLP was operated near the upper limits of the manufacture's specifications, and may well have contributed to the reference encoder failure discussed in the *Complications and Lessons Learned* section of this chapter. Apart from the possible ill effects that the extreme weather conditions can cause to the sensor in the LLP, the accuracy of the scan is in danger of being compromised. It is not unusual for the ambient temperature in the lab operating space to rise 13°C during the course of the day. This drastic change in temperature could conceivably cause considerable distortion of the material being scanned. Luckily, for the purposes of this study, it was not a serious concern. Wood is an excellent insulator and therefore does not change temperature very rapidly. Moreover, it was waterlogged and

remained wet throughout the scanning process, so the temperature of the timbers stayed relatively steady during the scanning procedure.

Once the timbers were scanned, the files were transferred to an external hard drive and copied to other computers for post processing. The majority of the post processing was done in a separate laboratory with access to several computers, which allowed multiple scans to be processed at a time, significantly cutting down on the amount of time spent away from the actual scanning process.

File Organization

Before moving on to the post-processing procedure, it is important to address the issue of file organization. When dealing with so many stages of data across so many timbers, meticulous organization is vital to the success of the digitization project. As detailed throughout this text, the stages that the data were saved at are as follows: *Design X* point cloud (.xrl), *Design X* unaligned mesh (.xrl), *Design X* aligned mesh (.xrl), an industry standard mesh file compatible with the 3D printer (.stl), and a decimated, or reduced resolution industry standard mesh file (.stl). Each stage was saved separately to ensure that any problems encountered during the processing pipeline could be recovered if necessary. Data was saved to two computers and an external hard drive, segregated into separate folders for each stage of processing. A non-segregated copy of all files created on the scanning laptop were also kept as a back-up.

For the initial point cloud scan, the files were named after the timber number assigned in the field, and then ‘SIDE 1’ or ‘SIDE 2’, etc. The field numbers were

designated based on the purpose and location of the timber. Frame timbers had the designator ‘F’, outer planking ‘P’, ceiling planking ‘C’, and so on. The ship was situated with the port side facing north, so all timbers from the port side were assigned an ‘N’ and all timbers on the south side were assigned an ‘S’. The framing numbers started with frame one as the aftmost cant frame on each side, and increased as the frames moved forward. The first floor was frame nine, and the forward most frame was frame 23. For the planking, the garboard on each side started as number one, and then increased as the strakes moved away from the keel.

For example, the first port side futtock for the forward most frame, frame 23 would be named FN 23-1. FN 23-1 required only two separate scans, and so the scan files were saved as FN_23-1_SIDE_1.xrl and FN_23-1_SIDE_2.xrl. Underscores were used to delineate spaces, just as a precaution against errors that can occur when opening files in non-native programs or across OS platforms (Apple Inc. 2016). These files were exported to the external hard drive, to a folder called ‘Raw Files’. Once the point file was processed and a mesh was created, it was saved in a separate folder called ‘Meshed Raw Files’. The word ‘MESHED’ was added to the file name when it was saved, i.e. FN_23-1_SIDE_1_MESHED.xrl.

Once the meshed sides were aligned and a water-tight mesh was created representing all of the scanned sides, the completed mesh was saved in a file called ‘Completed Files’, with the descriptors removed from the file name (FN_23-1.xrl). Once the mesh was complete, it was exported as the industry standard .stl file with the same name in a separate folder called ‘STL Files’. It was not necessary to change the file

name to describe the fact that it was a .stl file, the file extension made it obvious that they were distinct files. Finally, when the .stl file was decimated to a smaller file, it was saved in a distinct folder called ‘Decimated files’, and the word ‘DECIMATED’ was added to the file name, (FN_23-1_DECIMATED.stl).

The importance of a consistent, logical organizational scheme cannot be over emphasized. The number of files generated and the amount of data stored is useless if it cannot be tracked and accessed at all stages of the scanning project. Also, although it should go without saying, regularly saving all versions of the scan data across several distinct hard drives is mandatory. Anything less is inviting catastrophe. The failure to appropriately secure the data gathered during a project that deals with cultural heritage materials is tantamount to wanton vandalism.

Post-Processing

After the scans were complete, the next stage was to process and align the scans to create a watertight mesh. As mentioned in Chapter II, the scanned data is gathered by the LLP as a point cloud. The point cloud is by far the most accurate version of the data collected, because it represents the actual data points that were collected, as opposed to a mesh, which is an interpretation of the surface of the model based on the geometry of the point cloud. All of the raw point cloud data was saved and archived for this project, but for the purpose of the study and reconstruction of the WTC ship, the raw data files were too large to easily manipulate in a 3-D environment. Hundreds of sets of very dense point clouds would have ultimately overwhelmed all of the computing resources

available for this project. Having a model which is difficult and slow to manipulate hampered the ability to virtually reconstruct the ship. To overcome this, the point clouds were edited and meshed, which created smaller, more manageable file sizes, and also allowed the models to be arranged in *Rhinoceros 5* and printed out with a 3-D printer.

There are two ways that the scan data could have been edited, aligned, and meshed. The method outlined here was to edit and mesh the separate scans for each timber, and then align these separate meshes into a single model. This method produces a watertight, highly-detailed model, but if analyzed for its balance between detail and efficiency, it would lean slightly toward efficiency. The other method is to edit and align the point clouds of the separate scans, and then mesh the single aligned point cloud. This

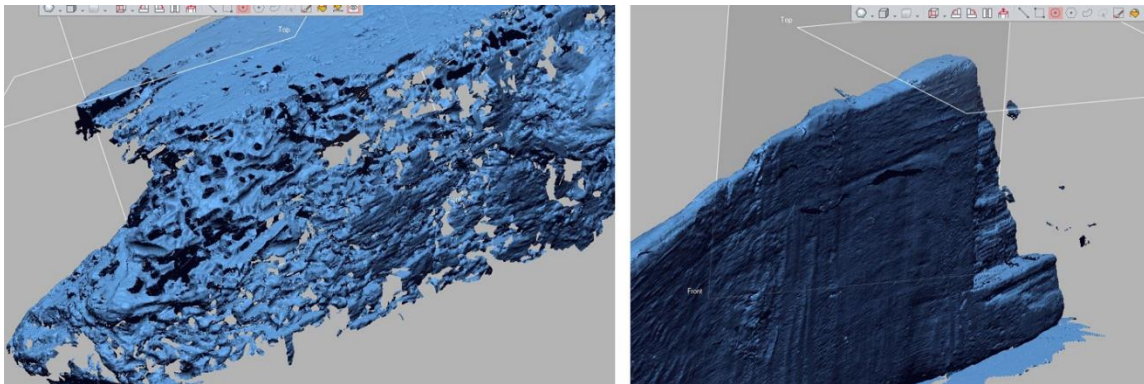


Figure 20: The LLP struggled to scan the *teredo navalis* damage on the stern post (ST 1), resulting in gaps (left). On the plank CN 3-5, excessive noise was picked up when the LLP was aimed away from the wood, and when part of the table was scanned (right). Image by the author.

provides a higher-quality mesh, but the time it takes to walk through the individual steps is substantially longer than the other method, and was deemed logistically unrealistic for this project. The raw data for each scan was archived, so when the computing resources

for this project reduce the time disadvantage, the scans could be remodeled in the more detailed method, which is outlined in Appendix II.

The raw point cloud acquired for each timber scan inevitably contained areas where the point cloud did not perfectly capture reality; there were gaps where the laser could not reach, or excessive points generated through interference or digital noise generated by the reflections and refractions of the laser line on the damp surface of the timbers (Figure 20). Before meshing, the point cloud was edited to remove these errant data points, as well as undesired scan data like the table or timber supports. All point cloud data editing was done using the same software that was used to capture the scan data, Geomagic *Design X*. The user interface in *Design X* is organized with tabs that represent the different stages of the data processing. There are four major steps to processing the scan data: selecting the data to be edited, editing the point cloud, aligning the scans if necessary, and the meshing.

To begin, because the first step deals with point cloud data, the POINTS tab was selected, and the Mesh Buildup Wizard protocol was used (Figure 21). There are five stages of editing in the Mesh Buildup Wizard: data selection, noise reduction and deletion, manual alignment, refined alignment, and data merging. As each stage is complete, the next stage is selected with a forward arrow. In some cases, not all stages are necessary. Because the FARO CMM arm and LLP tracks the movement of the probe, the segments of the scans generated when the data acquisition was paused were already pre-aligned, making the alignment stages unnecessary when processing the point data. Later in the process when there are meshes of the different sides of the timber, the

alignment stages are used. Because of this, under ‘Set Data Condition’, the ‘Is Pre-Aligned’ box was checked for point data (Figure 21).

As mentioned in the *Scanning Procedure* section of this chapter, every time the green button is pressed on the FARO Arm, the LLP pauses data acquisition and adds the data of the previous segment to the whole model. This means that when the scan is loaded into the Mesh Buildup Wizard, *Design X* sees each individual scan portion, not the overall whole (see Figure 21, towards the bottom of the screen capture). If during the

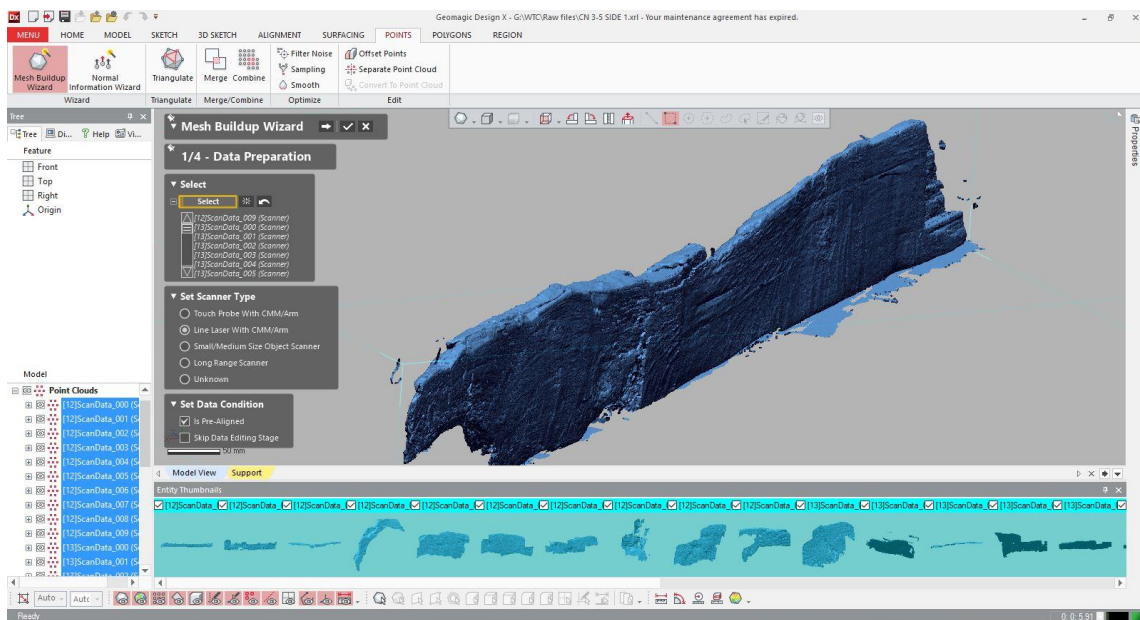


Figure 21: The first stage of processing utilizes the Mesh Buildup Wizard, found in the POINTS tab. Image by the author.

scan one segment generated excessive noise, it was occasionally easier to simply de-select that portion of the scan at this stage and not incorporate it into the rest of the model than to try and delete the excessive noise in the next stage. (This was only an

option if the portion of the scan in question was within an area of overlap with the rest of the scan).

Once the data to be used in the meshing process was selected, the next step was to select all the noise in the scan and delete it. There are several tools that can be used for this, each with a slightly different utility. The most obvious and consistent unwanted data in the majority of the scans was the table that the timber rested on during the scanning. One of the features of Geomagic *Studio* that was not imported over to *Design X* was the ability to create a clipping plane, or scanned area that could be designated as

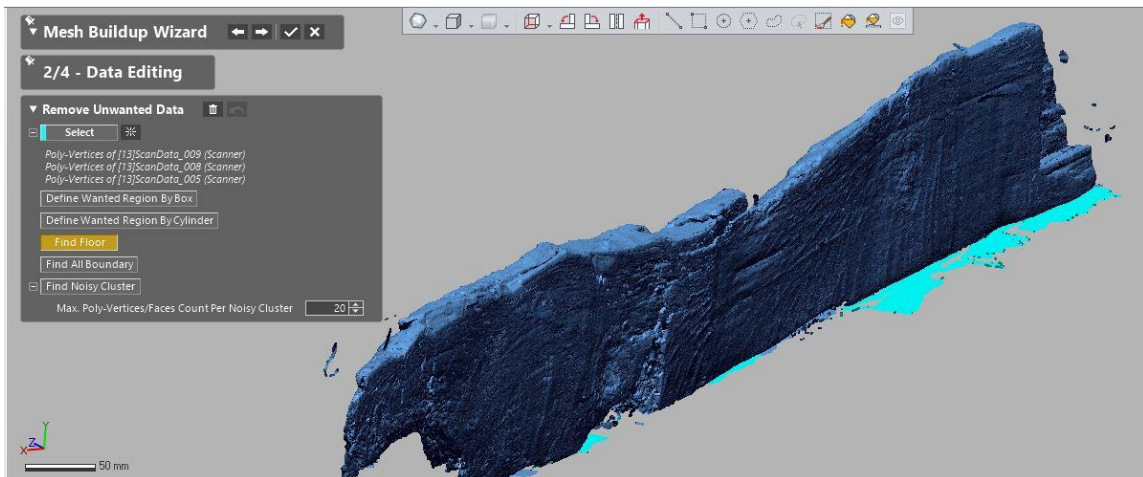


Figure 22: Using the 'Find Floor' selection tool, the plane of the scanning surface is automatically selected. Image by the author.

unwanted. This allowed for the scanning surface itself to be scanned, and then be designated as unwanted data and automatically ignored during the scan. Because *Design X* does not have the ability to do this, one of the data selection tools in the Mesh Buildup Wizard was optimized for the easy deletion of the scanning surface. By using the 'Find Floor' tool, clicking anywhere within the scanned table automatically selected anything

else along that plane (Figure 22). This worked with middling success; it often selected large swathes of the timber instead of just the table, and it often only selected small sections of the table necessitating dozens of separate selections. Though it can be made to work, if the three main faces of the timber are scanned for each side, there was almost always enough overlap to allow the user to simply select the bottom centimeter of the scan and delete the whole thing. This not only deletes the table, it also prevents any unwanted overlap of edges resulting in mesh noise.

For other obvious noise artifacts that do not belong to the model, there are a

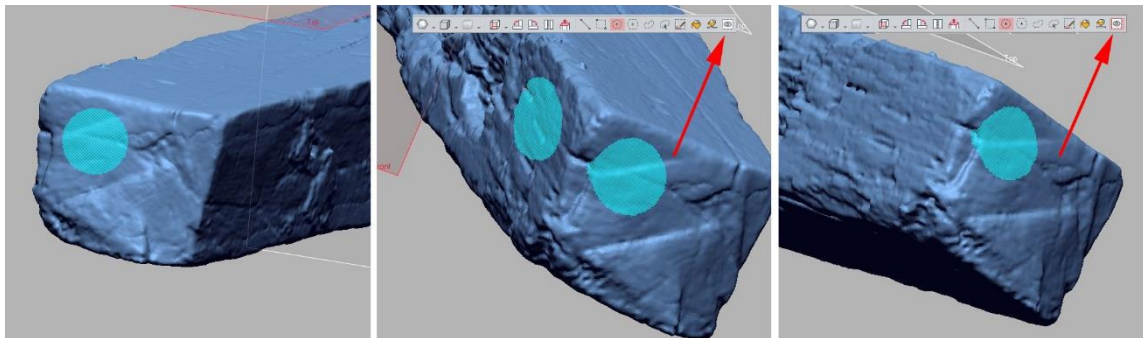


Figure 23: The differences when using the 'Visible Only' option when selection portions of the mesh. Image by the author.

variety of standard selection tools like square, circle, and lasso selectors, as well as a paint bucket tool to select large areas of adjacent data. One of the most important selection options in *Design X* or other 3-D data editing programs is the 'Visible Only' option. If the 'Visible Only' option is active, when an area of the model is selected, only the points oriented toward the screen are selected. If the 'Visible Only' option is not active, then when an area is selected, everything in the area specified, regardless of how far away it is from the selected surface is selected. Figure 23 shows the difference.

Once all of the obvious noise was removed, the data needed to be run through a ‘noisy cluster’ removal tool to remove any noise that was too minute to easily discern. A noisy cluster is a group of points that is not attached to the main body of the scan. The number of points that constitutes a noisy cluster is specified by the user, and for the

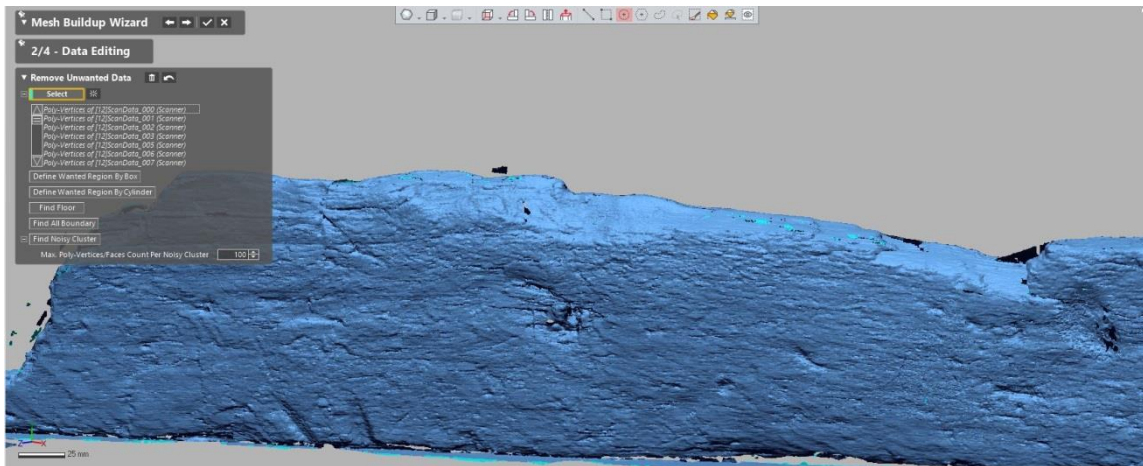


Figure 24: Noisy cluster selection (the light blue areas were noisy clusters). Image by the author.

WTC project, 100 was chosen. This meant that when the model was analyzed with the ‘Noisy Cluster’ tool, any group of points with 100 or fewer points that was not connected to the rest of the model was selected and then subsequently deleted. A major source of noisy data from these timbers was the refraction of the laser light from the LLP due to the presence of water at the surface of the timbers.

Continuing on with the forward arrow in the Mesh Buildup Wizard, the next two stages after data editing deal with alignment. Both of these stages can be bypassed for this stage of data processing, because as previously stated, the data is pre-aligned. The final step in the Mesh Buildup Wizard is Data Merging, which is the stage in which the point cloud is converted into a mesh by using the individual points as vertices to create a network of adjacent triangles. During this process, there are several options that can be selected that will affect the size of the model, the accuracy of the mesh, and the automatic data correction that is done. The settings used for the WTC ship project can be

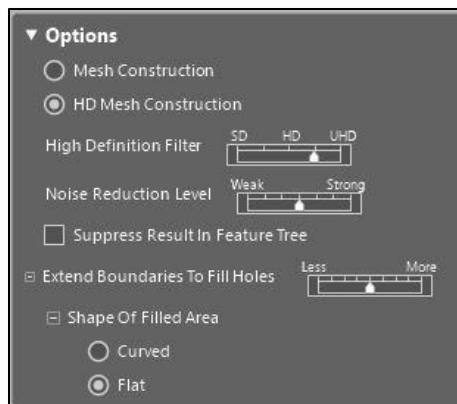


Figure 25: Mesh Buildup Wizard Data Merging settings used in *Design X*. Image by the author.

seen in Figure 25. Of the options for the mesh construction, the ‘HD Mesh Construction’ was selected to adhere as closely as possible to the geometry obtained in the point cloud. For the high-definition filter, the setting was selected to be one less than the maximum resolution. Though it might initially seem counter-intuitive, using a slightly-lower resolution mesh setting resulted in utilizing more of the primary point data than the highest resolution settings would have. Much like the settings of the LLP, the

meshing sequence also has thresholds for ‘noise’ that must be met if the data is to be retained. If the LLP settings are configured to retain data under a certain limit but the mesh settings consider that limit too loose, that data is classified as noise and the meshed model will discard the original point cloud data that does not meet its meshing standards. Through trial and error, (and with the guidance of the instructor of the *Design X* workshop the author attended in September of 2015), the mesh settings seen in Figure 25 were used for the meshing of the individual point clouds and again for the merging of the individual meshes into a complete model.

Figure 26 shows the original point cloud for the floor timber FN FS 14-0 compared to the UHD model made with no noise reduction vs. the second highest HD to UHD setting and moderate noise reduction and moderate boundary extension. The higher-resolution model does indeed show more detail in the areas where the data was dense enough to meet the noise threshold for the UHD setting, but for the purposes of the WTC ship project timber documentation, the slightly-lower resolution model was perfectly acceptable and proved to be the best compromise between the quality of the model and file size. Once the scans of each side were individually meshed, they needed to be aligned to one another and merged into a single mesh model of that timber.

To align and merge the different sides of the timber, the mesh of the first side was opened in *Design X*, and then the mesh for the second side (or third, etc) added by importing it. (Home -> Import -> Import Only). Much like during the scanning process, the program prompts ‘Do you want to run Mesh Buildup Wizard’. Despite the fact that this is the process by which the two sides were merged, it is recommended to not run the wizard until the import was complete; it was found that if run when prompted, there was a high incidence of the program freezing or crashing. Once both files are loaded, the

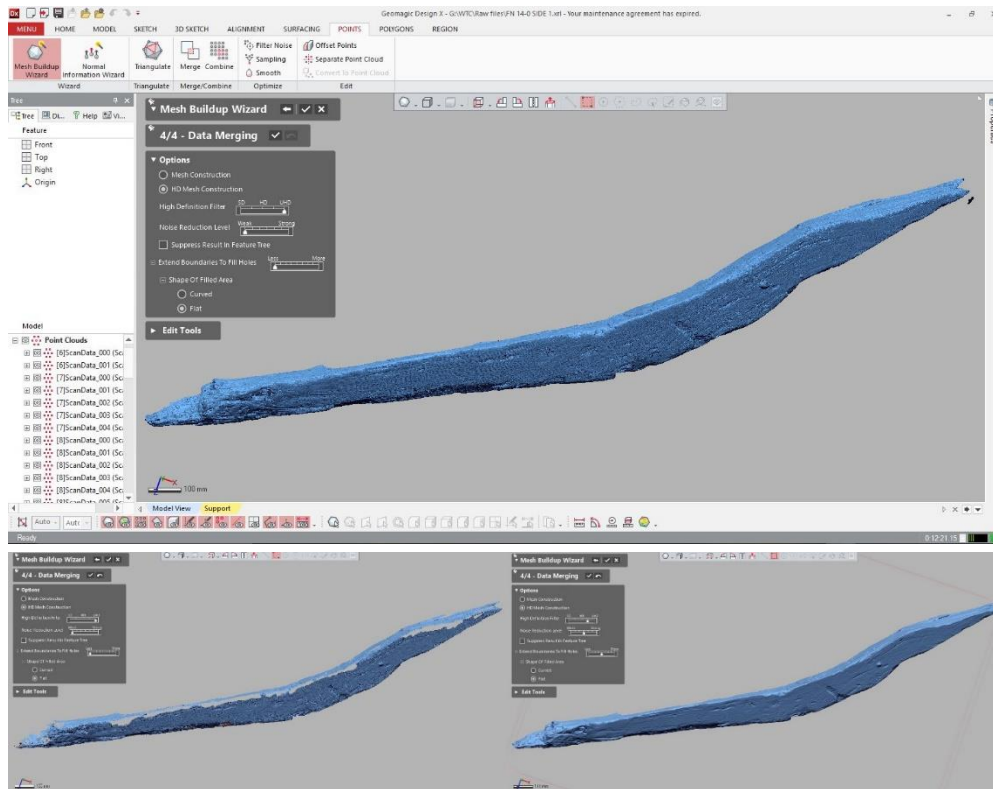


Figure 26: The unaltered point cloud (top), compared to the UHD version of mesh with no noise reduction and no gap filling (bottom left) vs HD version with moderate noise reduction and gap filling (bottom right). Notice the holes around the edges on the UHD mesh. Image by the author.

Mesh Buildup Wizard was selected to align and merge the scans. The stages for the Mesh Buildup Wizard are mostly similar when dealing with two meshes instead of a point cloud, but since the data is in mesh form, instead of selecting the mesh buildup wizard in the POINTS tab, it is selected in the POLYGONS tab.

The major difference between running the wizard on the two meshes versus the point cloud is that the data was no longer aligned; in order to align the two scans, the box that says ‘Data is Aligned, skip the editing stage’ needed to be unchecked. After this was

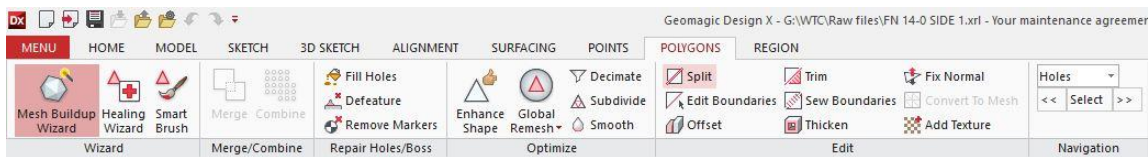


Figure 27: Under the POLYGONS tab, select Mesh Buildup Wizard to align two mesh halves. Image by the author.

done, the steps that follow were mostly the same as with the point cloud, except for the addition of the alignment of the two meshes, and the fact that the data editing stage is no longer necessary. The second stage of the wizard prompts for data editing just like it does when meshing the point cloud, but with that having been done in the point cloud stage, it was skipped. The third step is pre-alignment of the meshes, and to accomplish this there are two main options, either to go through and manually arrange the scans, or let the computer try and figure out how to automatically arrange it. The prospect of automatic alignment is tantalizing to anyone that has spent significant time in other software suites aligning scan data, but it was found to be too slow and error prone to be of any real use to this project. The manual alignment in *Design X* is substantially easier

and more streamlined to use than it was in the previous Geomagic reverse-engineering program *Studio*, and the process only takes a few minutes. Direct interaction for a few minutes is more work than the setting-and-forgetting approach that could be done with automatic alignment, but without an unlimited amount of computing resources, the time it took to automatically align these very complex models tied up a work station for too long (often upwards of an hour), and on top of that the results were only acceptable about 75% of the time. Manual alignment ensured accurate alignment quickly, and the human involvement precluded subtle errors that might have gone unnoticed otherwise by the software.

The manual alignment process consists of finding the same exact points in the overlapping sections of the two scans, and placing a pin on those points so the software knows that they are the same. To do this, both scans were loaded and arranged so that they are in exactly the same position (Figure 28). The overlapping sections were zoomed

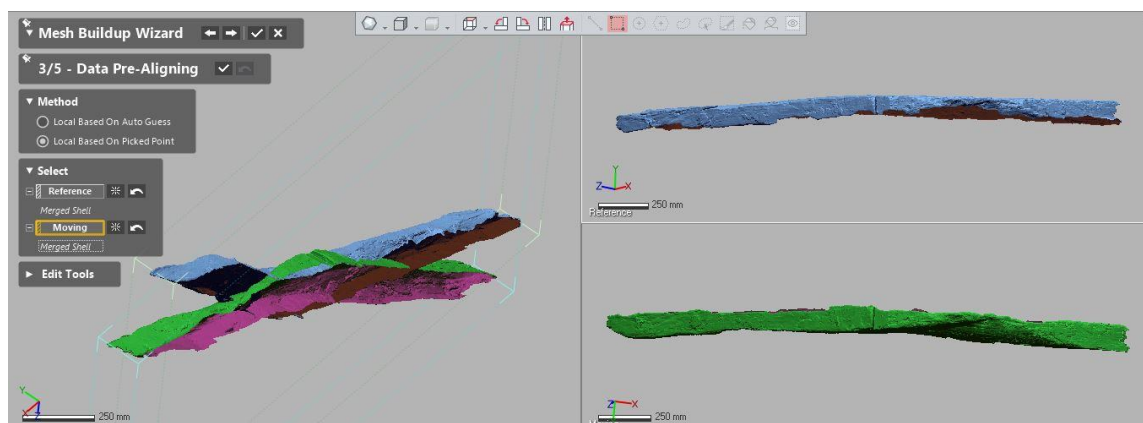


Figure 28: Arranging the two scans for alignment. Image by the author.

in on, a unique point common to both scans was identified, and a pin was dropped in exactly the same position by left clicking on the point. As pins are added, the software refined the alignment between the scans, as seen in Figure 29. This is why it is so important that certain steps be taken during the scanning process to ensure enough overlap is present for each of the scans (see *Scanning Procedure* in this chapter for more information). With *Design X*, the software often has enough information with only four or five points selected to align the scans. As long as the manual process is aligned to

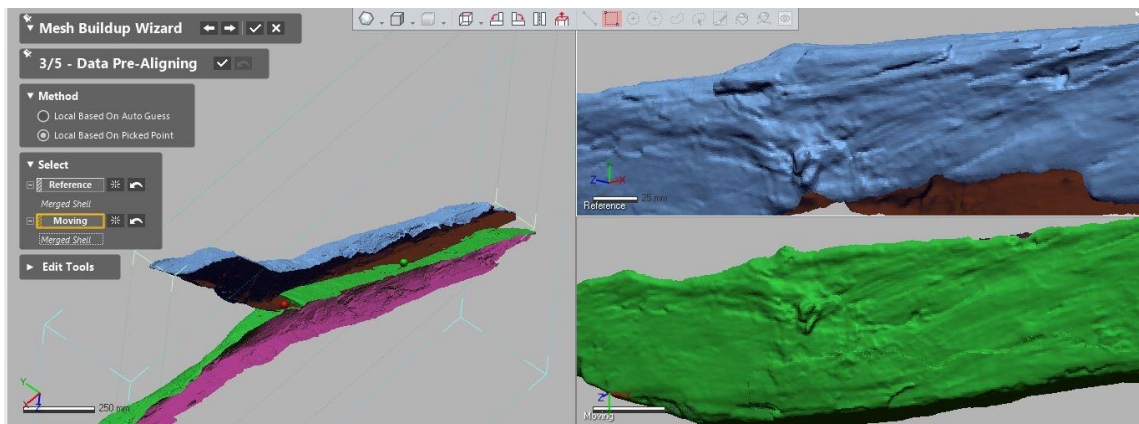


Figure 29: As pins are dropped on the same point in the overlapped section of each scan, the software will begin to align the two meshes. Image by the author.

within a centimeter or two, the next step in the alignment process will correct minor mismatches.

Before moving on to the next step, it should be mentioned that while selecting these points, it occasionally happens that the wrong area is clicked accidentally. If this problem is noticed when it happens, points can be removed by pressing ctrl-z to undo and then simply clicking the correct area. If it is not initially noticed, the points will begin to diverge on the aligned model in the left window pane. If all of the same-color

dots are not in the same area, the alignment process must be abandoned and begun fresh. When aligning between sections of a long plank that took more than two scans to capture, it was easier to align between the scans of the same wide face first for both sides, and then align between the two wide faces. This resulted in better alignment for the separate scans of each side, which in turn allowed for better alignment between the two sides.

Once enough pins were dropped to align the model to the users satisfaction, the

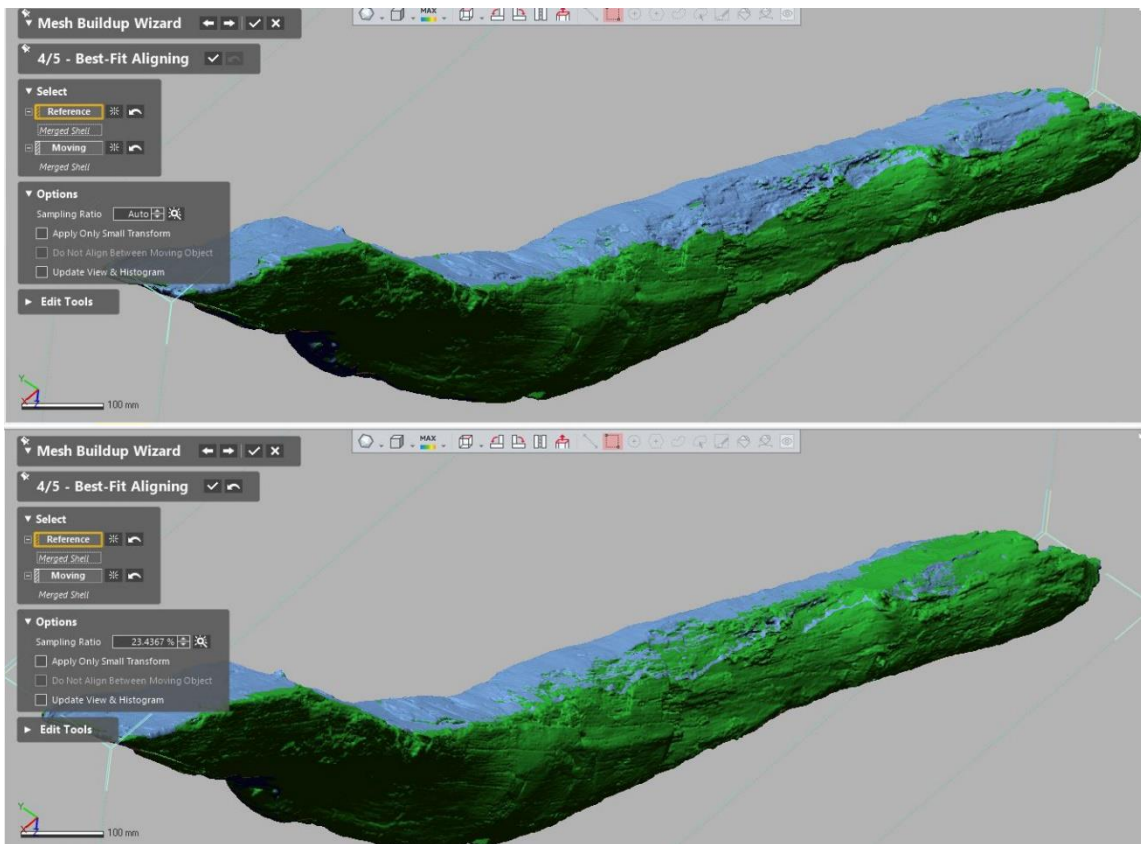


Figure 30: Manually aligned model before Best-Fit Alignment (top) and after (bottom). Note subtle change in overlap. Image by the author.

next step was an alignment refinement that is done automatically by the computer. In this process, the software analyzes the areas immediately surrounding the pins selected and looks for similarities, nudging the meshes to increase the fidelity of the alignment. The amount of mesh that the software analyzes is controlled in the options menu; for this project, the automatic setting was used, allowing the software to determine what was necessary to sample. Figure 30 shows the before and after with the automatic setting used for best-fit alignment. The ‘Best-Fit Aligning’ was used on nearly all models for this project, though on very rare occasions, it did not work correctly. When ‘Best-Fit Aligning’ resulted in unacceptable results, the manual alignment was re-done with 12-15 pins instead of the 4-5 to verify that it was correct, and ‘Best-Fit Aligning’ stage was bypassed.

Once the two scans were aligned, the final step in the Mesh Buildup Wizard was the same as it was when meshing a point cloud, but instead of meshing a point cloud, the data merging stage re-meshes the entire model to create one single unified mesh. The settings here were kept the same as before, though if too much detail was lost, the noise reduction could be reduced and the high-definition filter put all the way to UHD. The majority of the scans processed for this project were done with the same settings as the point cloud though, and the resolution of the resulting model was high enough to pick out the fastener markings necessary for virtual reconstruction. If there is any problem in the future and it is decided that the mesh is not quite to the high-definition standards for a particular task, the raw point data can always be re-meshed with higher resolution.

After the point cloud was meshed and aligned, two additional steps were taken to ensure that the meshes were uniform, watertight, and as free from errors as possible. The first step was to re-mesh the model with uniformly-sized triangles. During the meshing process, the point cloud data that is used to calculate the trigonometric vertices of the mesh is not always uniformly placed, resulting in scalene triangles. Once the mesh shape

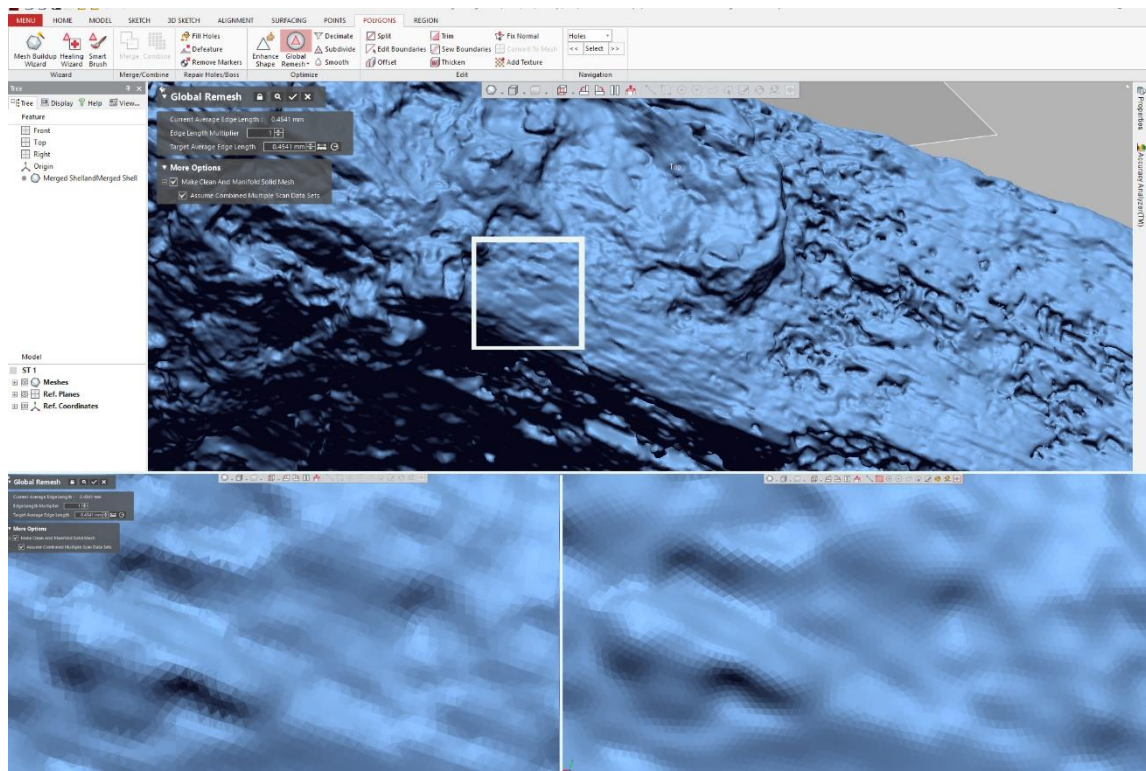


Figure 31: Global Remeshing ST1, the sternpost. The upper image shows the model, with the white square showing where the two lower zoomed in windows are focused. On the bottom left, the mesh before remeshing. On the bottom right, after remeshing. Image by the author.

is calculated, it can then be re-calculated to remove all scalene triangles, maintaining the geometric shape of the model with a more stable, less error-prone mesh (Figure 31).

In the 'Polygon' tab, the icon 'Global Remesh' was selected, which brought up the dialog box for the re-meshing process. To estimate the new triangle side lengths,

Design X analyzes the model and determines the average length, and then suggests that the model be re-meshed with that length as the new length of every side of all of the triangles in the model. This option can produce very large file sizes depending on the type of the model. For the timbers that were heavily damaged by *teredo navalis*, the complex geometry caused by hundreds of small tunnels in the wood meant that the average edge length was much smaller than needed to convey the data. In these cases, the goal side length was specified to 0.75 mm.

Once the model was remeshed with uniform side lengths, the last step in post-processing the model before export was to run the model through an error detection and repair routine, known in *Design X* as ‘Healing Wizard’. (Polygons tab -> Healing

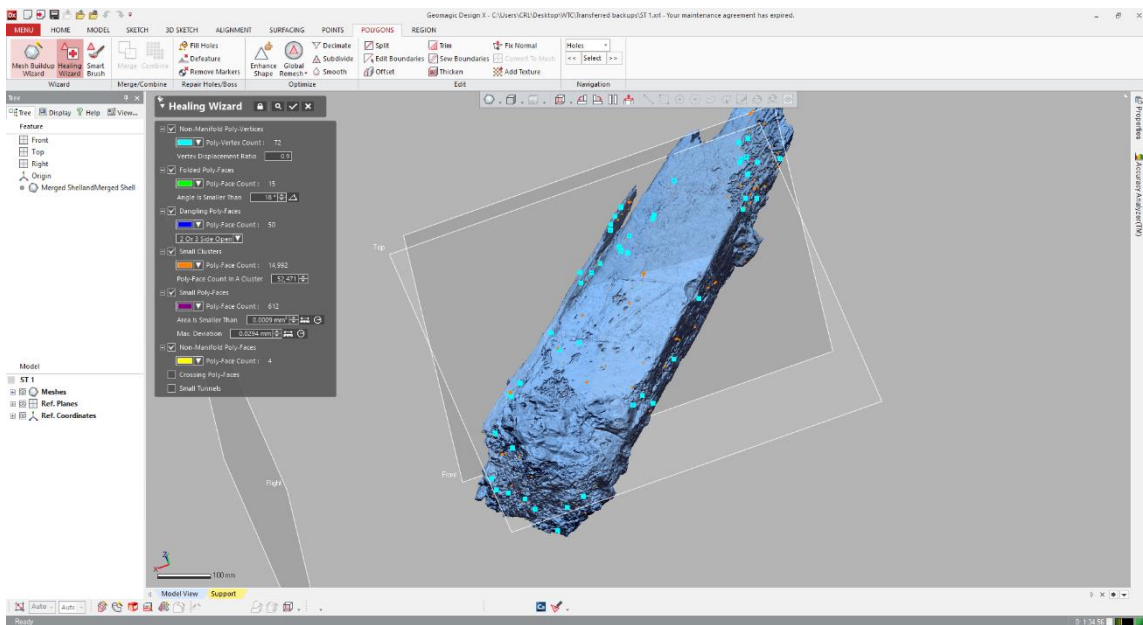


Figure 32: The mesh for ST2, the disarticulated portion of the sternpost after being analyzed by the Healing Wizard. The blue squares are all problems with the mesh that need to be corrected. Image by the author.

Wizard). The Healing Wizard analyzed the model for common mesh errors, like non-manifold poly faces or vertices, small clusters, folded, dangling, or crossing faces, and small tunnels (Figure 32). Essentially, it looks for areas of the mesh that would defy the laws of physics if they existed on the physical timber, and eliminates them. The healing wizard can be run before the Global Remesh procedure, though it is not recommended. Remeshing actually corrects a number of the problems that the Healing Wizard would have to identify and correct, so remeshing first substantially reduces the time needed to heal the model.

After all of the post-processing is complete in Design X, the models were re-saved, and then exported as a .stl file for use in *Rhinoceros 5*, the computer graphics program used to arrange the timbers for the virtual reconstruction (see Chapter V), and for use in the Z-Suite slicing software to prepare the models for 3-D printing (see Chapter VII).

Accuracy Verification

To verify that the scans accurately reproduced the dimensions of the timbers being scanned, a random sampling of timbers were selected periodically and distinct markings were identified and measured, and then the same spots were identified on the full resolution and decimated versions of the mesh for the timbers and the results compared. Ten timbers were analyzed this way of the 134 total scanned at the time of this writing. The measurements that resulted from these checks revealed an inherent weakness in this method of accuracy verification: it is practically impossible to replicate

the exact beginning and end points of the physical measurement on the 3-D model. The inability to consistently replicate the measurement results prohibited this from being an

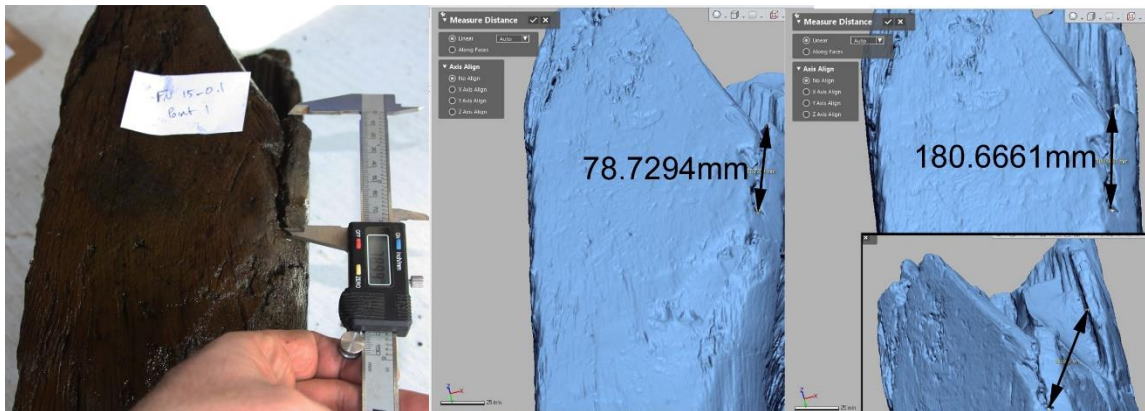


Figure 33: FN 15-0.1 measured physically and virtually. Note the arrow on the left looks like the middle arrow from the same view, but when the object is rotated it is obviously not measuring the same spots. Image by the author.

appropriately reliable method of verification. It is relatively easy to subtly adjust the location of the measurement on the 3-D model until the distance perfectly matches the physical data, ‘proving’ that the model is perfectly accurate. It is also easy to adjust the measurement in such a way that the difference between the two is too great, showing that the model is not accurate enough to be valid.

Figure 33 shows what this can look like with the measurements taken on the broken port side end of floor 15, FN 15-0.1. The image on the left is the physical timber with a pair of calipers adjusted to measure the length of a distinct crack, 78.99 mm. The image in the middle shows that same crack being measured at 78.7294 mm. A difference of 0.17 mm is well within the margin of error. (Note: darker arrows were added over the original faint arrows for visibility). The image on the right shows an arrow over the same

area, with a measured distance of 180.6661 mm. In the inset for that image it is apparent that the 180 mm measurement is across a totally different area, but the model was rotated so that the arrow lined up over the original points. The result is a measurement that seems to replicate the original distance, but with extremely different results. The ease with which these measurements can be manipulated disqualifies them from being reliable gauges by which to assess the veracity of the digital models, but careful utilization of these measurements can still be useful to the user as a feasibility check; if there is a concern that the model is not accurate, a few quick measurements can at least verify that the units are correct and the distances measured are within the ballpark, so to speak.

The companies that produce CMM arms and LLPs like FARO offer a calibration service in which they will put the scanner through a series of tests to verify that the scanner meets the technical specifications for which it was designed (FARO n.d.). As long as a scanner is within the calibration period recommended by the manufacturer, it is reasonable to assume that the resultant scans are accurate. The newness of the technology and the complexity of the data may cause some to rankle at the idea of simply accepting that the data is accurate, and frankly, that has been the position of the author as well. That said, the verification standards to which this study have adhered to for 3-D scanning with the LLP is well beyond what other methods of archaeological documentation utilize. There is no rigorous procedure by which all photographic scales and measurement tapes are verified to accurately represent the distances they should, and measurements and sketches of archaeological sites are often done by students with little

or no training. Even so, given that this is a relatively new technology, extra verification of accuracy is recommended to mitigate potential critiques. Along with using the calibration procedures that were recommended by FARO using a calibration plate, another reliable method by which to verify the accuracy of a scanner is to scan an external calibration standard. As seen in Figure 34, a pair of calipers and a ruler were scanned and the distances they were set at were measured in *Design X* for verification. The calipers on the left measured within 0.004 mm, and the ruler on the right measured within 0.083 mm, which can be accounted for by the thickness of the incised lines. It stands to reason that if these scans are well within a 0.1 mm margin of error from their admittedly non-certified standards, the scans of the timbers meet or exceed the margin of error found with every other conceivable method of documentation available today.

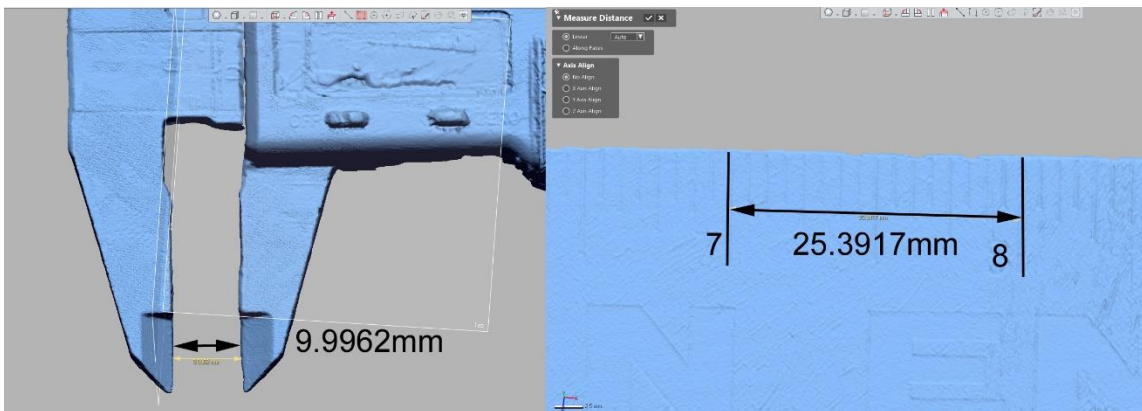


Figure 34: Verifying accuracy by scanning a pair of calipers set to 10 mm (left) and an etched steel ruler (right). Note the ruler is in inches (1 in = 25.4 mm). The arrows and measurements were emphasized in black for visibility. Image by the author.

Complications and Lessons Learned

As with any major scientific undertaking, there are a number of things that, in hindsight, would have been very helpful to know prior to beginning work. The most significant lesson learned from this project was the realistic estimation of the amount of time it took to prepare the timbers for scanning, and the amount of time that it took to post-process the raw scan data. Biological growth in the outdoor timber storage vats often took upwards of 30 minutes to clean off of the larger timbers before scanning, and with up to four large timbers scanned on a given day, this stage took up to two hours of time *per day* that was not initially considered when planning the project. When assessing the time needed to complete a project of this scale, it is advisable to run trial scans with comparable material prior to committing to a schedule, and to allow for extra time to compensate for issues like this.

Another issue that arose was the pacing between the scanning and the processing. It is tempting to simply focus on scanning for several weeks and then do all of the processing at once, and this is indeed what was done for the majority of this project. There were four computers available with *Design X* for this project, which meant that four files could be processed simultaneously, which essentially eliminated the time wasted waiting for each step to complete. One step could be started on one computer, and then the same step started on the second, then the third, and then the fourth. The time it took to initiate one step on all four computers was typically enough time for that step to process on the first computer, and so by the time that first computer was reached again in the rotation it could immediately be set to start the next step, then on to the

second computer, and so on. This meant that there was a big advantage to having a great number of raw files that needed to be processed, because a weeks' worth of scanning could be processed in just one or two days. There was a major drawback to this strategy though, which was that sometimes there were errors in the scan that were not revealed until the data was processed. Finding a timber from several weeks back that needed to be rescanned due to inadequate overlap or uneven flexing can be cumbersome. Additionally, if the same error occurred across multiple scans, it could potentially go unnoticed for weeks.

The discovery of problematic scans well after the scan date was something that became more prevalent when scanning long planks. Wooden planks are flexible, especially those that are partially degraded and waterlogged. Because these planks were twisted and warped to fit the curvature of the hull of the ship, many of them did not lay flat on the scanning table. To accommodate the bend of the wood, foam blocks were used to prop up areas that did not lay flat so as to minimize the stress on the timber.

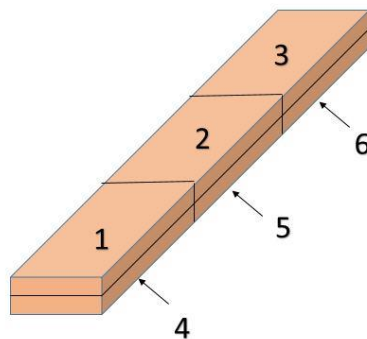


Figure 35: A guide to aligning a plank that requires six separate scans. Image by the author.

After the first side of the plank was scanned, the plank had to be flipped over so the other side could be scanned. During this repositioning, even the slightest variation in the curve recorded by the first scan meant that the scans of the two sides would not perfectly align. Because this misalignment was subtle, it would not be discovered until the final stage alignment of the separate mesh sections. To mitigate the misalignment and to minimize the amount of re-scanning needed, a shift in the post-processing procedure was done when the structural timbers were complete and the planks were scanned. The planks most susceptible to flexing were the longest ones, measuring approximately 3.5 m - 5 m. At this length, three scans of each side of the plank, for a total of six scans, were necessary to capture them in their entirety. To align the separate meshes, the three meshes of the same face (i.e. one, two, and three) were aligned first, and then the two halves were aligned. In Figure 35, scans one, two, and three were aligned, then four, five and six would be aligned, and then the two groups would be aligned to each other. For the planks that did not align properly, instead of aligning the two faces separately and then combining them, each section was aligned to the same section on the other face. For example, in Figure 35, scans one and four were aligned, then two and five, then three and six. When these pairs were aligned to each other, the areas where the sections met could be very subtly bent to provide the give needed to make the scans align.

As mentioned in the *Scanning Procedure* section of this chapter, prior to scanning, the FARO Arm needed to have the encoders in each articulated joint referenced by walking the arm through its full range of motion. Once all of the encoders were referenced, the arm was ready to scan. In some cases, if undue stress was placed on

a particular joint due to the position of the arm, a warning dialog box would appear and indicate which reference encoder was being stressed. The dialog box does not go away until the stress is alleviated, and while the dialog box is present, all signals from the LLP are interrupted.

In mid-July of 2016, at the height of the scanning process, the FARO Arm began to produce the over-stress reference encoder warnings for the rotational joint at the base of the arm when there was clearly no stress on the joint. The warning could only be cleared by rotating the arm to certain seemingly-random positions. Even when cleared, the scanning could only continue within a limited range of motion, because extending beyond that range would trigger the warning again. FARO technical support was contacted via phone, and they suggested that since the arm was being used in an environment that could potentially contain dust or other airborne contaminants, it might help to spray compressed air into the joint to try and dislodge whatever contaminate might be causing the issue. Through the rest of July and into August these errors persisted, despite the dozen cans of compressed air that were emptied into the joint in an attempt to fix it. By September, the error was happening with much more regularity, slowing progress significantly and limiting the range of the arm to a roughly 35° arc where it could function without error.

In October of 2016, the reference encoder error was no longer able to be cleared. In an attempt to ensure it was not simply a loose wire or something otherwise obviously out of place before spending upwards of \$5000.00 to have it repaired by FARO, the circuitry housing around the base of the arm was disassembled to troubleshoot. Of all of

the obvious things that could have been easily identified, none could have been more surprising than what *was* discovered: a colony of hundreds of ants (Figure 36). Tawny crazy ants, or *Nylanderia fulva*, a recent invasive species to Texas and other gulf states, had found the circuit housing to be an ideal place to make a nest. Since the mid-2000's, these ants have become notorious in Texas for their tendency to nest in electronics and cause damage.

Tawny crazy ants originate from Argentina, Paraguay and Brazil, and have managed to successfully establish themselves in Texas despite the presence of another invasive species that typically drives out other ant types, the fire ant (*Solenopsis invicta*) (Lebrun, Jones and Gilbert 2014, 1014). Crazy ants excrete an unusual type of formic acid that neutralizes the venom of the fire ants. It is not yet fully understood how exactly



Figure 36: Crazy ant infestation of the FARO Arm circuitry housing. Image by the author.

the ants damage electrical equipment, but the acidic excretion is certainly a possibility. Even so, despite the glaring fact that the FARO Arm was not designed to host a colony of ants, it is possible that they were not the cause of the failure of the reference encoder. There is no way of knowing how long the ants had taken up residence in the arm prior to discovery, and because the arm was already seven years old at the time of the scanning, it is a possibility that the reference encoder might have simply broken down from wear. An insect infestation in the scanning equipment is not something that the CRL personnel would have likely anticipated, but as a precaution and best practice for future scanning projects at the CRL or elsewhere, ensuring that a clean and insect-free work area is maintained around the scanning equipment is highly recommended.

Another unforeseen issue that was encountered during the WTC ship timber scanning was the interference caused by excessive ambient light in the work area. The reflection and refraction of light caused by the standing water on the surface of the wood has been previously mentioned to contribute to errant data points known as noise, and this noise is exaggerated in environments where there is bright light. When sunlight coming through the CRL windows was shining directly on a portion of the wood, the automatic exposure sensor in the LLP struggled to pick up the brighter sections of the wood surface. To minimize the glare that came through the windows, the work space for this project was rigged with tarps and cardboard to cover the windows, and the scanning table was rearranged at different parts of the day to avoid the sun. After the new FARO Arm was purchased and the scanning area relocated, the new room was outfitted with

blinds on the windows and cardboard was taped over areas where the blinds failed to block out the sunlight.

Another lesson learned in the course of this project was the importance of developing a standard method for identifying which timbers had already been scanned. As mentioned in the first section of this chapter, an initial sampling of 15 small timbers were scanned to develop and refine the scanning procedure, and after each of these small timbers were scanned, they were stored in a separate vat to prevent confusion about which timbers had already been scanned. This was a perfect solution until the time came to scan the larger timbers like the floors and the first futtocks. At the time they were scanned, there were no empty vats large enough to store these timbers, and so a method of easily identifying the scanned timbers was needed. Initially, it was thought that if the paper ID tags from the field were removed, that would serve as a good enough identification of a timber that had been scanned. This was quickly determined to be a terrible idea, as it required a full inspection of each timber to ensure that there was no small paper tag. Additionally, during the initial inventory of the timbers by the CRL staff, some of the paper tags fell off or were discarded, making this method of distinction as unreliable as it was time consuming.

The method that was eventually adopted was the use of neon-orange flagging tape. For large timbers, both ends of the timber were wrapped in flagging tape and tied, making quick visual distinction easy, even in overcast days. Later in the process more vats were constructed or re-purposed for this project and the scanned timbers were all transferred to separate vats. While being transferred, it was observed that the flagging

tape that had been in the original storage vat for more than three months was almost completely devoid of its original color, and was starting to deteriorate. For this reason, flagging tape can only be recommended for short-term identification. Having designated vats ready to store scanned timbers is recommended for any future projects.

CHAPTER IV

VIRTUAL RECONSTRUCTION

Once the timbers were scanned and processed, the meshed models were virtually assembled in *Rhinoceros 5*, a computer graphics program that allows the individual models to be imported and arranged based on the archaeological evidence. This ‘virtual reconstruction’ allowed the component timbers of the ship to be put back together for study without the constraints of gravity or friction, and allowed for feasibility testing for the different arrangement of the timbers.

Mechanics

Rhinoceros 5 is a 3-D, nurbs-based computer graphics modeling suite produced by McNeel and Associates. This program was chosen because of its ubiquity in the nautical archaeological community, its accessible price point, and ease of use. It should be noted that making 3-D models with nurbs modelling is fundamentally different than polygonal mesh modelling. Whereas polygonal mesh modelling utilizes small triangles to convey the shape of the object, nurbs models use mathematically-derived curves to define the shape of an object. The benefit of these curves is that they are immune to pixilation when zoomed in on, but this benefit is not necessarily helpful for the recording of archaeological material. Mathematically-calculated curves cannot accurately capture the same level of detail in the irregularities and flaws of natural materials that a mesh can.

The major 3-D-modeling suites like Autodesk *Inventor*, *Solidworks*, Geomagic *Design X*, and *Rhinoceros 5* all use mutually-exclusive proprietary file formats for the models generated in each program. Because of the difficulty that this lack of compatibility brings, there are a number of formats that are readable across platforms, such as .stl, .obj, and .ply. For the meshes obtained in *Design X*, it was necessary to convert from the native .xrl format to a more universal format, in this case .stl. The .stl format is compatible with both *Rhinoceros 5* and the Zortrax 3-D printer software *Z-Suite*. When converting from one file format to another, it is common for small errors to be generated in the model, such as triangles that overlap or intersect each other, small holes, etc (McHenry and Bajcsy 2008, 16). To account for this, the exported .stl models were opened in Geomagic *Studio* and run through the diagnostic and repair routine.

The average file size of a WTC ship timber .stl model was 300 to 400MB, and the average triangle count for the meshes was 2-3 million. These models were very high resolution, which is excellent for studying the diagnostic features of the timber, but the file size and triangle count meant that they were very resource intensive for manipulation in *Rhinoceros 5*. To mitigate the impact of the file size, each model was run through a decimation routine, where the triangle count of the mesh is lowered by increasing the length of the triangle sides, all while maintaining the shape and measurements of the model. Through a series of trial-and-error experiments, it was determined that after reducing the mesh to 2-3 thousand triangles, or about 10% of the original triangle count, sufficient surface detail remained for the purposes of reconstruction while allowing the software to handle the manipulation of the models without too much lag.

Once the .stl file decimated, it was imported to *Rhinoceros 5* via the File -> Import command. Each file was imported to whatever X,Y,Z coordinates were already associated with the model. In each case, the X,Y,Z coordinates varied slightly based on the position of the timber to the FARO Arm, but they all imported to roughly the same area around the 0,0,0 coordinate. Immediately upon import, it was important to name the mesh and to organize it. The organizational scheme for *Rhinoceros 5* is a layer system that allows certain meshes to be arranged in groups and sub-groups. The main layer groups created for this project were based on the type of timber, i.e. floor, futtock, ceiling planking, etc. Each individual timber was then given its own unique sublayer. After renaming the imported file to its appropriate name, it was then assigned to its appropriate layer.

The layer system of mesh organization is important for the mechanics of the virtual reconstruction. Even with the meshes decimated to 10% of their original size, when all of the meshes were displayed at the same time, *Rhinoceros 5* operated slowly, making adjustments difficult because of the lag between user input and the reaction on the screen. One of the features of the layer system is the ability to turn layers and sub-layers on and off. Turning a layer or sub layer off helps the program run faster, and it is also useful for clearing up the visibility when arranging timbers. Along with the ability to hide certain timbers, the layer system also allows timber meshes to be locked. This prevents selection and accidental movement of a timber.

Arrangement Methodology

The first timber model arranged in *Rhinoceros 5* was the keel. As mentioned in Chapter II, the keel is the backbone of the ship, and was certainly the first timber laid down during the original construction of the ship (Goldenberg 1976, 88). During the excavation, the keel was snapped into thirds by drilling two 2.5 cm holes through it in

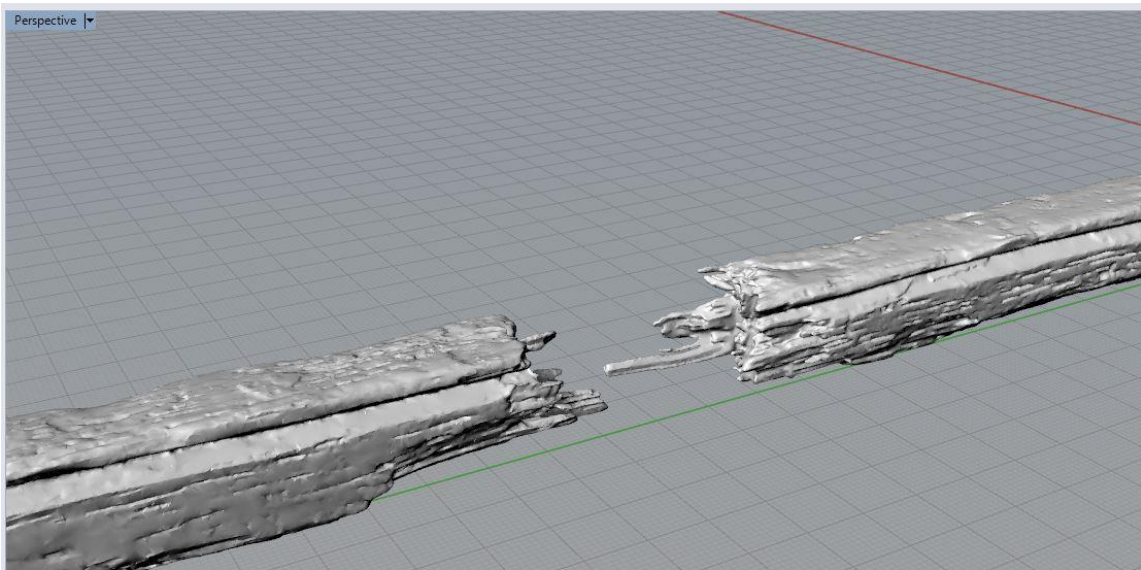


Figure 37: Damaged ends of the keel. Image by Author.

two places, then holding down one side with a backhoe bucket and pulling up the other side with a strap attached to a crane. The reason the keel was broken into three pieces was to allow for easier transport and storage. As an aside, it is the opinion of the author that if the keel could be transported intact in the 18th century, it could have been done in 2010. Moreover, the adage that it is better to break waterlogged wood than to cut it is not applicable to reasonably-sound waterlogged wood. The keel, which is made of hickory, did not snap cleanly when it was broken, and the fibrous broken ends made physical and

virtual re-assembly very difficult (AKRF Inc. 2013, S-2) (Figure 38Figure 37). If the funding is not available to keep longer timbers in one piece, they would be better served being cut at an angle than snapped.

The three separate models of the pieces of the keel were imported and aligned to one another based on similarities in shape, the grain of the wood, and the drill holes (Figure 38). Once they were perfectly aligned, all three pieces were selected and then grouped to act as a single timber. This prevented accidental misalignment during the next phase of the reconstruction. To make it easier to place the rest of the timbers in the model, the keel was aligned vertically through the Y-axis, horizontally bisecting the X-

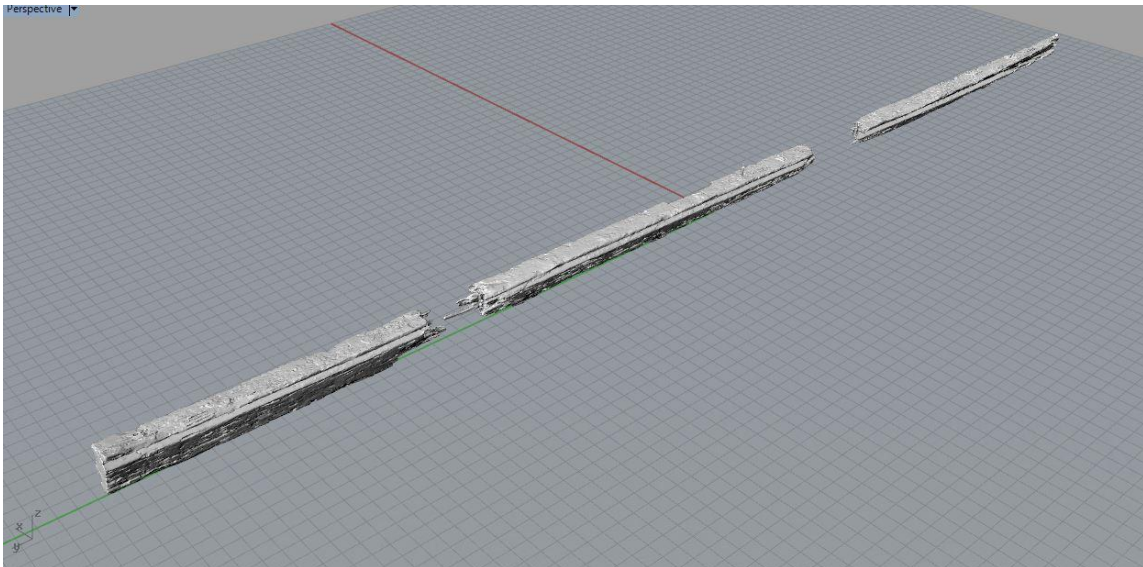


Figure 38: Aligning the keel pieces. Image by Author.

axis, and resting atop of both the X and the Y axes. This placement allowed the axis markers in *Rhinoceros 5* to act as centerline markers, which was useful for centering floors and mirroring halves of frames to check for symmetry.

After the keel was placed, the stern knee was added. The stern knee is a massive single block of wood that acts as the main structural component for the stern of the ship,

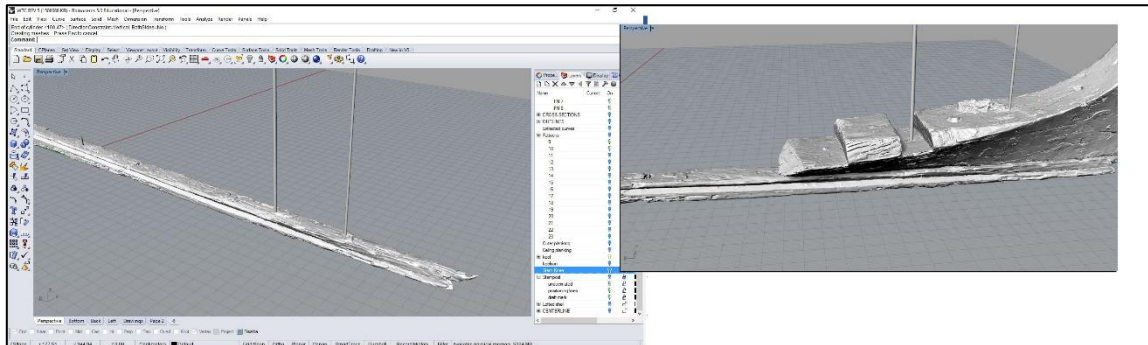


Figure 39: Aligning the stern knee. Image by author.

and was fixed directly to the keel and the sternpost. The width of the base of the stern knee tapers in the same way the keel does, so it was simple enough to place it. After the knee was roughly in line with the keel, cylinders were created to simulate the spikes that would have fastened the original two pieces, and the stern knee was nudged into place to match up the corresponding marks (Figure 39).

Once the stern knee was aligned, the two pieces of the stern post were added. Though the original construction sequence would have likely added the stern post first, it was not practical to follow that sequence here for two reasons. First, the section of the keel that was mortised to accept the stern post was destroyed during the excavation process, and so a precise placement would have been impossible without the stern knee in place. Second, the forward face of the stern post is not perpendicular to the top of the keel, and determining the exact angle is much more difficult without the stern knee in

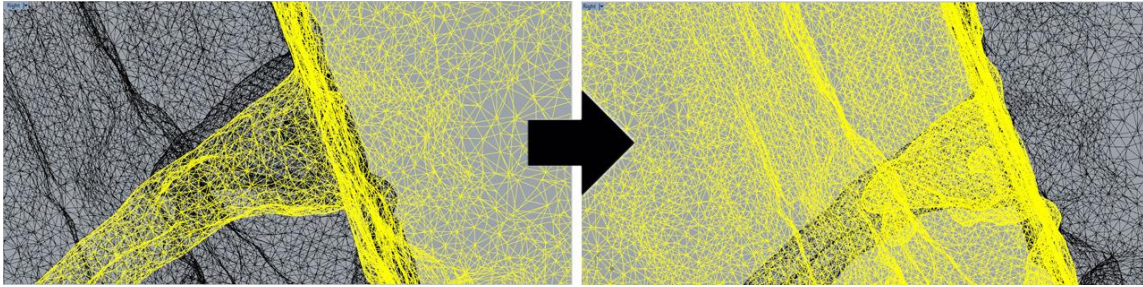


Figure 40: Positioning ST-1, the lower portion of the stern post to the stern knee by aligning the fasteners. Image by the author.

place. Of the two pieces of stern post that were excavated, only the lower piece (ST-1) was *in situ* and still fastened to the keel and the stern knee. The second piece (ST-2) was found disarticulated, and its placement in the model was not determined until the lower portion was placed. Positioning ST-1 in relation to the stern knee was particularly easy, because the fastener positions were so prominent. With the aft face of the stern knee lined up to meet the forward face of the stern post at the appropriate angle (measured in Rhinoceros, 112° from the top face of the keel), the model was viewed in mesh mode to allow for transparency through the surface, and the surviving bolt on the knee was easily lined up with its hole on the stern post, even though the scanner could not reach all the way to the end of the hole (Figure 40).

Once the lower portion was in place, the upper piece was aligned based on the geometry of both pieces. The molded dimensions of ST-1 tapered as it moved from the keel towards the deck. Starting from the top of the keel, three lines were drawn along ST-1, one on the forward face, one on the aft face, and one along the corner of the rabbet. These lines were drawn so as to follow the lines of the timber and extend beyond

it, creating a virtual template showing the extent of the taper. Once these lines were in place, orienting ST-2 was merely a matter of finding where it would best fit in that virtual template, as seen in Figure 41.

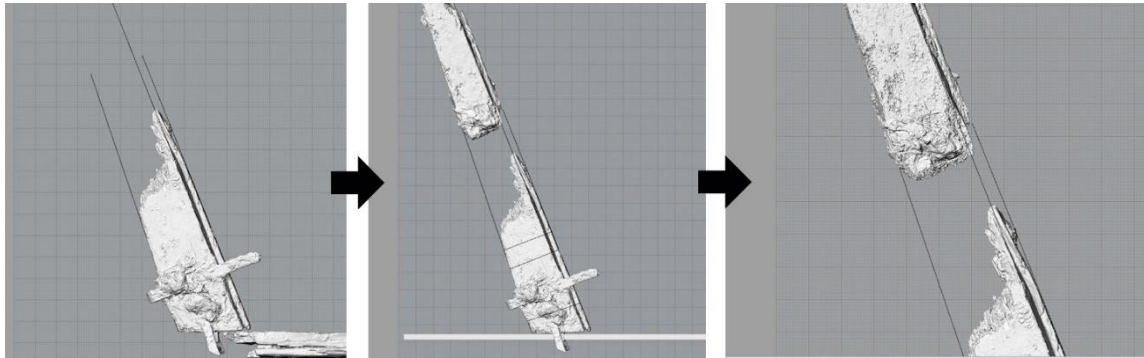


Figure 41: Positioning the disarticulated portion of the sternpost

Carved into the side of ST-2 was the Roman numeral V, indicating the 5 ft (1.52 m) draft marking (Figure 42). The bottom of the V, (marked by a horizontal line in Figure 42) must have been the point where the draft was measured, because at a depth greater than 5 ft, the top of the V would have been submerged and obscured from view. Therefore, to verify the accuracy of the placement of the ST-2, once it was aligned to the

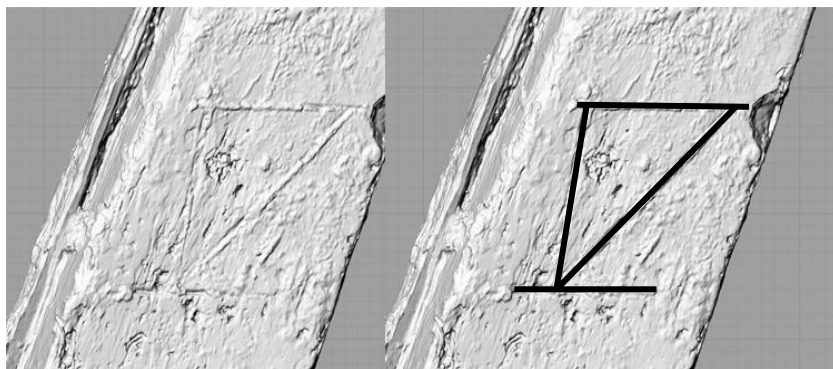


Figure 42: Five foot draft marking on the sternpost. Image by the author.

lines extrapolated from ST-1, the distance from the bottom of the V to the rabbet of the keel was measured, and was found to be 155cm, or 5.0853ft.

After the stern post pieces were in place, the floors were added to the model. The placement of the floors along the keel were arranged based on the location of the fastener markings, much like how the stern knee and ST-1 were arranged. To make the location of the fasteners easier to identify while trying to arrange the floors, rectangular prisms were created that passed through the keel at the location of the spikes from a top-down view. The prisms were simple shapes to create in *Rhinoceros 5* that could more obviously mark the location of the fasteners from a zoomed-out view of the model. The prisms were used instead of cylinders to aid in arranging the frames perpendicular to the keel. Once the floor was added to the model, the view was switched to a bottom-up view, and the floor was matched to the location of the rectangular prism. When the floor

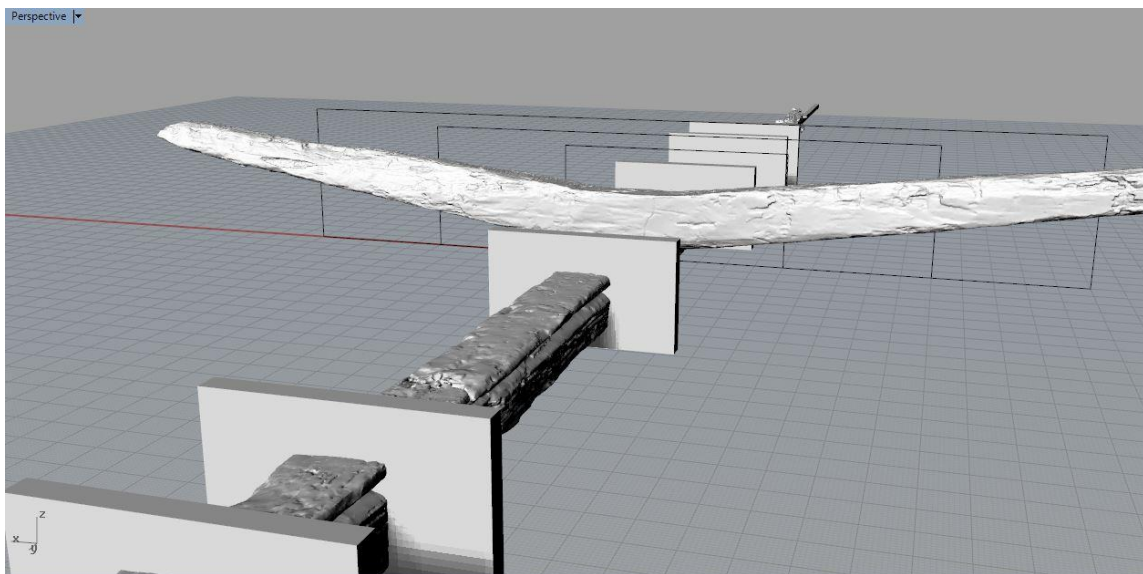


Figure 43: Rectangular prisms were placed along the keel at the fastener to aid in placing the floors. Image by the author.

was imported, the fastener hole on the base of the floor was then placed in line with the rectangular prism (Figure 43). Once the floors were arranged along the keel, they needed to be aligned along the X-axis and balanced on the keel.

To align and balance the floors, a series of rectangular wire boxes were drawn on the grid in the top and the front views of *Rhinoceros 5* respectively, and each individual floor timber was rotated along the appropriate axis until both the port and the starboard sides aligned to points on the wire boxes. For intact timbers, three points were referenced on each side by measuring out from the centerline and noting the intercept points (Figure 44). If a floor was tilted either on the X-axis or towards the port or the starboard side, it was rotated until it was balanced. The axis of rotation was always the exact area where the floor was fastened to the keel; if it were anywhere but there, the

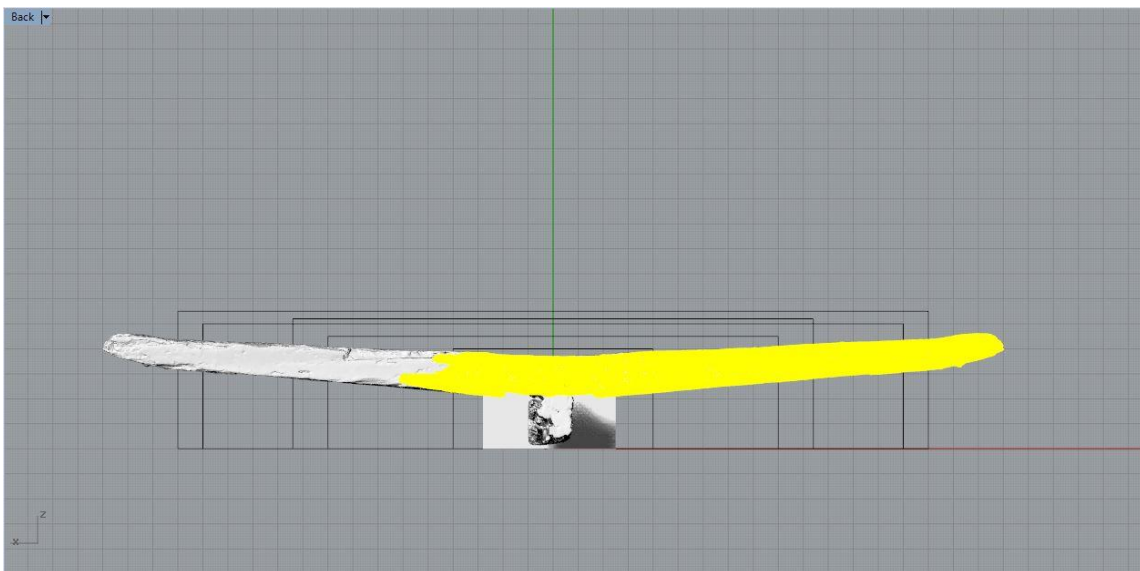


Figure 44: Balancing and mirroring a copy of incomplete floors. Image by the author.

position on the keel would be altered by the rotation. Each floor was double checked after any rotation to ensure this did not happen.

Balancing the floors using wire boxes in *Rhinoceros 5* only works if the timbers are roughly symmetrical. Several floors were either asymmetrical or only partially preserved, and balancing half of a frame by comparing the two sides is obviously impossible. In these cases, the floors were digitally halved, and then a mirrored copy was placed 180° from the original half (Figure 44).

The aft-most floor, FN FS 9-0, could not be balanced using the wire box technique, because it was bolted to the notch in the stern knee. This meant that balancing the floor took more than simply ensuring it was symmetrically balanced. It meant that the base of the floor had to completely match up with the base of the stern knee, which was a much larger and more complex surface than that of the keel. To visualize the placement of the floor, a virtual cast of the surface of the notch was created. To create

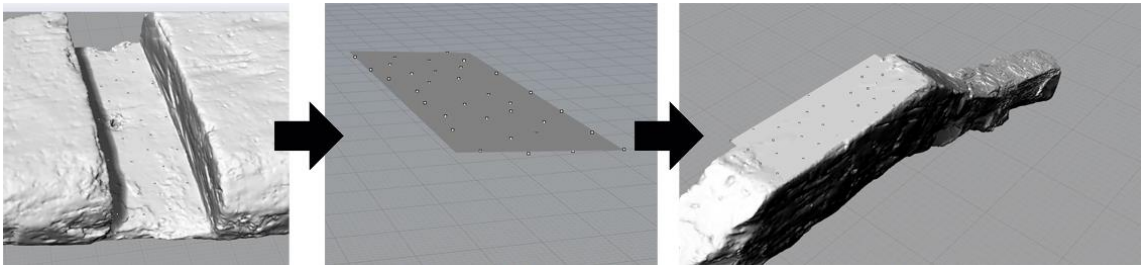


Figure 45: Positioning FN FS 9-0 on the stern knee. Image by the author.

this cast, dozens of points were placed along the surface, and then a plane was drawn through all of these points. The resultant plane mimicked the shape of the surface of the knee, so the knee could be hidden and the floor aligned to the plane (Figure 45).

Once the floors were all balanced on the keel, the futtocks were added. Based on the construction sequence outlined in Chapter II, most of the futtocks were added after the garboard and the first several rows of outer planking had been added, because the majority of the futtocks were not fixed to the floors. It was not necessary to plank up to the first futtock of the made frames in the virtual model, because the first futtocks for all frames could be positioned in ‘mid-air’. The main challenge was accurately positioning the futtocks in relation to their floors, as there were no transversal fasteners to align them.

The first two futtocks added were to frames 10 and 14. During the excavation, three futtocks were found directly abutting their corresponding floors, at frames 10, 14,

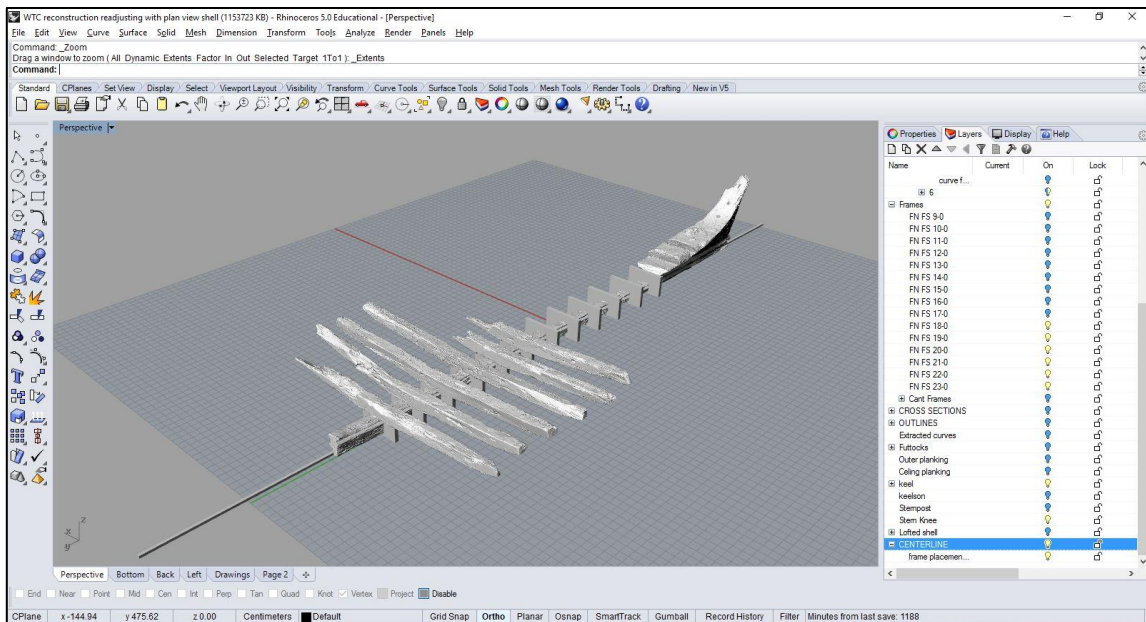


Figure 46: Placing the floors on the keel. Image by the author.

and 20 (AKRF Inc. 2013, 173). These three were theorized in the AKRF report to have been used as molds for the rest of the futtocks, though only 10 and 14 were actually fastened to the floors. X-rays of the futtocks for frame 20 confirmed that there were no transverse fasteners. After all of the floors and futtocks had been scanned, the data showed that frames 10 and 14 had the heads of the floors and the heels of the futtocks cut at a 45° angle, which meant that instead of having to drive a spike through the entire width of the floor and futtock, spikes could be driven through the narrow edge. Though frame 20 did not share this trait, it was discovered that frames 18 and 23 did. Upon closer examination, transverse fasteners were found between the floors and first futtocks for frames 18 and 23, which meant there were a total of four made frames to guide the placement for the rest of the frames. As each floor was added and balanced to the model, a series of nurbs curves were drawn along the exterior of the four made frames and faired, (substituting for the battens described in Chapter II), and the floors for the rest of the frames were checked to ensure they did not extend beyond it. This procedure was repeated for each frame until all of the floors were in place and the model position was locked by clicking the padlock icon next to the file name in *Rhinoceros 5*.

The next step in the construction sequence of the actual ship was for the outer planking to be fitted and fastened out to the floor head line. This was done because the actual ship was built under the harsh constraints of gravity, something that was not the case for the virtual reconstruction. The decision was made to install the first futtocks next on this model, for two reasons. First, because the structural timbers were all scanned before the planks were scanned, and the models were available much sooner.

Second, and more importantly, the planks were long and thin, and they were much more susceptible to distortion while scanning than the floors and futtocks. Installing the futtocks first allowed for a more precise positioning in line with the associated floor, and it gave greater guidance when installing potentially-distorted planks.

To position the first futtocks, all of the layers except for the futtock being positioned and its associated floor were turned off. This allowed for easier manipulation of the meshes, and also allowed an unobstructed view of the floor when positioning the

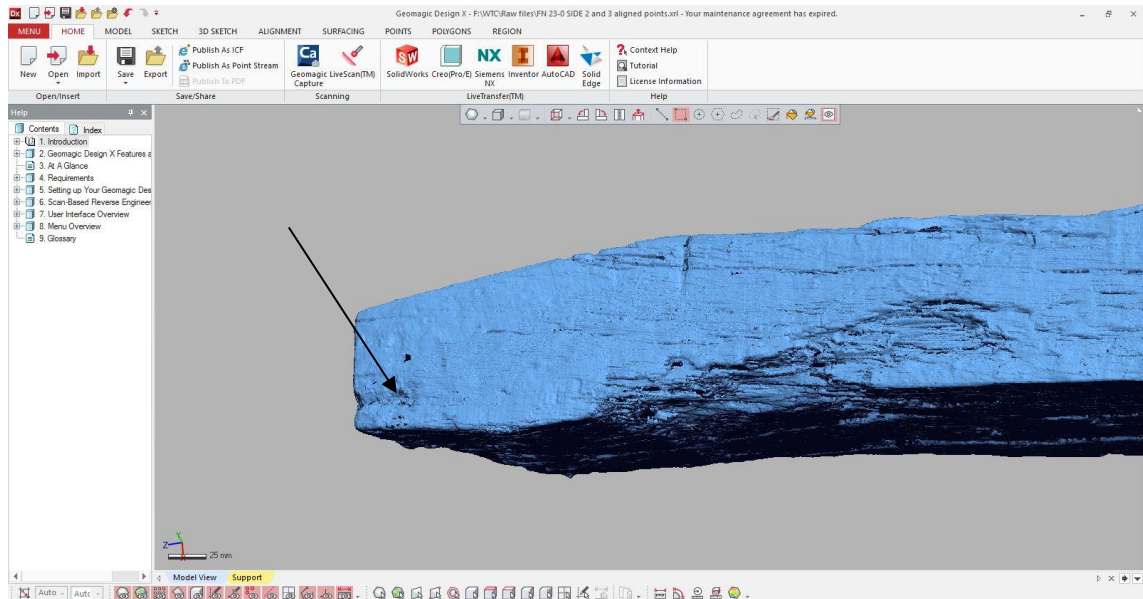


Figure 47: Aligning the master frames to the futtocks was done by aligning the fastener locations, as notated by the arrow. Image by the author.

futtock. The first futtocks added to the model were the ones for frames 10, 14, 18, and 23. They were by far the easiest to position, because the fastener holes between them and their floors were easily visible in the scans (Figure 47). Much like the method used to position the floors along the keel, a cylinder was created to represent the original

fastener through the floor, and the futtock was then dragged into position until the fastener hole on it lined up with the cylinder. Next, the futtock was rotated in the front and top views until it was aligned with the floor both forward to aft and top to bottom. The angle that these futtocks were set to was extremely important, because they determined the angles and positions of the rest of the first futtocks, which were not at consistent distances from the keel.

Once the four made frames had their first futtocks, a similar procedure was followed where a nurbs curve was run along the exterior of those four frames to create a positioning guide, similar in function to a batten. Each first futtock was then installed to match the position of the floor, and then the futtock was adjusted inboard or outboard

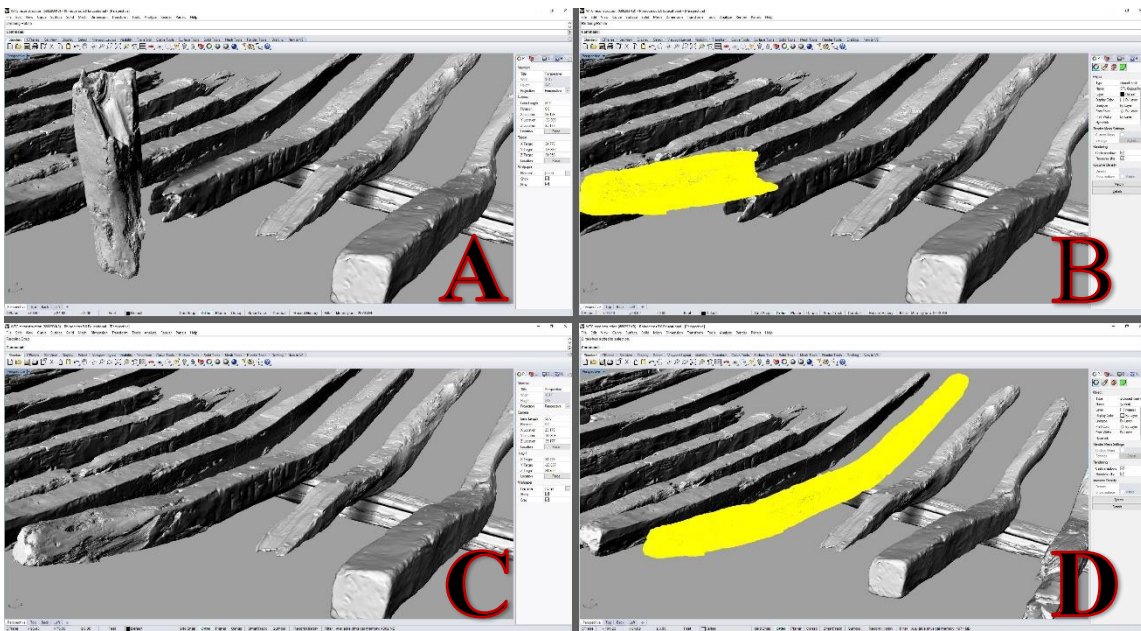


Figure 48: Repairing a timber in *Rhinoceros 5*. Step A: Importing the broken piece. Step B: Rotating the broken piece to match the position of the floor timber. Step C: Positioning the broken piece. Step D: Grouping the two pieces together. Image by the author.

until it was lined up with the positioning curve. The placement of the few extant second futtocks was less precise, because the only made frame with an associated second futtock is frame 10, which is all the way aft attached to the stern knee. This was very useful for positioning the cant half frames in the stern of the ship, but it was not particularly useful for positioning the second futtocks forward of that. Further, the ship did not survive much past the first futtock, so the placement of the second futtocks was done with the understanding that there is likely some difference in their position in the model versus their original position.

Like the keel, several of the floor timbers were broken before they arrived at the CRL, most notably frame 10 and frame 15. These breaks were either the result of site formation processes or excavation, and some of them were still intact enough to be reassembled. To ‘repair’ the models, the two parts of the broken timber were aligned until they were perfectly lined up, and then they were both selected and grouped together using the ‘Group’ command in the command prompt. This allowed the reassembled timbers to be manipulated as a single timber for the remainder of the reconstruction, though it should be noted that grouping two meshes did have some implications for printing and for creating the support structures, as discussed in Chapter VII. Figure 48 shows the steps involved with this process.

Because the planking was not yet scanned when this part of the dissertation was written, the plan for the placement of the planks on the model can be discussed, but it would be premature to outline a procedure without a trial-and-error period to refine it. Adding the planking to the model will be a very tedious operation, as many of the planks

were broken during the excavation, and there are over 100 pieces smaller than 25 cm long. The planking of the digital model will be done in tandem with the planking of the 3-D printed physical model, so that any theoretical placements can be tested in the real world for feasibility.

The order in which the planks are placed will mimic the proposed construction sequence of the actual ship. The garboard fragments will be oriented and installed first, then the next strake up, etc. The fractured pieces will not be reassembled using the procedure outlined for the keel and floors, instead, they will be aligned to their correct positions without grouping them to the other fragments. This will allow the broken pieces to act as a correction for distortions in the planking that would prevent a successful reconstruction. Once all the major planks are added, the fragments will be added based on the excavation notes and by studying the model to see where they fit.

Calculating a Lines Drawing

As stated in the Workflow Overview section of Chapter I, the eventual goal of the modeling process was to extract a set of lines drawings for the remains of the WTC ship. Lines drawings are a 2-D projection of the 3-D form of the ship, generally drawn on paper for publication. The lines represent the shape of the ship from the side view, (the sheer plan), a top-down view, (the half-breadth plan), and a cross-section view, (the body plan). These drawings represent an idealized version of a ship, perfectly symmetrical in each view, with each curve perfectly faired. Figure 49 shows an example of this: the lines for the 17th-century French light frigate *La Belle*, reconstructed by

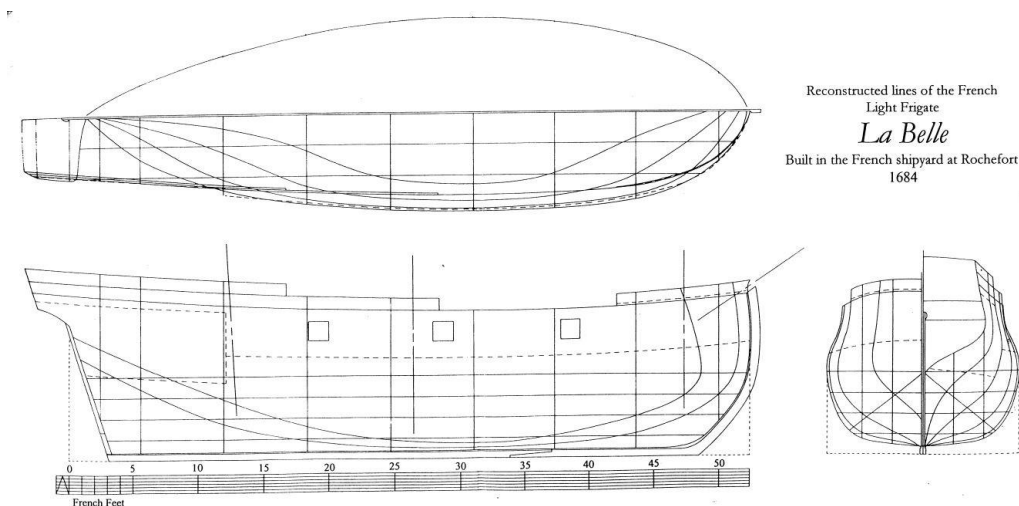


Figure 49: Lines of the French light frigate *La Belle*. Reprinted from Grieco, 2003.

master model maker Glenn Grieco (Grieco 2003, 58). The prerequisite for generating a lines drawing with the virtual model in *Rhinoceros 5* is ensuring that all of the structural timbers that can be placed with confidence are in place. It is recommended that any

timbers that are not necessary for this operation have their layers turned off to minimize the strain on the computer while trying to manipulate the entire model.

To build the lines of the WTC ship off of the 3-D model, dozens of data points needed to be derived from the outboard faces of the structural timbers. These points, once established, were aligned and then connected in the three views to establish each set of lines. To start, the 'Top' viewport was maximized, and using the line tool, a series of longitudinal lines were drawn through the length of the ship, extending beyond the forwardmost point and the aftermost point (Figure 50). The first line was drawn as

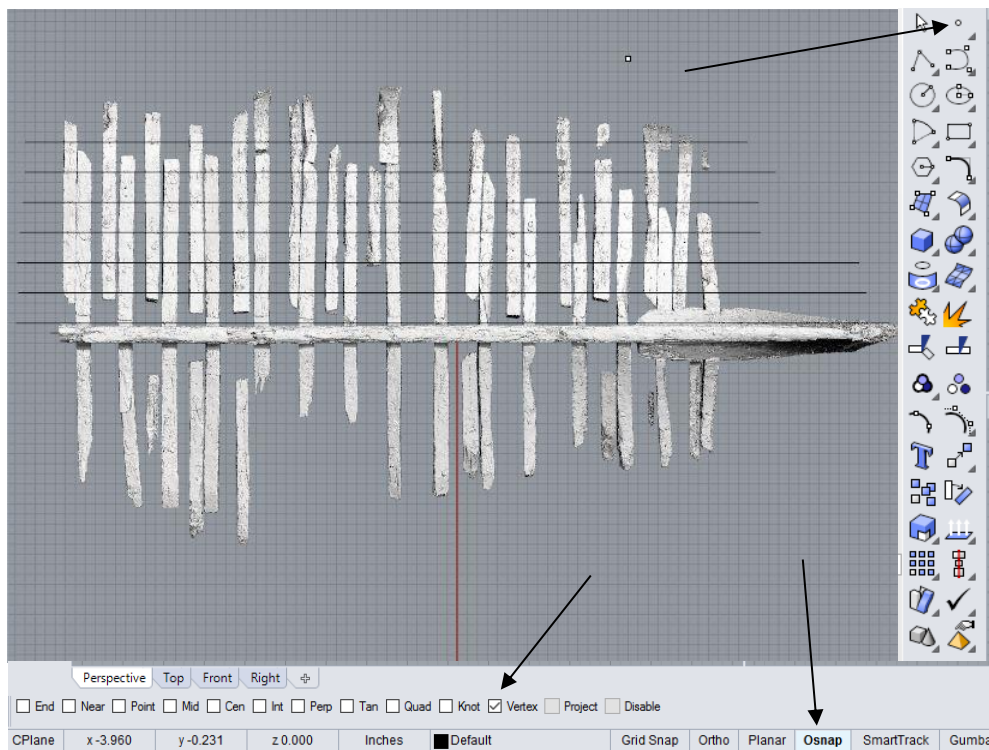


Figure 50: A series of guidelines were drawn to aid in the position of the points along the bottom of the structural timbers. The top arrow is pointing to the 'point tool', and the bottom two arrows show the 'Osnap' tool with 'Vertex' selected. Image by the author.

closely as possible to the keel, and then additional lines were added at a set distance away from the keel, as if the lines were being used to plank the ship. These lines served as a rough guide for the placement of the data points, and so they needed to be placed close enough together that the points placed along the timbers adequately represented the curve of the timber, but not so close together as to become too cluttered.

Once the guidelines were in place, a series of points were added to the outboard face of each frame where it intersected the guidelines. Adding a point is done using the point tool in the tool bar or the command 'Point', and to make it adhere to the surface of the timber instead of being placed on the default $Y=0$ point of the X -axis, the object snap feature must be used ('OSnap'), and the box next to 'Vertex' checked. This action places the point at the vertex of a mesh, which as discussed in the *Post-Processing* section of Chapter III, is what the models of the timbers were made of. Along each line, a point was placed on each floor or futtock until the port side of each frame had been assigned points along the transverse guidelines. When placing the point, there is an unfortunate flaw in *Rhinoceros 5* in which a large white text box appears next to the point whenever it comes into contact with a vertex, which often obscures the placement of the point. To work around this, the point can be placed near the line, then simply dragged into place once the text box disappears, provided the 'Ortho' option is checked. If it is not, dragging the point will reposition it to the $Y=0$ point of the X -axis.

Once all of the points were placed, they needed to be aligned to one another for use in the other viewports. Placing the points using the guidelines helped to ensure that the points were arranged in an orderly fashion in the top view, but from the front and right views, the points were disarrayed. Before continuing on to build curves with the points, each set of points needed to be precisely aligned in each view, top, right, and front. In the right viewport, each set of lines needed to be arranged to have the same Y-axis value, in the top viewport, the same X-axis value, and in the front viewport, the

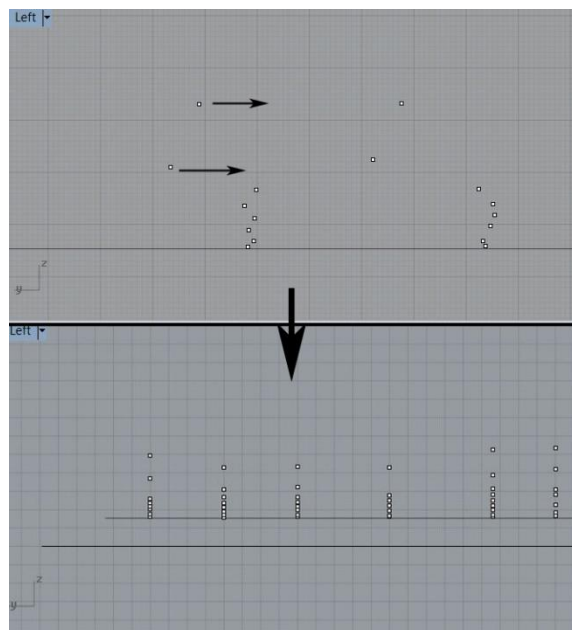


Figure 51: After the points are placed on the outboard of the frames, they need to be aligned in the Left or Right view so that they have the same Y-value. Image by the author.

same Z-axis value (Figure 51). To drag the points along one axis without resetting the other axes' values, the 'Ortho' option and the 'Grid Snap' option were both checked.

Ortho only allows the point to be moved across one axis at a time, and grid snap places the point at one of the grid intersection points, allowing for precise alignment.

Once each set of points were aligned across the three axes, they were used to build the lines (or more precisely, curves). There are a number of options for using control points to build a curve, and the best for the purpose of adhering as closely to the geometry of the points is to build the curve through the points. (Command: CurveThroughPt). The command line then asked to specify which points would be used to build the curve, and the set of points for each curve was selected. The points must be selected in either top-to-bottom order or bottom-to-top order. The command will draw a line through the points in the exact order specified, so if a point is skipped and then added out of order, the line will skip the point initially and then cross back over itself in the order it was selected.

The first set of lines derived were the buttock lines of the sheer plan. To build the buttock lines, each set of aligned points were selected in the front viewport and a curve drawn through them. Each set of lines are representative of the precise hull shape created by arranging the timber scans, and as such they will almost never reflect the ideal shape that faired lines drawings have. If there are any abnormalities in the shape of the exterior of the timbers as a result of decay, uneven wood working, or deformation over time, the lines will not have a perfectly smooth, faired appearance. Additionally, because each of the available 15 frames were used to create their own line, there were more lines created than were necessary to depict the shape of the ship. To compensate for this, each line was analyzed for redundancy and if deemed to be a suitable representation of shape, it

was faired using the 'Fair' command (Figure 52). Once faired in the sheer view, the original points used to draw the curve were moved to match the faired curve, using the 'Ortho' option and the 'Osnap' option with 'Int' selected. This only moved the point in one axis, and snapped the point to the intersection of the line when they became close to

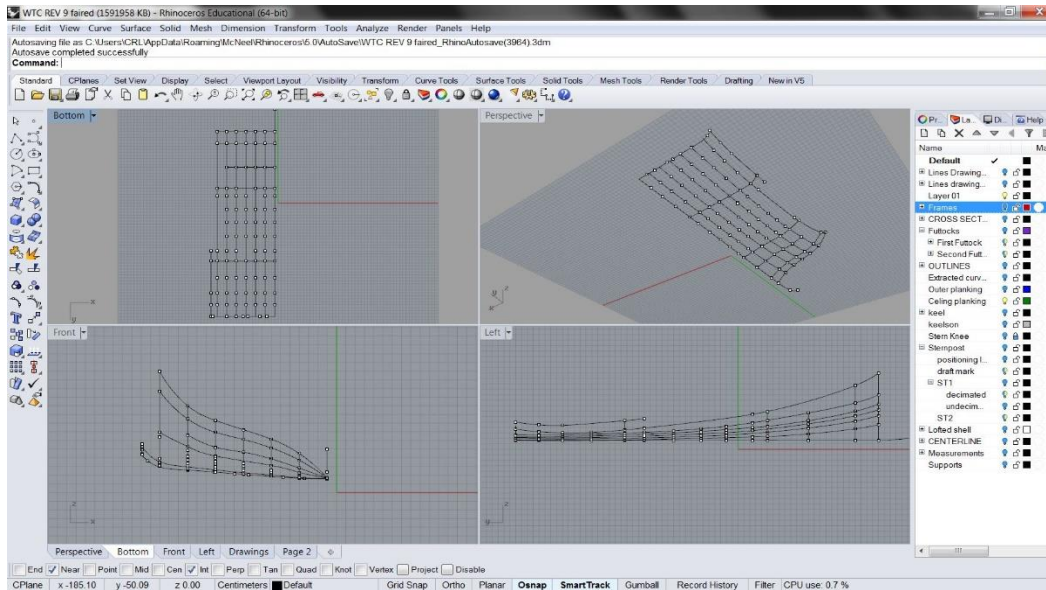


Figure 52: Each curve produced was faired using the 'Fair' command. Image by the author.

one another.

To generate the waterlines of the half-breadth plan, six fixed Z-values were chosen and a horizontal guideline was drawn across the model at those points in the front viewport, and then a separate set of points were made where the body plan lines intersected that Z-value line along the X-axis (Figure 53). To ensure that the points were being selected along the body plan lines and not the placement lines across the Z-Axis, the 'Ortho' option was used with 'Osnap' and the 'Int' option again. This allowed the point to lock onto the intersection of the guideline and the body plan lines. Once each of

the points were placed, the CurveThroughPt command was used again to build a curve along those points. Because so little of the ship survived, the top two guidelines did not provide enough information to establish a curve, so in the end only four half-breadth lines were established (Figure 54).

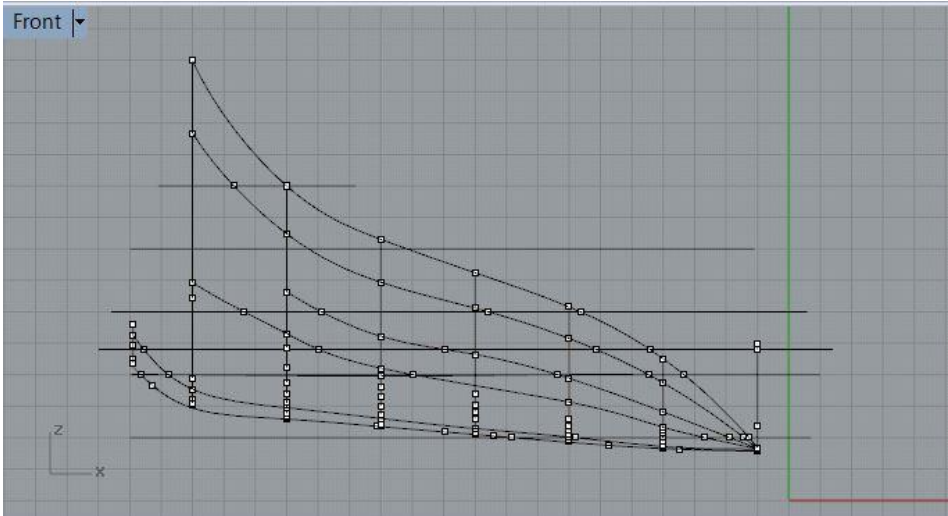


Figure 53: Horizontal waterlines were drawn, then a point placed where each waterline intersected with the body plan curve to produce the curves for the half-breadth plan. Image by the author.

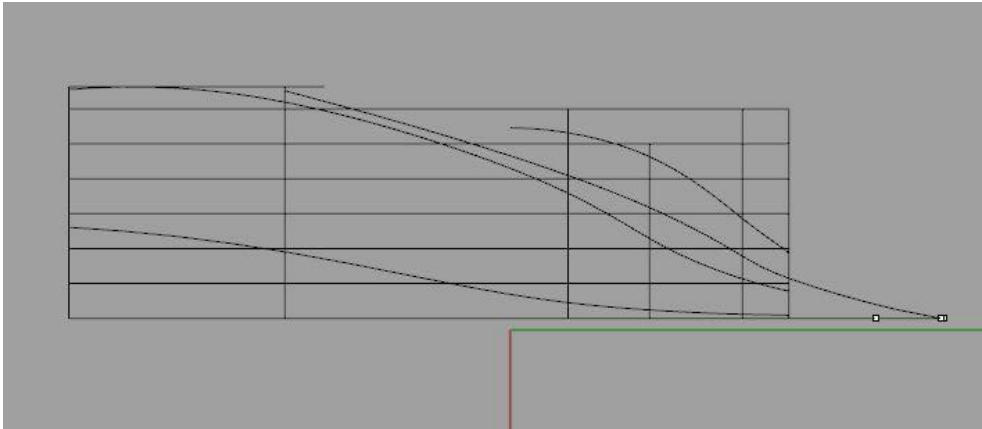


Figure 54: Half-breadth lines representing the remains of the ship. Image by the author.

The shape that the line drawings depict is for a flat-floored, beamy hull. When compared to the examples Paul Fontenoy's *The Sloops of the Hudson River*, the lines for the WTC ship show a vessel with less deadline to the floors and a harder turn of the bilge than even the beamiest Hudson River Sloops, like the 1848 *Victorine*. (Figure 55). The apparent form of the WTC ship's hull, with its low length-to-beam ratio, near-flat floors, harn bilges, full after end, and shallow draft accords with our limited knowledge of typical Hudson River sloops of the late 18th century. The lack of the forward end of

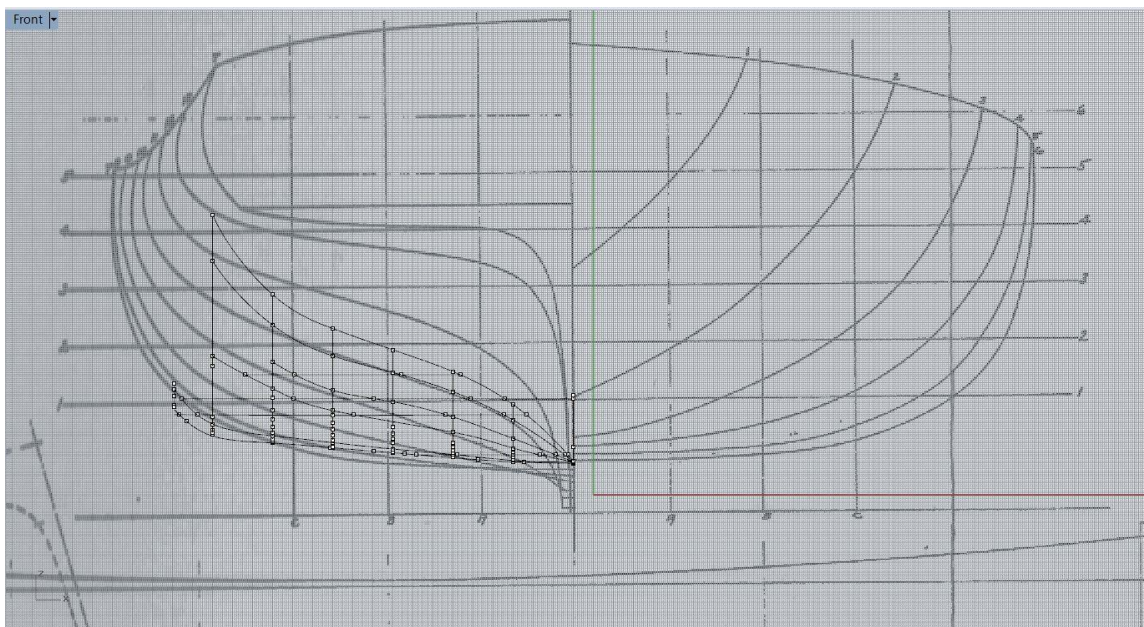


Figure 55: Body plan lines from the WTC ship overlying a set of lines from for a beamy Hudson River sloop. Image a composite of Fontenoy 1994, plan 12 on page 100 and the lines produced by the author.

the keelson and the maststep makes it difficult to say definitively that this is certainly the suggested by the surviving hull structure (Fontenoy 1994, 40-41).

CHAPTER V

MESH MODELS TO TIMBER CATALOG

There are multiple stages and components to the documentation procedure for archaeological material conserved at the CRL. The scanning of the timbers was the second phase for the WTC project, the first being the initial photography and measurements that were taken during the inventory of the materials when they were delivered. At a minimum, all CRL projects have photographs and measurements taken for all materials before and after conservation. If an artifact is unusual or noteworthy, or if there are concerns about how the artifact will respond to the conservation process, additional documentation such as in-process conservation photos, artifact sketches, and X-ray radiographs are taken as well. This comprehensive documentation ensures that the information that can be gained by an artifact is preserved even if something goes awry during the conservation process and the artifact does not stabilize as hoped, or in the worst-case scenarios, the object does not survive the treatment at all.

For something as complex and nuanced as the remains of an entire shipwreck, it is vital that every pertinent detail is collected and documented throughout each phase of the conservation process, both to aid in the final reconstruction of the conserved timbers and to continuously re-evaluate the efficacy of the polyethylene glycol (PEG) freeze-drying treatment. For the conservation of the 17th-century French ship *La Belle*, the CRL used a combination of 1:1 tracings and pioneering 3-D digitization techniques with total station and CMM arm data to create CAD drawings that were the basis for the

timber documentation (Fix, *Archaeological Watercraft: A Review and Critical Analysis of the Practice* (Doctoral Dissertation) 2015, 131-135). Although the high-definition laser scanning done for the WTC ship project provided an unprecedented level of detail to the documentation process, after the pre-conservation scans were completed, a means for documenting additional details as timbers moved through the stages of conservation

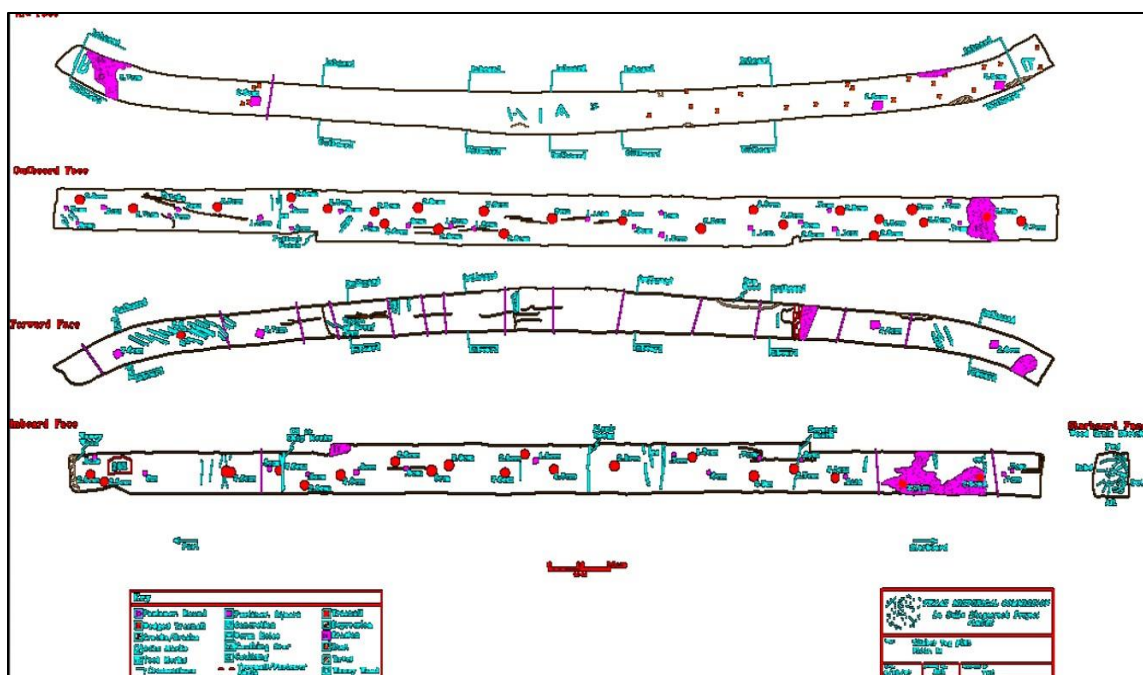


Figure 56: CAD Timber drawing from *La Belle*, used as a template for the design of the WTC timber drawings. Image from Peter Fix.

(akin to the timber drawings used for *La Belle*) was needed (Figure 56). Notes about the location of concretion patches, fastener sizes and orientation, and markings uncovered during cleaning had to be incorporated into the scan data. Most of this data is acquired

during the mechanical cleaning of the timbers. After the laser scanning was complete, each timber was removed from its fresh water storage tank and placed onto a large, stainless steel table, and all of the fasteners were removed using pneumatic chisels. Initially, the plan was to add the information gained during this phase directly to the 3-D

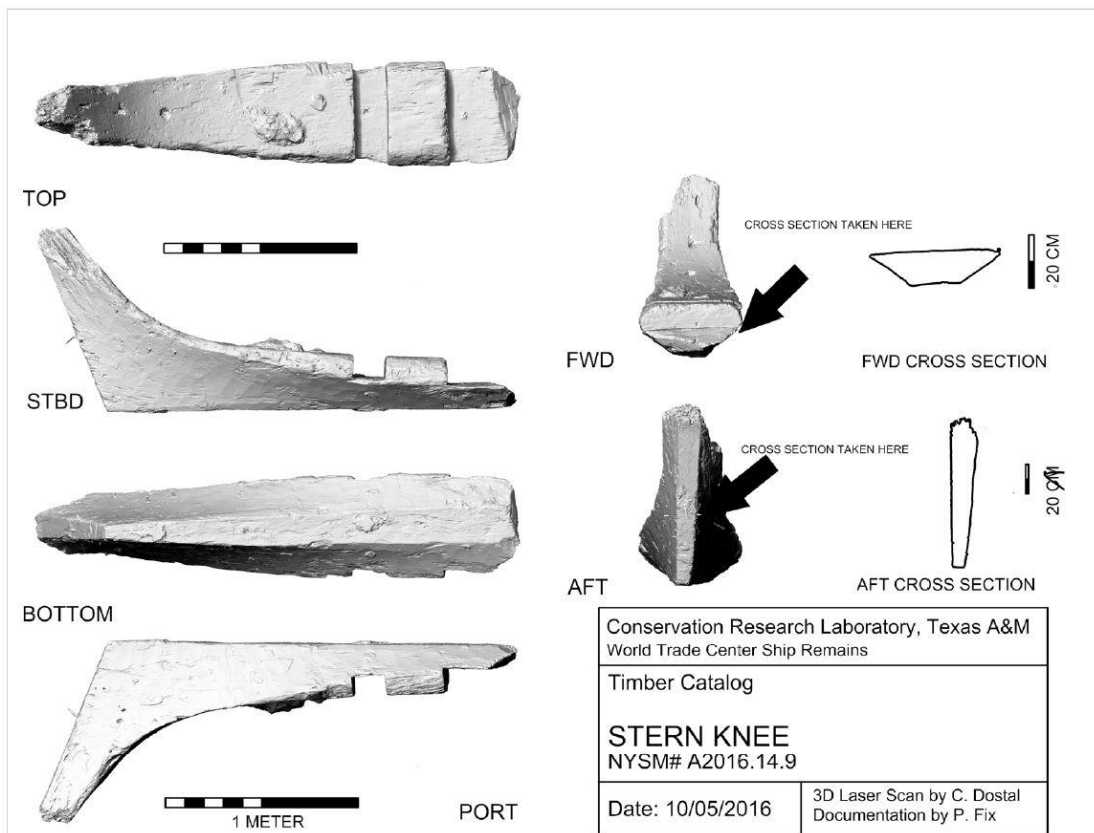


Figure 57: Timber catalog entry for the stern knee. Image by the author.

model in *Rhinoceros 5*, but the constant re-wetting of the timber meant a high likelihood of splashing the computers, and the task itself was too time consuming to do while the timbers were out of water. In the end, paper copies modeled after the *Belle* drawings were made from the scans, and then these faux drawings were printed out and annotated

with the pertinent data, which was added back to the 3-D model in *Rhinoceros 5* at a later date.

With the importance of a timber catalog well established before the commencement of the WTC project, the generation of the each drawing needed to be done in a way that was easy to replicate hundreds of times, and also maintained the high standard expected and necessary for timber comparisons to be made with other ships documented with 1:1 drawings. At the outset of the project, it was assumed that creating drawings with the meshed models would be relative easy to do, though the exact method by which this would be achieved was not fully understood at the time. This assumption of ease proved to be one of the more frustrating time management miscalculations made

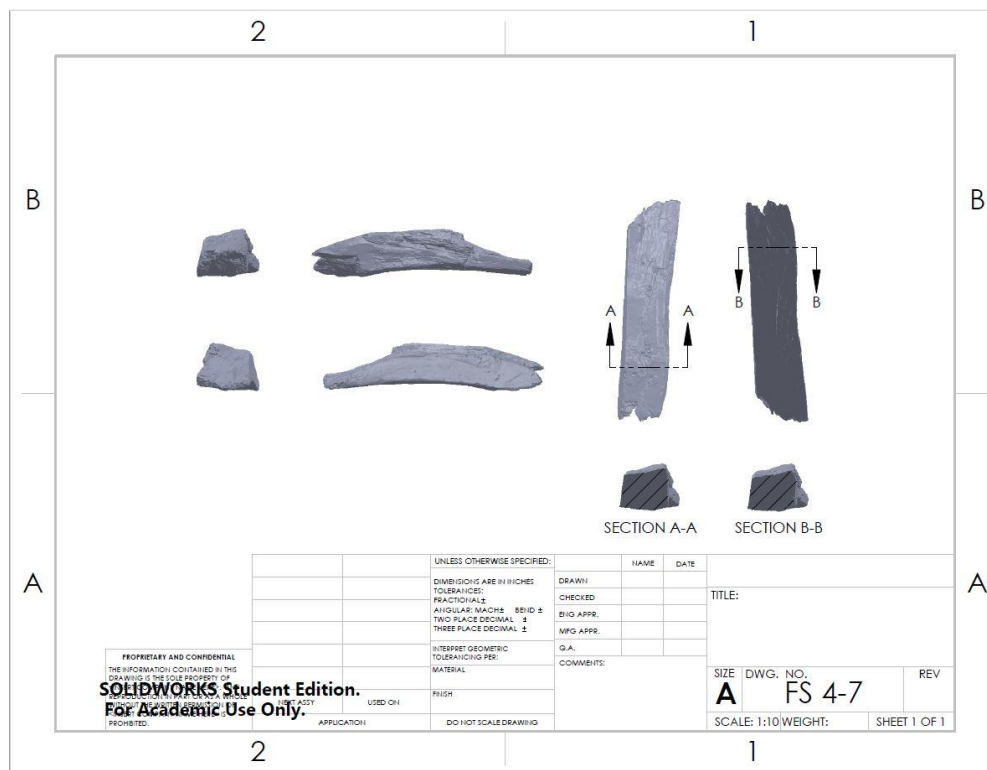


Figure 58: A timber catalog entry generated with a converted CAD body in SolidWorks. Image by the author.

during this project.

As mentioned above, the desire for the catalog entry was to show each of the six faces of a timber as well as two cross sections. The projection of a variety of distinct views onto a blueprint-like page is relatively straightforward when using computer assisted design (CAD) software suites like AutoCAD, Autodesk Inventor, or SolidWorks. These programs are well integrated into the world of engineering and manufacturing, and the ability to generate a blueprint showcasing all faces of an object is crucial to their applicability to industry (Figure 58). With that said, these programs are designed to handle CAD models, not mesh models. Projecting the various faces of mesh models as complex and large as those generated by the LLP is not something that these programs are capable of achieving.

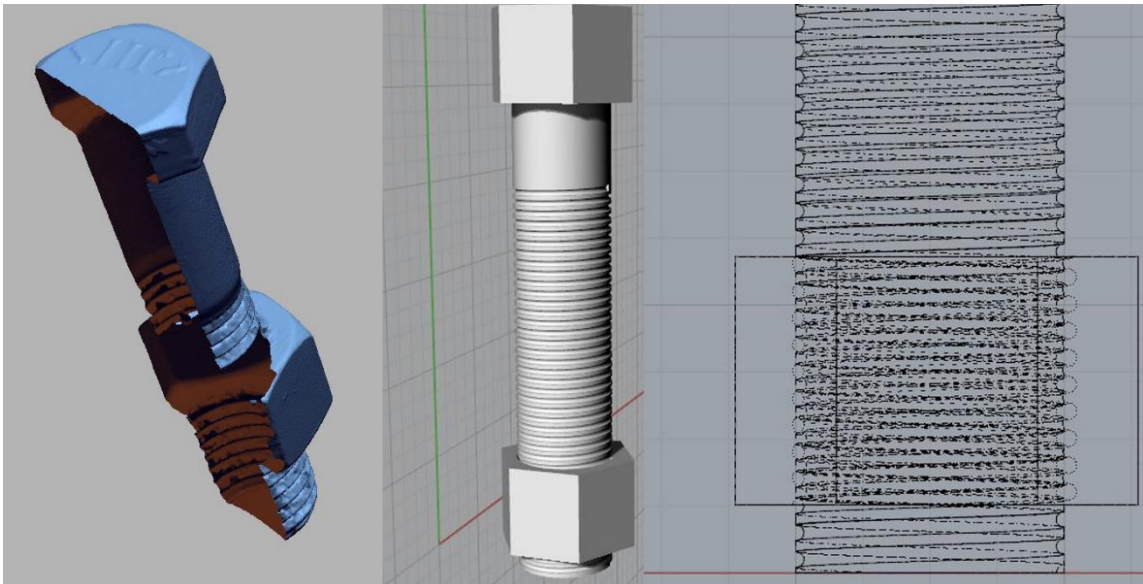


Figure 59: A mesh of the bolt (left) vs. a solid model of the bolt (center). Note the interior of the mesh (left) compared to the interior of the solid (right). Image by the author.

The shortcomings in CAD software were well understood at the outset of this project, but the abilities of *Design X* to easily transform the mesh data to CAD data were overestimated. The main difference between a mesh model and a CAD body is that a CAD body is a 3-D model with fully-realized internal structure. As mentioned in Chapter III, the LLP gathers data as a point cloud, and then a watertight mesh is calculated from that point cloud. The mesh only represents the structure of the timbers visible at the surface; if an internal detail is obscured from the laser, it is not going to be a part of the 3-D model. A solid body is different in that it has all of the internal structure accounted for. To visualize this difference, Figure 59 shows a cut-away of a meshed scan of a bolt with a nut threaded on it and a solid model of the same. Looking at the interior of the mesh, if the bolt is laser scanned, the threads hidden by the nut are not part of the model. For a CAD solid model, the bolt and nut are created separately, and if the nut is hiding the threads, they are still accounted for in the model (the far right image is the x-ray view of the middle image). To convert the mesh on the left to a solid, the missing section has to be drawn in based on the information available in the rest of the model.

The *Design X* software used to capture the scan data can capably turn most scan data into a CAD-ready solid; in fact, it is specifically designed to be a comprehensive reverse engineering solution (Geomagic n.d.). Despite having access to one of the premiere software solutions for converting mesh models to CAD models, the initial plan to convert the scanned timbers to CAD solid bodies was discarded for two reasons. One, it was quickly discovered that the computing resources required to convert the complex

shapes of degraded water-logged timber meshes into solid bodies was considerably higher than initially anticipated. Several powerful computers were designated for the post-processing portion of this project, but even so, the conversion process nearly doubled the already substantial amount of time needed to convert the scan data to mesh form.

Two, it was difficult and time consuming to preserve the archaeologically-important data when converting from mesh to CAD body. From an engineering standpoint, the conversion process is not designed with the idea of perfectly preserving the detailed surface flaws during the conversion. To use the nut and bolt featured in Figure 59 as an example, turning the mesh into a solid body does not need to preserve

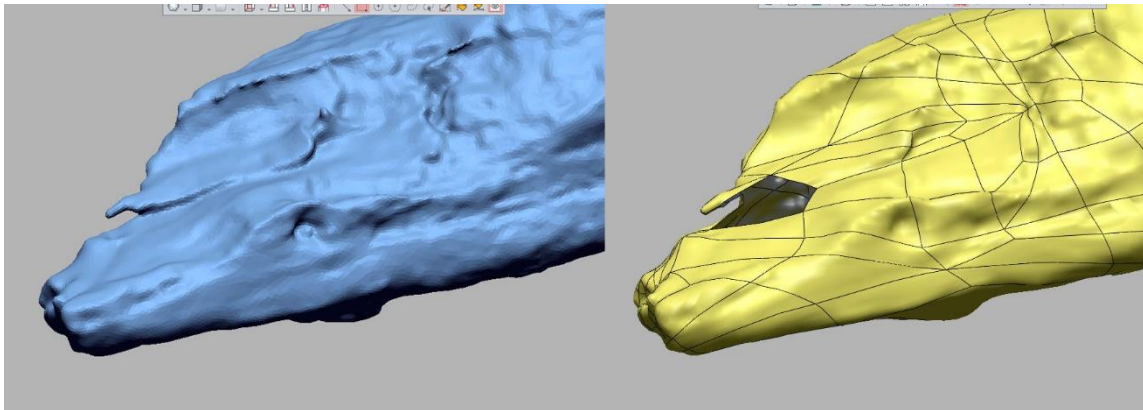


Figure 60: The mesh for FN FS 10-0 (left) and the resultant error in the solid model. Image by the author.

every nick and scratch that was captured by the scanner. Quite the contrary; there is rarely a need to manufacture an item that perfectly mimics the wear and tear evident on the part it is replacing. The broken and degraded surfaces of the wood that needed to be preserved were very difficult for *Design X* to model, and the process of conversion often

resulted in missing sections or incorrectly calculated surfaces, as seen in Figure 60. To rectify the type of error seen in Figure 60 is an achievable goal, but the process was deemed too time consuming to be worth the effort.

With the decision to forgo CAD body conversion from the mesh, a mesh-friendly option to generate the timber catalog entries was needed. After dozens of failed experiments and frustrating dead ends, *Rhinoceros 5*, the software used to virtually reconstruct the ship, ended up being the best solution for generating the timber catalog. *Rhinoceros 5*, like other 3-D modeling programs, shows several views of a model at once to allow for manipulation in 3-D space. Using its ability to visualize a model from a

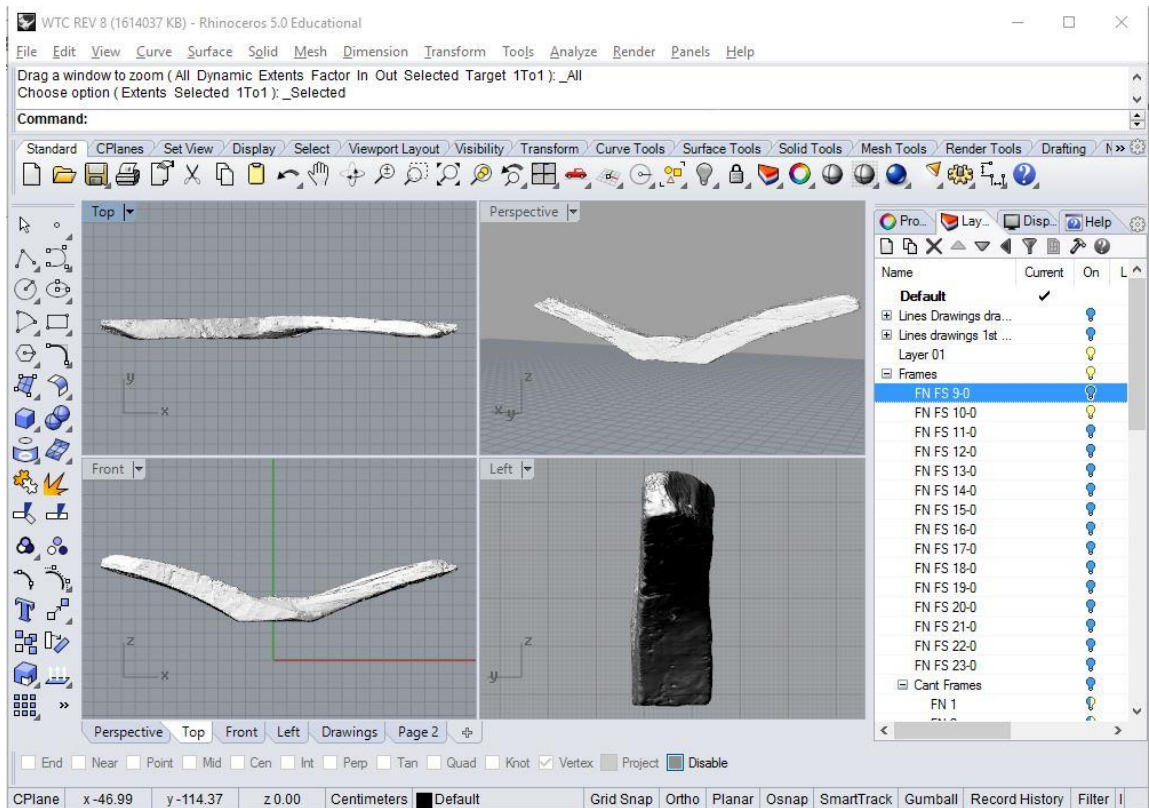


Figure 61: FN FS 10-0 being prepared for a timber drawing. Note the rest of the timber scan layers are off in the panel to the right. Image by the author.

variety of angles at once, the program has a drafting option that allows the user to create a blueprint-like document that has distinct windows, each window displaying a different view of the model. In essence, creating the timber catalog for each scan was akin to setting up an array of security cameras, each pointed at a timber from various angles, with the drafting page acting as a bank of monitors showing all of the different views. The goal was to show six views for each timber, one featuring each face. The document was arranged to have the six windows feature the six faces of each timber as if it were being rolled for each separate view.

The procedure for the production of each timber drawing is essentially the same. In order to illustrate the methodology, the drawing for the floor timber FN FS 10-0, the after-most made frame, is outlined here. The floor timbers were the most straightforward to make the drawings for, because they were already arranged parallel to the X-axis and perpendicular to the Y-axis in *Rhinoceros 5* for the reconstruction. For the timbers that were arranged differently, like the cant frames or the futtocks, the timbers had to be rotated and positioned into the desired arrangement prior to this procedure. To do this, the first step was to turn off all of the layers in *Rhinoceros 5* except for the one containing the timber in consideration. This is done for two reasons; one, it allows for smoother manipulation of the timber, as *Rhinoceros 5* only has to render one mesh, and two, as will be shown below, other visible timbers may potentially obscure views of the desired timber. In Figure 61, the right side of the screen shows every layer turned off with the exception of FN FS 10-0.

At the top of the viewports in *Rhinoceros 5*, there is a series of tabs that bring up different sets of contextual menus. In Figure 61, these can be seen stretching across the

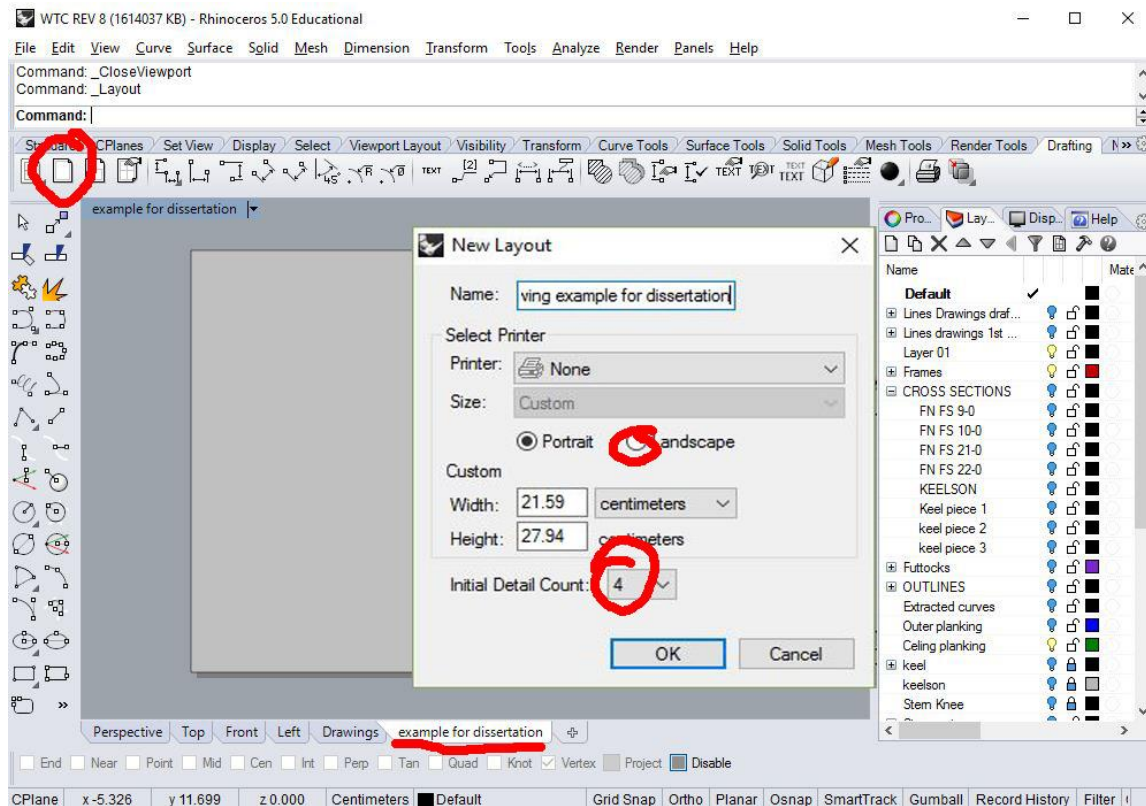


Figure 62: Creating a new layout for the timber drawing using the ‘Drafting’ tab. Image by the author.

top of the display, starting with the ‘Standard’ tab, ‘CPlanes’, ‘Set View’, etc. At the far right side is the ‘Drafting’ tab, which contains the necessary tools to create a template for the timber drawings. Once the drafting tab is selected, a new view tab is created by clicking the blank page symbol (circled in the top left of Figure 62). The new layout dialog box will open, as seen in the center of Figure 62, and the size and orientation of the drawing should be selected. For the WTC project, the size entered was that of standard A4 paper, 8.5 in by 11 in (27.94 cm by 21.59 cm). The landscape option was

selected, and the initial detail count was set to 0. This prevents the new layout from having predesigned detail windows, which would have to be either resized or deleted. The new layout will generate as a blank page, and the name of the layout will be displayed in the bottom left of the screen (Figure 63).

With the canvas set, the next step is to create the template features like borders, text box areas, project information, and any other metadata pertinent to the project that will not change from drawing to drawing. For WTC, a border was added around the sheet, and then a text box was created in the lower right-hand corner of the page that

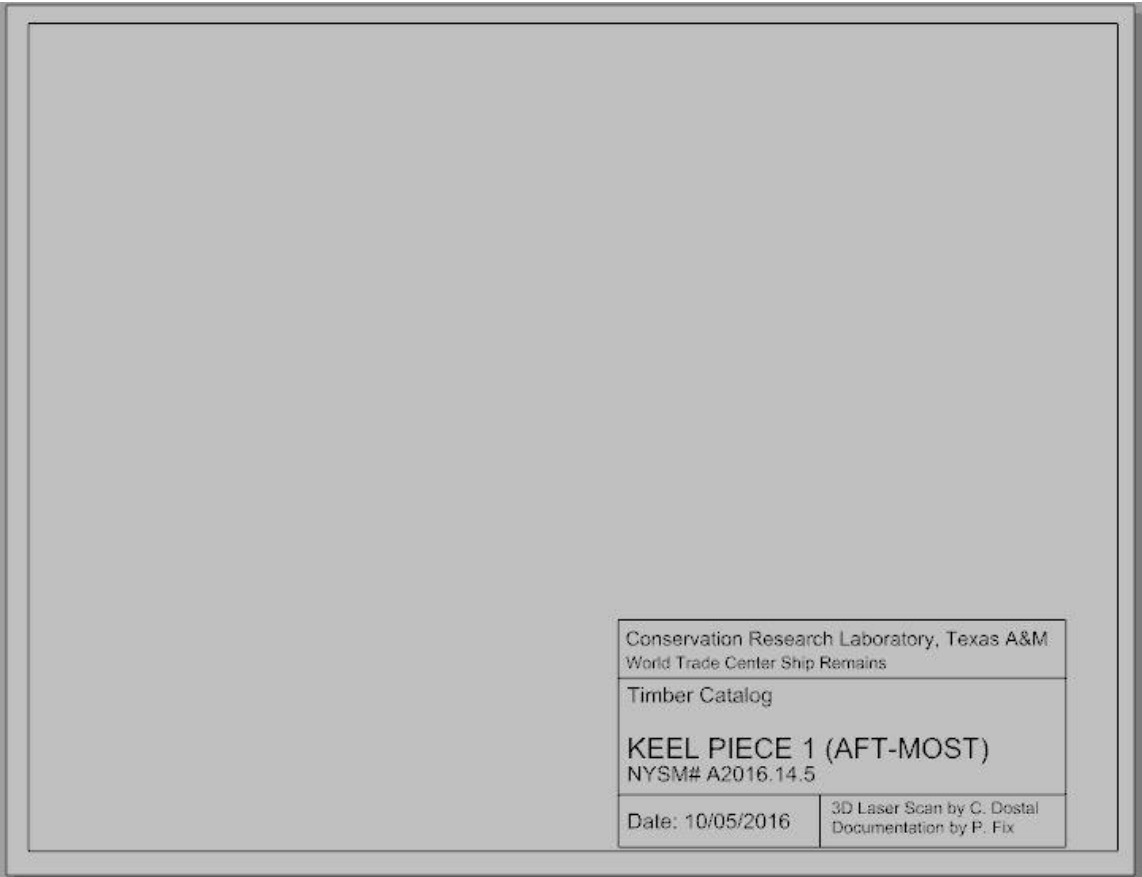


Figure 63: New blank layout page, after a border has been drawn and an information box drawn in on the bottom right. Image by the author.

displayed the laboratory designation, the project name, the field designation for the timber being cataloged, the accession number for the timber (which was generated at the CRL), the date, and the authorship of the document. With the template layout finalized, it can be exported to other projects, which lends to standardization of the documentation format.

The next step was to create the detail views that were desired for the drawing. The goal for these timbers was to follow the standard framework set by past projects,

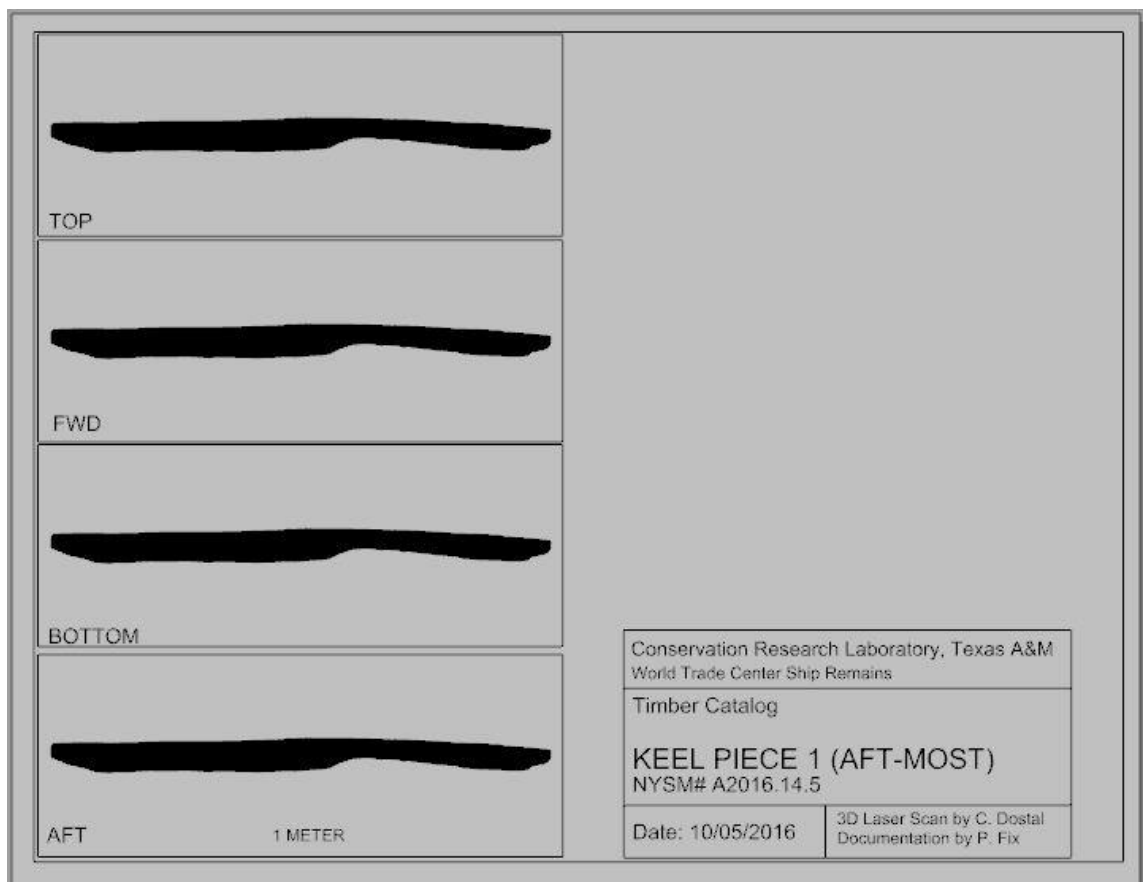


Figure 64: The four larger viewports being added to the timber drawing sheet. Note that they all display the timber in the orientation it was on the previous active window. Image by the author.

which shows each of the six faces of the timber, as well as a cross section of each end (Fix, *Archaeological Watercraft: A Review and Critical Analysis of the Practice* (Doctoral Dissertation) 2015, 134). The dimensions of the port and starboard ends of most of these timbers are much smaller than the top, bottom, forward, and aft dimensions, so the layout was designed to have four larger detail views and two smaller views. This decision was made for the sake of maximizing the detail visible on the page, despite the problems presented by the fact that the end views would be displayed at a different scale than the other four faces.

When designing the page layout for the drawings, the plan was to print each drawing on standard ANSI A sized paper, which is 8.5 in by 11 in (21.6 cm by 27.9 cm). This meant that in a landscape layout, maximizing the size of the larger detail views meant a 5 cm height, and with that height, a 13 cm width fit nicely in the space available on the left side of the page (Figure 64). It was later decided to increase the paper size, because when the timbers were being mechanically cleaned and inspected, the 5 cm x 13 cm windows did not provide enough space to properly document the details needed. The timber drawing template was resized to ANSI B, which is 11 in by 17 in (27.9 cm by 43.2 cm), but for the purpose of demonstrating the creation of a timber catalog in *Rhinoceros 5* with the mesh models for this project, the ANSI A dimensions will be described below.

When inserting a new viewport on the drawing page, each viewport defaults to the view that is active on the main screen, and to the 'mesh' option for the display. If the perspective window was active before switching to the drafting layout, then each new

window will display the view from that window. Since each new window is meant to display a separate view, it is necessary to double-click on each one and change the view to the desired position. To do this, the viewport must be double-clicked, which will change it from static to active, then in the display tab at the top of the screen, the icon representing the desired view can be clicked. Once the view is created, then the display tab should be selected and the display option changed to 'rendered' to allow for an academically-useful view; the mesh for each model, even decimated, contains hundreds of thousands of polygons, so when displayed as a mesh without zooming all the way in

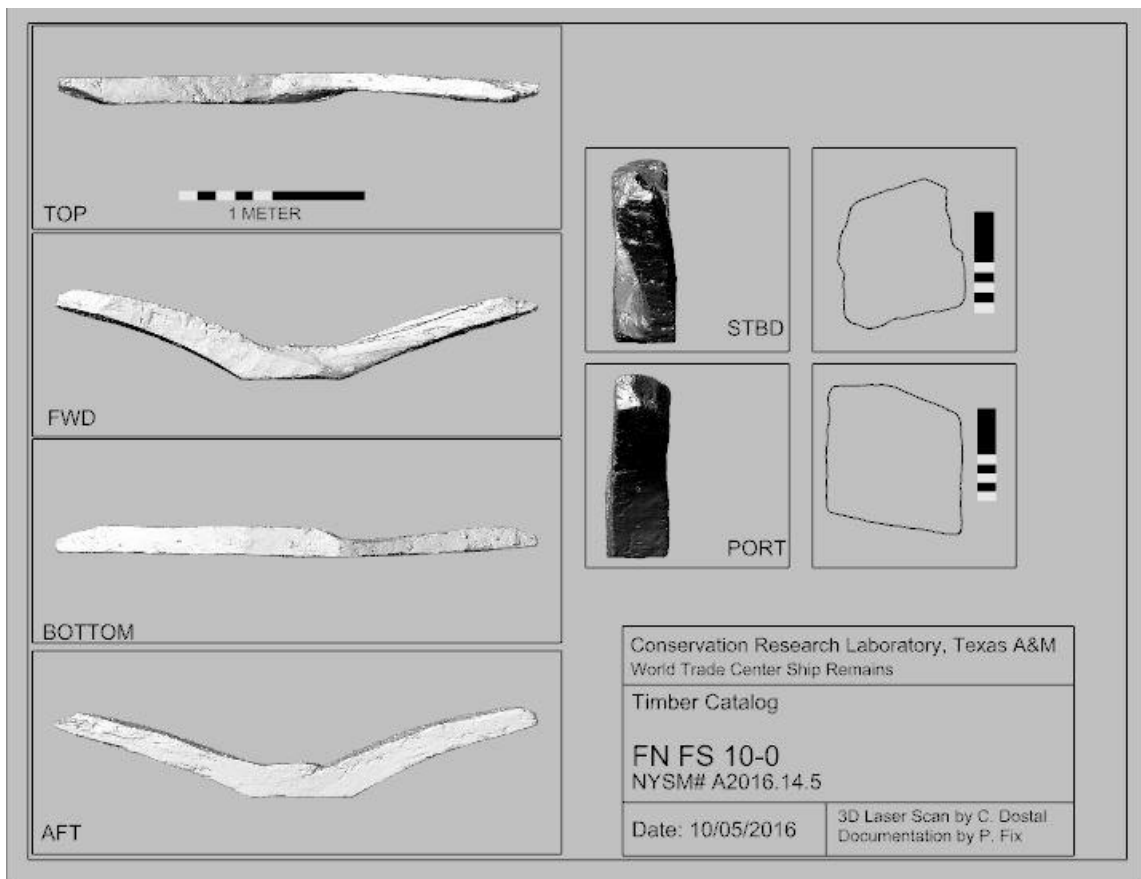


Figure 65: Standardized timber drawing layout for the WTC project. Image by the author.

on the model, the model appears to be solid black (see Figure 64 for what the mesh display mode looks like from afar).

Designating the order of the views should be done consistently across all timber drawings, and for this project the standard view order for all transverse timbers were top, forward, bottom, then aft, top to bottom. To the right of these four views, four other smaller detail views were created, two for the port and starboard views, and two for the timber cross sections (Figure 65). The size of the viewports is of course up to the person designing the timber drawing page, but there must be plenty of empty space to accommodate notes and other metadata that is gathered while the documentation of the timbers is undertaken.

To extract the cross sections of the timbers, in the standard, non-drafting view, the section tool was used to cut through the mesh at the desired cross section point

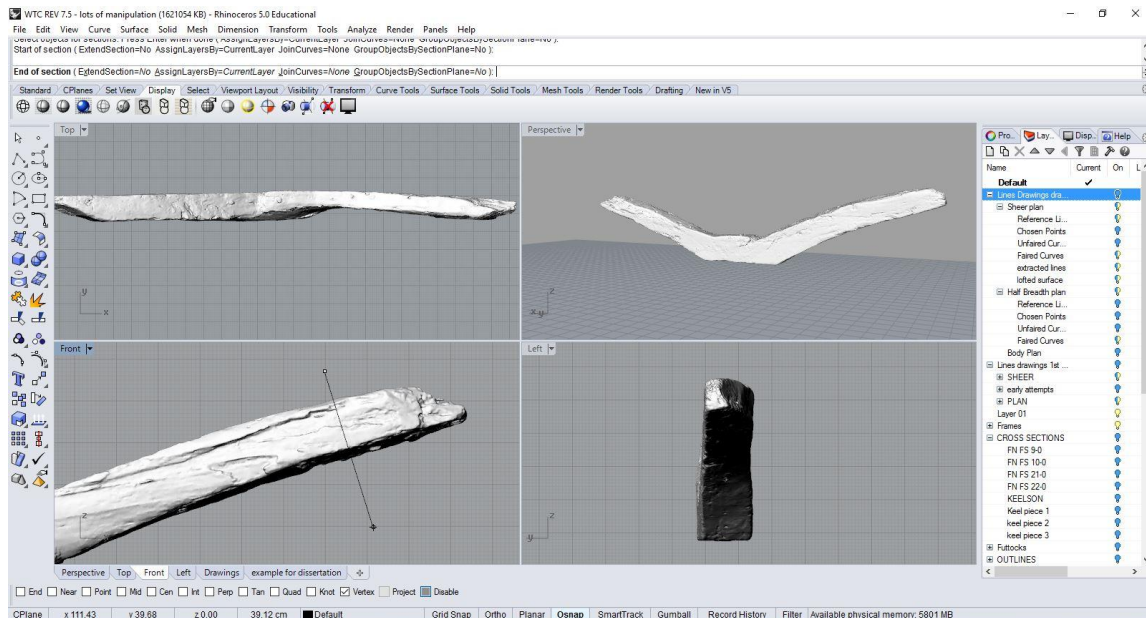


Figure 66: Using the section tool, a cross section can be extracted from the mesh model. Image by the author.

(Figure 66). In the command prompt, 'section' was typed, the mesh for the timber to be sectioned was selected, then the cross section tool was dragged across the area of the timber to be sectioned. When using the section tool, the angle of the cross section should be as perpendicular to the timber as possible, so as to minimize distortion, as seen in Figure 66. This angle is selected by eye and not by any mathematically-derived angle, and therefore it can be argued that there is a margin of error being introduced here that should be avoided, but the cross section achieved via this method is still substantially more accurate than what could be achieved by any other method, and so for now this is a level of error that is acceptable and understood to be a part of the model. After the cross section was complete, it was rotated back to a 90° angle perpendicular to the X-axis to present the accurate cross section for the drawing.

Arranging the viewports was straightforward, but there was a complication that needed to be accounted for; as described above, each viewport is a window looking at the same object, and so anything placed around the model was visible in all views. This proved to be a hurdle when it came to the placement of the cross sections and the scale

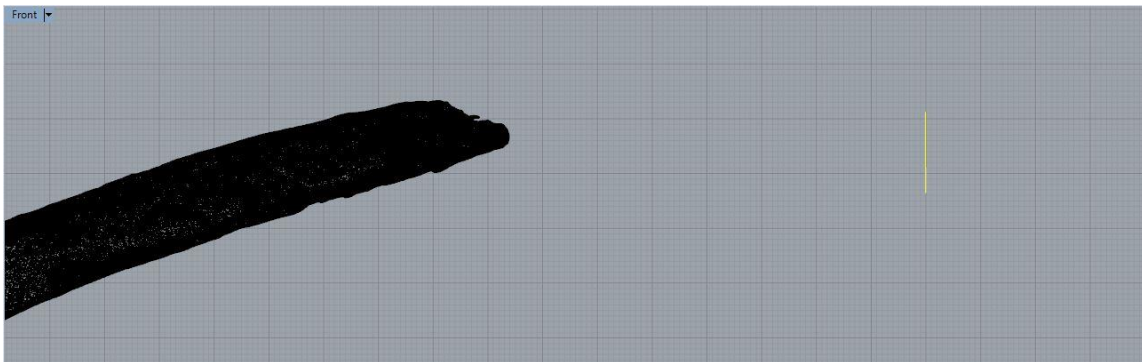



Figure 67: Moving the cross section (in yellow) away from the mesh to prevent it from being visible in the other views. Image by the author.

bars. The cross sections needed to be moved far enough away from the model that the viewports that featured them would not accidentally show any of the model in the background. Likewise, if the scale bars that were created for one view were not arranged in such a way so as to be hidden in competing views, they appeared as stray lines in the other views that were distracting at best, confusing at worse. To remedy this, the scale bars and the cross sections were placed in such a way as to only be visible in the view desired.

Figure 67 shows the cross section moved away from the timber, but in a side view this would not make any difference. In order to properly remove the cross section from the field of vision, one side needed to be moved further outboard and above the model, and the other side was moved further outboard and down. Once they were out of the way, if they were selected (highlighted yellow), the viewport on the drafting page could be opened and manipulated to show only that section. The easiest way to do this is to open the drafting page, set the viewport for the cross section for either the 'left' or the 'right' side view, depending on which side the cross section was taken from, then clicking on the 'Standard' tab at the top of the work area and selecting the 'ZoomSelected' icon . This maximizes the view of the cross section in that particular window.

Creating a scale bar is straightforward, despite not having an automatic tool for the task. Before outlining the creation of the scale bar however, it is pertinent to discuss the choice of measurement units. For this project, *Rhinoceros 5* was set in the metric system, despite the potential problems that might occur when dealing with a ship that was built using the imperial system. For the USS *Westfield* conservation project that was carried out by the CRL, the project director, Justin Parkoff, decided to use the imperial

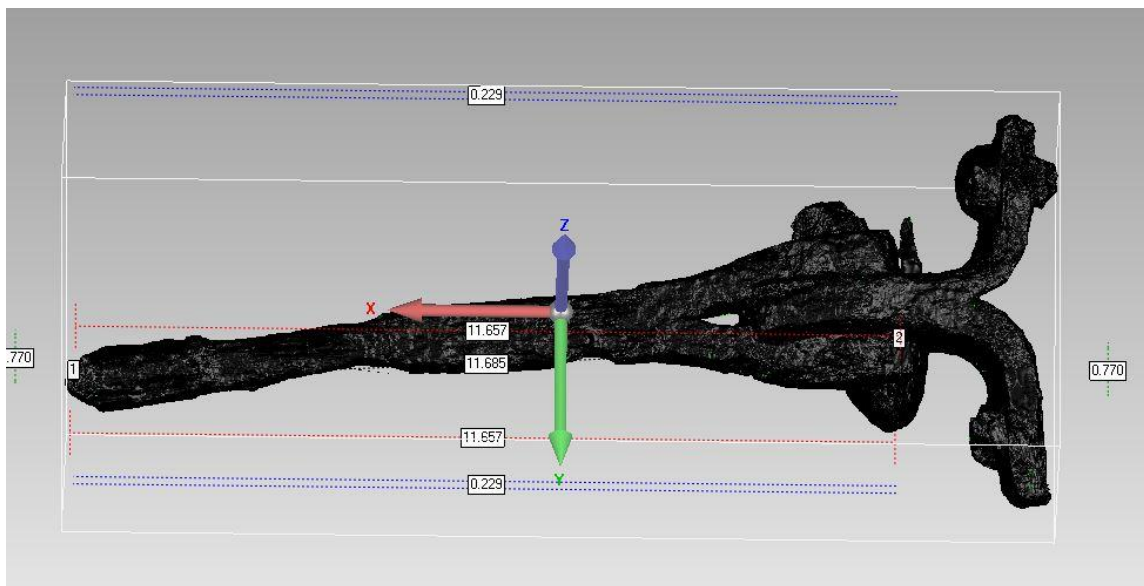


Figure 68: The FARO scan of USS *Westfield* artifact 121-52 C69. All units were kept in imperial. Image by the author.

system for all of the scale drawings, photography, and digital modelling to ensure that all measurements were the same as those used by the original designers (Parkoff 2016, 6). This made it easier for conservators working on the project to pick up on patterns or rules of thumb that might have been used in the original design.

Though the WTC project could be measured in feet and inches for the same reason, there are a number of reasons why the metric system was chosen instead. The first (and most obvious) reason is that because with the exception of the United States, Burma, and Liberia, every country on planet Earth has adopted the metric system, and it is the principal system of units utilized by the scientific community (Central Intelligence Agency 2017). Second, with a single exception, every scanning project that had been done prior to the WTC ship project at the CRL was scanned using the metric system, and so determining the configuration settings was much easier to do in metric. Finally, it was determined that any interpretation issues that might arise due to the scanned model measurements being in different units than those used to build the ship were not significant, due to the ease with which *Design X* and *Rhinoceros 5* can switch back and forth between the measurement systems.

With that established, the design of the scale bars can be as intricate or as basic as one desires. The scale bar is just an object created in *Rhinoceros 5* with precise dimensions, with surface features to delineate those dimensions in a way that is easy for the viewer to identify. For this project, a 100 cm by 5 cm plane was created as the base for the scale bar. When a plane is placed in *Rhinoceros 5*, the default settings allow the plane to interact with the light and shadows from surrounding models, which was not something that was desired for the purpose of a scale bar. It would be counterproductive to place a scale bar under a timber and then have the units masked in shadow. To keep the scale bar from being affected by shadows, the plane was selected, and in its object properties panel, the 'Casts shadows' and 'Receives shadows' options were deselected

from within the rendering settings. For a basic design, the plane was assigned a black color in its material properties panel, and then three white 10 cm x 5 cm planes were placed atop the black plane 10 cm apart starting at the far side of the black plane. The 10 cm white planes created a smaller increment for half of the scale bar, which is typical of



Figure 69: The scale bar for the timber drawing is a 100 cm x 5 cm black plane with 10 cm x 5 cm white planes atop it. Image by the author.

their design (Figure 69). If the white planes disappear, it may be necessary to raise or lower them away from the surface of the black plane by 1mm.

It was found that enlarging the end view for most timbers was necessary to convey detail, which meant that on the timber catalog the side views were not at the same scale as the other four views. If more than one scale is going to be present on the same page, it is important that the scale bar be visible in the non-standard viewport, to prevent confusion. Once the scales are in place and each view is properly prepared, the drawing can be saved, either as an image file or a PDF (with the drafting tab active, File > Print > Save as PDF). All of the drawings for this project were exported as PDFs. Once the drawing for one timber was done, the next could be done by simply turning off

the layer of the completed timber and turning on the layer for the next one in the sequence. The windows and scale bars sometimes needed to be nudged into place to align with the next timber, but the process moved very quickly once everything was set up. It is a good idea to double and triple check to ensure that all of the legend information is updated correctly before saving and moving on to the next timber, because once the next drawing is started, if there are errors on the previous drawings, they will have to be redone.

CHAPTER VI

3-D PRINTING AND PHYSICAL RECONSTRUCTION



Figure 70: The digital model reconstructed and the 3-D printed structural timbers for the WTC ship project prior to reconstruction. Image by the author.

During the process of reconstructing the ship remains virtually in *Rhinoceros 5*, the timber models were individually printed out at a 1:10 scale using a fused deposition modeling (FDM) 3-D printer. FDM is a process in which a material is extruded through a small nozzle in thin layers to create an object, stacking layer upon layer until a 3-D shape is built. The FDM printer used for the WTC ship project was a Zortrax m200, which extrudes the plastic filament acrylonitrile-butadiene styrene (ABS). ABS is one of

the two most commonly used materials for FDM printing, the other being polylactic acid (PLA) (Mueller, et al. 2014, 277).

To print, a spool of 1.75 mm diameter ABS filament is fed into the nozzle of the extruder, heated to 275°C, and extruded onto a heated printing platform. To visualize the

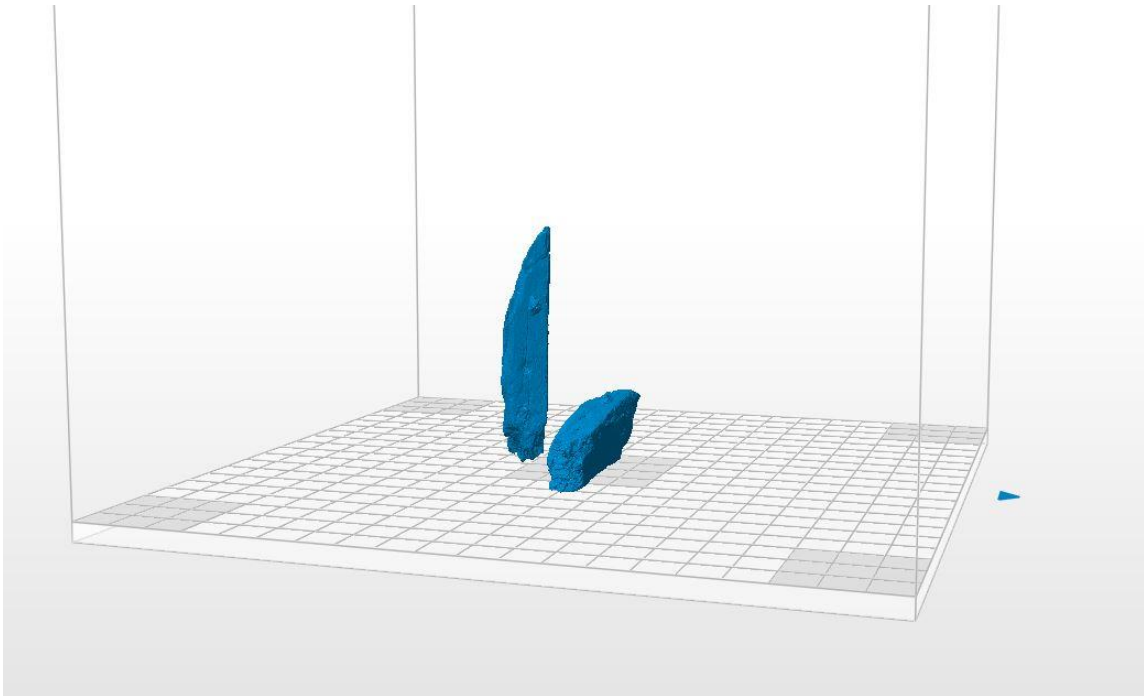


Figure 71: Orientation of BF 3 in *Z-suite*. Image by the author.

process, think of adding rows of frosting to the sides of a round cake with a piping bag. The first layer of frosting ‘filament’ is piped, or ‘extruded’ around the base of the cakes, and each layer that is applied after that builds a certain height of frosting, until the entire cake is frosted. This is the principal by which FDM 3-D printing operates, except the layers of filament are much smaller and the shape that they are ‘piped’ can be much

more complex, and instead of the piping bag moving up to add to each layer, in the case of the printer, the cake would be dropped down for each new layer.

The path that the extruder takes while depositing the ABS on the printing platform is determined by a program that analyzes the 3-D model file and ‘slices’ it into layers. If it were slicing the cake to determine the frosting path, it would virtually cut the cake into layers that are the thickness of the piped frosting, and map out the path that the piping bag would need to move to match that shape. Once the 3-D model is sliced, an optimal path can be calculated for the extruder to move during the filament extrusion for each height interval of the platform.

Preparing the Models for Printing

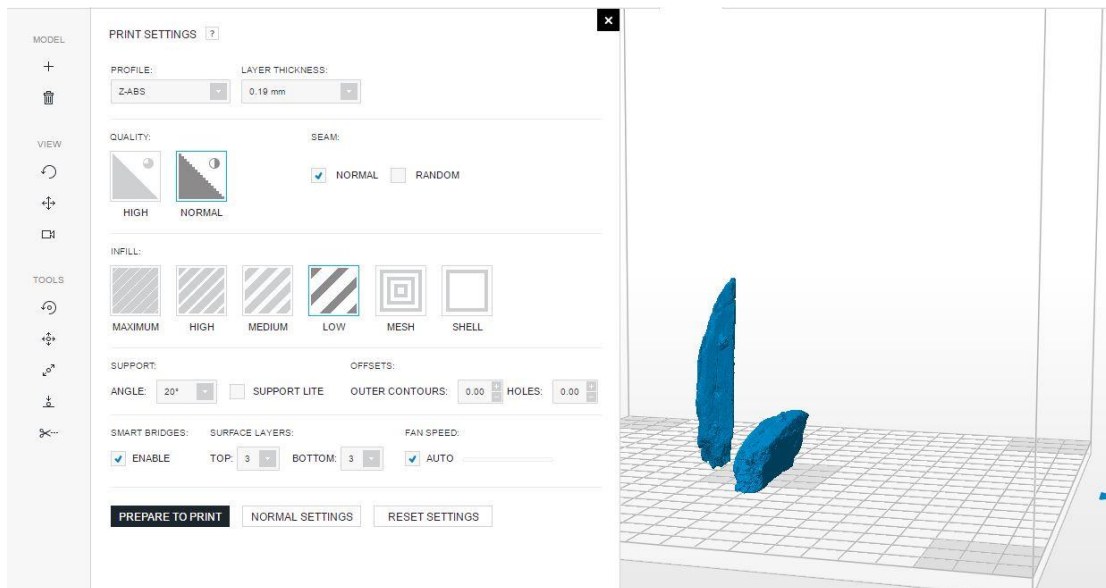


Figure 72: Customization options in *Z-Suite*. Image by the author.

The slicer program used for this project was *Z-Suite*, provided by Zortrax with the purchase of the printer. Third-party software options like the excellent open-source program Slic3r offer much more nuanced customization than *Z-Suite* offers, but *Z-Suite* was used because of its user-friendly interface and reliably excellent results with the m200, the printer it was designed around. The *Z-suite* program allows for a certain level of customization, as seen in Figure 72. Of the options available, there are eight major components for the configuration of a model to be printed: model orientation, printing material, layer thickness (resolution), speed, infill, surface layers, number of shells, and supports. With the exception of orientation and material, these options are used to change the balance between the quality of the print and the time needed to print. As a general rule, the longer a print takes, the higher the quality.

Before adjusting the speed of the print though, the first thing that must be done when preparing a file to be printed is to consider the orientation of the object. The orientation can significantly impact the quality of the finished model. Even with the highest-resolution settings of the m200 printer, the individual layers of the print are still visible to the naked eye. With this in mind, the way that the model is oriented means that when the model is sliced and printed, certain features can either be highlighted or obscured based merely on the orientation of the model in the slicing software. Because of the physical limitations of the printing process, one face of the model must be printed first, and the rest of the faces printed atop it. The first face to be printed is the one that is oriented towards the printing platform, and this face will have to adhere to the platform, which results in it having the least amount of detail visible when printed. With each

layer being extruded atop the previous layer, areas with low relief should generally be oriented vertically if possible. If these areas are horizontal, when they print they will tend to look like topographic maps. Figure 72 shows the timber BF 3 oriented vertically and horizontally. Figure 73 shows the final print of each orientation. Note the topographic map-like appearance of the detail in the horizontally-oriented timber on the top.

Once properly oriented, the next step is to choose the material and the layer

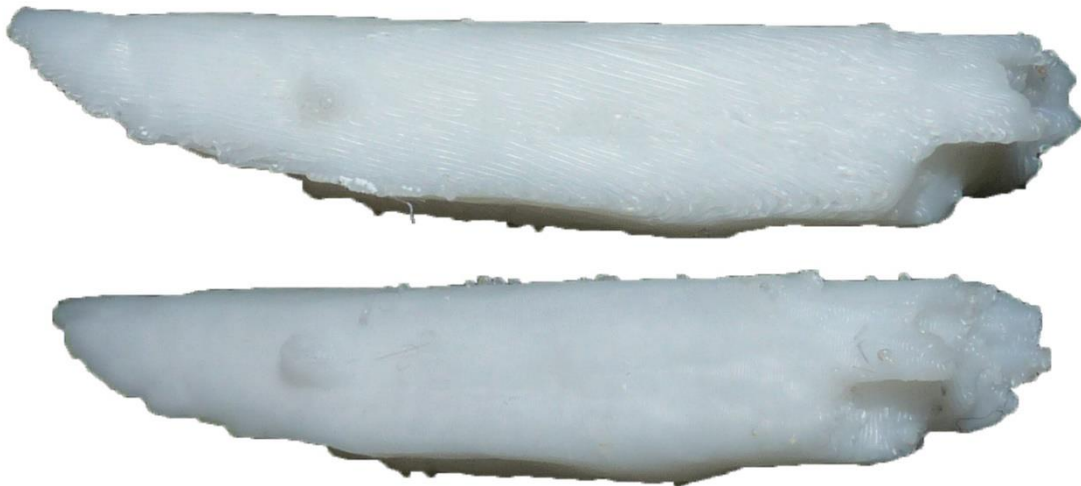


Figure 73: The effects of orientation on print quality. The top version of BF 3 was printed with the visible face parallel with the print platform, while the bottom version was oriented perpendicular to the print platform. Image by the author.

thickness. Along with ABS, there are a host of other plastic formulations that can be used with the m200 printer, but none of these options were utilized for this project. ABS is inexpensive and reliable, and therefore other materials were not considered. The layer thickness determines the thickness of each individual print layer, meaning that the layer

thickness is in effect the determining factor for the resolution of the print. Different materials have different thickness options, but for ABS and the m200, the maximum layer thickness for the m200 is 0.39 mm, and the minimum is 0.09 mm. As mentioned earlier, the smaller the layer thickness, the higher the resolution and the higher the detail in each print, but the printing takes more time. A middle ground between quality and time was chosen for this project, and all the timbers were printed with a layer thickness of 0.19 mm.

As a side note, the resolution of the print being set to 0.19 mm at a 1:10 scale meant that the layers of the printed model represented 1.9 mm on the actual object. As mentioned in the *Post-Processing* section of Chapter III, the .stl files were decimated to between 10% and 20% of their original resolution depending on the size of the timber. As mentioned in the *Configuring the Settings* of the LLP section of Chapter III, the settings for this project specified a grid size of 0.035 mm. This means that when the models were meshed, the maximum resolution possible would be an average triangle side length of 0.35 mm. (In reality, this was not achieved, nor desired; see Chapter III: *Post-Processing*). With an average maximum edge length of 0.035mm, a 90% decimation resulted in an average edge length of 0.35mm. Though at first glance this may seem much coarser than the 0.19mm layer thickness, in reality, the diameter of the extruder nozzle, 0.4mm, determines the maximum resolution achievable for a single point. This means that even decimated, the resolution of the 3-D model exceeded the resolution of the printed model. Trials were done in the planning phase of this project for prints with full-resolution models, and apart from the negligible change in print quality,

the file size was so large that manipulating the models in the slicing software was slow and clumsy, and any time saved by printing at 0.19 mm instead of 0.9 mm was wasted when trying to orient the models with the lag.

In Chapter V, the difference between a mesh model and a solid CAD model was discussed. Because a mesh model consists entirely of external features, the printer can be configured to print the model as a shell of sorts; a thin layer of the external features of the model are printed, and then the interior is filled with a grid-shaped lattice for support. The desired strength, durability, and rigidity of the final model can be specified in the settings by selecting the amount of infill, number of shells, and the number of surface layers. The infill determines the size of the internal grid lattice (Zortrax 2016). As seen in Figure 74, the low infill setting creates larger grid squares and therefore takes less time and material to print. The high setting creates smaller squares, and though it takes longer to print, the final model is more stable and rigid. For the largest timbers, the keel, keelson, stern knee, and stern post, the high infill setting was used. For all of the floors

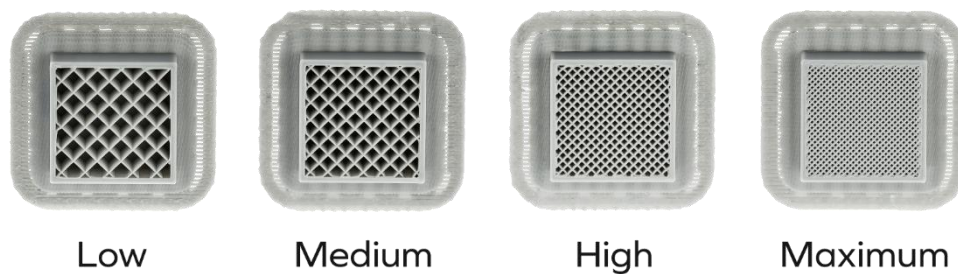


Figure 74: Different levels of infill. Reprinted from of Zortrax.com (<http://support.zortrax.com/wp-content/uploads/2016/07/infill.png>)

and futtocks, low infill was used, as their square profile made them structurally sound regardless of infill. For the planking, low infill was also used so as to maximize the flexibility in the print to aide in the reconstruction of the model.

The number of layers that make up the external structure of the model are known as shells and surface layers. Changing the number of shells changes the thickness of the exterior of the mesh model on the sides, while the number of surface layers controls the thickness on the top and bottom of the model (Zortrax 2016). The number of shells and surface layers will affect different faces of the model based on the orientation chosen by the user, so it is something that must be considered after the orientation is decided upon. For this project, three shell and surface layers were used for every model.

The movement speed of the print head can be adjusted to change the quality of the print; as mentioned above, generally the longer a print job takes to complete, the better it will look. In some printers it is possible to adjust the speed to a specific mm/sec, but the Z-suite only allows for 'High' or 'Low' quality; high referring to quality and therefore printing at a slower speed, and low being a lower quality but printing at a faster speed. The speed of the print head is one area where the *Z-Suite* is particularly restrictive. In other printers and slicer programs, the specific speed of the extruder can be set separately depending on whether the extruder is printing or just moving to a new area (see Makerbot 2017, Hodgson n.d.). For this project, the low quality was used. The first two batches of test prints were printed on the high setting (i.e. at a slower speed), and the third batch printed on the low setting. There was no discernable difference in the quality

of the two sets of prints, which was likely a by-product of the middling resolution selected.

The final configuration option is choosing the level of support that must be provided for the model. For the purpose of an exaggerated example, printing an arch-shaped model is ideal; so consider printing a scaled copy of the St. Louis Gateway Arch. As discussed above, FDM printing works by depositing layers of filament atop layers of filament to build the model. What about models with overhang? How can the printer print the top of the arch without any previous layers below it? Without some kind of support, the filament would simply fall down to the printing platform. In these situations,

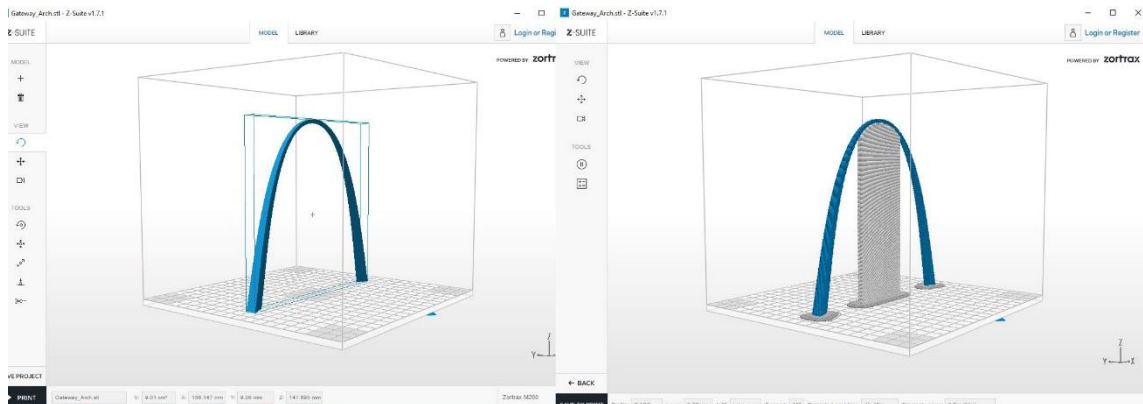


Figure 75: Preparing the Gateway Arch (left) for printing requires supporting any area of the print that is not overlapping a previous layer by 20°. Image by the author.

the slicing program will build a lightweight support bridge up to the portion of the print where the overhang begins (Figure 75). The standard support setting is 20° for Z-suite; this means that overhanging parts of the model will have a support structure built at 20° or higher from the surface.

Once the .stl files are oriented and the setting chosen, the model is sliced and formatted for the printer. Figure 76 shows the way the slicer builds the path. Note that this is not a typical print batch. The timbers were not printed individually, they were printed in the largest groups possible. Without sacrificing the maximum detail achievable through ideal orientation, as many models as possible were added to each print job. Printing efficiency is an economy of scale; though the numbers are not exact, the idea is that if a single model could be printed in two hours, printing 10 models at once would take 10 hours, not 20. At any rate, the first step of the slicing is to generate the ‘raft’ that the model is printed atop, which allows for the print to be removed from

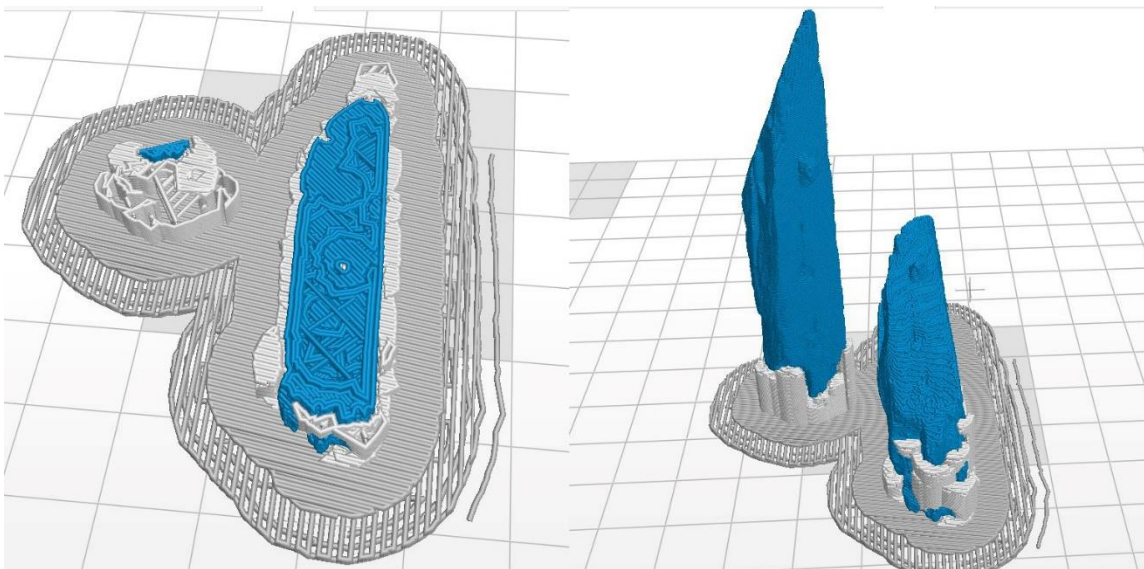


Figure 76: Slicing maps the route for the extruder to take during each layer of the print. Image by the author.

the platform without damaging the bottom face of the model. Then the pathway the extruder must take for the exterior and infill of the object is mapped out for each individual layer, and the supports are generated (in white) on the outside of the model to

allow any overhanging parts to be printed without compromising the print. Once the slicing was done, the printer instruction file was saved on an SD card and loaded onto the printer.

For some of the print files that contained a number of long, sturdy timbers extending across the length of the print platform parallel to one another, as they would print the ends would warp and curl, lifting off of the printing platform. At a 1:10 ratio, all of the floors and many of the first futtocks and planks spanned the entire print platform. In several cases, the timber models were too large altogether and had to be sliced in *Rhinoceros 5* to fit on the printing platform. This is covered in the next section of this chapter. The working theory is that the longitudinal torsion on the print itself created when printing several parallel timbers was great enough to overcome the adhesion that the raft had to the printing platform. The base of the prints would lift off the platform at opposite edges, giving the timbers a false curve and ruining the dimensional accuracy of the print. To overcome this, two approaches were taken. First, steps were taken to increase the adhesion to the print platform. At the suggestion of Dr. Donny Hamilton, the supervising professor for this project, the print platform was sprayed with Krylon Maxx clear adhesive sealant. The adhesive was easy to remove either by scraping or by wiping off with a rag soaked in acetone, and it greatly improved the adhesion of the first layer of the print to the print platform. The Krylon adhesive greatly reduced the print warping, but it did not eliminate it for some of the more extensive print batches with long timbers. The second way to overcome this warping was to simply reduce the number of timbers being printed per batch. This increased the

number of prints, but it was still more effective to print smaller batches than print larger batches and have them fail.

Modifying Oversized .stl Files in Rhinoceros 5 for Printing

As mentioned above, many of the timbers printed at the 1:10 scale were too large to fit the printing platform of the m200, which is only 200 mm x 200 mm x 180 mm (Zortrax 2016). In order to fit the full length of the timbers onto this platform, the models were imported into *Rhinoceros 5* and split. It is not enough to simply split the mesh though; recall that there is no internal structure for the mesh model, and so cutting the mesh would leave a 2-D border at the intersection of the cut. Instead, the mesh tools in *Rhinoceros 5* allow the mesh to be split with a plane, and the intersection created by

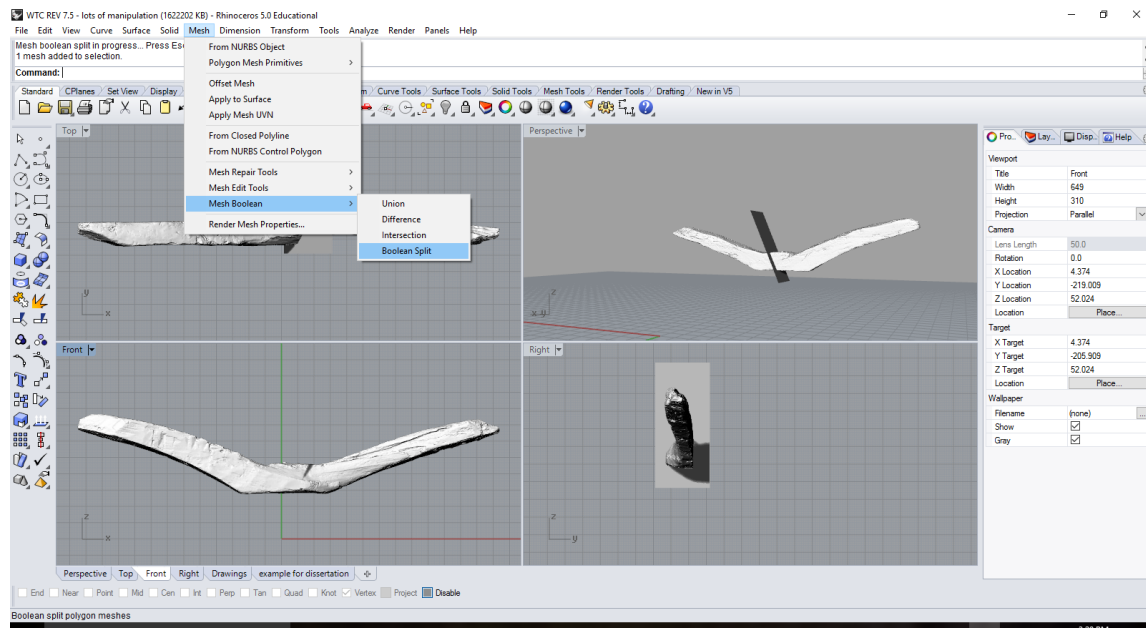


Figure 77: Cutting a timber model in *Rhinoceros 5* so that it will fit on the 3-D print bed. Image by the author.

the plane is meshed to create two distinct watertight models.

The first step was to import the decimated .stl file into *Rhinoceros 5*. (File -> Import). Then a cutting plane was created and oriented to the most advantageous position on the model for the cut. The best practice for orienting the cutting plane was found to be off center, and at an angle. Though a complex scarf might have allowed for a cleaner re-assembly after the print, a simple flat plane seemed to work perfectly fine. Putting the plane at a slight angle helped with orientation when reassembling, and putting the cut off center helped reduce the pressure on the seam. Once the plane is in place, in the mesh menu, select 'Mesh Boolean', and then 'Boolean Split' (Figure 77). This will split the model and automatically patch the hole where the cutting plane was, which results in a watertight mesh that can be printed. From there, select each half and in the file menu, click 'export selected', saving as a .stl file and not the native *Rhinoceros 5* .3-Dm file. With the model split, the two halves were added to *Z-Suite*.

It should be noted that if *Rhinoceros 5* is not set to millimeters, (the measurement units native to *Z-suite*), there will be scaling issues with the model halves and they will be imported at a fraction of the size of the other timbers. To rectify this, the scale that the model halves were saved in must be converted to the scale used in *Z-suite*. As an example, if a model was split with *Rhinoceros 5* using inches and imported to *Z-suite*, the model would be selected, the scale tool selected, and the model would be scaled by 254%, as 1 in is equal to 254 mm.

Printing

Once the print file was complete, the file was written to an SD card and inserted into the printer. The steps for printing are very straightforward, but there were a few things that needed to be considered prior to starting. The first thing was to verify the amount of filament remaining on the printer spool. When each print file is processed by Z-Suite, the estimated amount of filament needed to complete the print in grams is calculated and displayed. To track this, a log sheet was kept near the printer with the starting weight of the filament spool, and the estimated print weight was subtracted after each print. On the rare occasions that this was not done or if there was an error encountered with the print, the spool in service was removed and weighed, then the weight of an empty spool was subtracted to ascertain the amount of filament remaining.

The second thing was to ensure that the printing surface was perfectly level. If it was not, there would be areas that were too close to the print head, and areas that were too far away. Areas that were too close prevented the filament from coming out, which clogged the print head, which leads to a phenomenon called 'air printing'. The printer has no way to detect that the filament is not coming out, so it will continue to run the extruder head through the entire routine before it stops. If the nozzle becomes unclogged for any reason while air printing, the platform will be out of place and it will just spew filament out and create a bird's-nest-like ball of filament. If the print surface was too low and therefore too far away from the nozzle, the filament would not adhere to the surface of the printing platform or the layer it was printed atop, and the next time the nozzle passed over that area, it would snag the unsecured layer and drag it along as it prints. To

level the print bed, each printer has its own procedure to follow, which involves adjusting the platform with leveling screws and checking the level with the print head.

Third, platform adhesion is something that needed to be considered before each print. As mentioned above, when printing several long timbers, the longitudinal torque was enough to cause the print to curl up off the platform. Even when printing smaller objects though, it is important to ensure that the filament will adhere to the platform. The Zortrax printer has a heated printing platform, which helps. The Krylon spray method mentioned earlier works very well, and dissolving the filament used to create the rafts and supports in other prints in acetone creates a runny glue that can be painted onto the platform. If utilizing adhesives to help the print stick to the platform, after two or three print batches, the printing platform should be disassembled and cleaned of any residual adhesive that may have worked its way through the plate. If the resin is allowed to build up, there will be subtly uneven areas on the platform that can cause print failure.

ABS filament is prone to warping if it cools at an inconsistent rate, so it is helpful to maintain a steady temperature around the printer. To effectively protect the print from changing temperatures, an enclosure around the printer prevents air from moving heat away from the print, and it is good practice to ensure the printer is not near any HVAC vents, personal heaters, fans, etc. The Zortrax m200 used for this project has optional side panels and a door on the front that were used while printing, and only minimal warping was seen due to the longitudinal stress mentioned above.

Cleaning and Labelling the Prints

Once the models were printed, they needed to be separated from the raft, (the layer between the print and the printing platform), and the supports that were necessary for printing, which was done with only a few small tools. A stainless steel spatula was used to separate the raft from the printing platform, and a small pair of needle-nose pliers were used to break away the majority of the support material. For small pieces of support that were wedged into deep overhangs, a dental pick was used to flick at the support until it popped out. The flicking tended to work more cleanly than pushing or pulling, because the rapid movement released the support at the seam where it connected to the rest of the model. For some of the prints that had to be halved in *Rhinoceros 5* to fit on the print platform, a small section of the seam would not perfectly line up, and so these were sanded down with a grinding wheel until they were smooth and would fit together. A variety of files and sanding tools were used to grind down these areas in the first several batches of bisected prints, but it was found that the grinding wheel worked much faster and cleaner, and produced excellent results. If a small divot was created by overzealous grinding, glue could often patch the gap.

After the timber prints were removed from their supports, each one was tagged with its field designation number using a fine-tipped Sharpie marker. Depending on the orientation needed to get the best print of the timber, some sides of the timbers were smoother than others. It worked much better to mark the smoothest side with the Sharpie, as this prevented unwanted spreading of the ink. After everything was labeled and sanded, the bisected timbers were dry fitted to ensure they would match up

correctly, then they were glued together with hot glue. Hot glue was used for two reasons: it was easy to remove by heating if necessary, and it was hard enough to fasten without sagging. Initially polyvinyl acetate (PVA) in acetone was used to glue the pieces together, but the acetone solvent reacted with the ABS, and the joints were too strong to break without damaging the model. Further, the acetone weakened the walls of the models, and allowed the inner support structure to be visible.

Assembly

Once all of the structural pieces were printed out, the actual assembly of the model began. Virtual assembly in *Rhinoceros 5* guided this process, but the limitations of having to contend with gravity and adhesives meant that it was not ultimately a good step-by-step model to follow. The model was assembled almost entirely, then disassembled almost entirely after the discovery of a subtle error (described below), and then reassembled. Both assemblies will be discussed here, because separate methodologies were utilized for both builds.

The first step was to assemble the keel. As mentioned in Chapter V, *Rhinoceros 5* allowed for easy reconstruction of the keel because it does not prevent two objects from occupying the same virtual space. The messy overlap from splintering that occurred due to the snapping of the keel during the excavation was irrelevant, because the pieces could be aligned without considering it. With the 3-D printed keel, the real ramifications of the splintered breaks in the keel needed to be dealt with. Because of the limitations of the LLP and the need for a water-tight model, deep gaps at the broken ends

of the keel pieces were artificially filled and printed solid, which meant the pieces would not simply fit back together. To get around this, the digital reassembly of the keel was printed on paper at an exact 1:10 scale and put on the table, then the keel pieces were trimmed until they lined up with one another at exactly the correct position. Once everything was trimmed and aligned, the three pieces were glued together. The hot glue, mentioned above, worked very well for adhering the various pieces of the model together; but this was not entirely true for the 3-D print of the keel. Because of its length

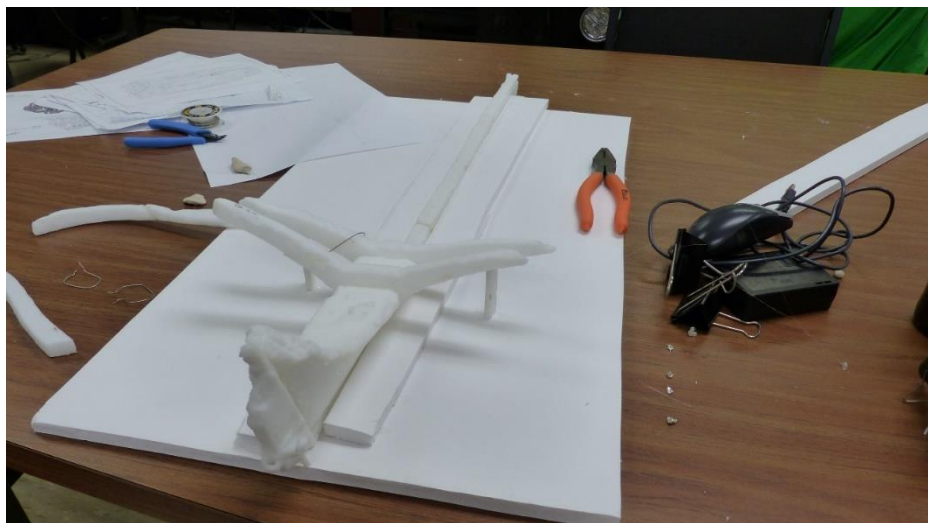


Figure 78: The reassembled keel with the stern knee and stern post attached. The aftmost floors were inserted because of the notches in the stern knee. Image by the author.

(80 cm), the weight of the three pieces caused it to sag at the adhesion points if held by one end. Luckily, this keel replica did not have to meet the rigors of seaworthiness, and it was placed onto a large foam core board atop the 1:10 digital reassembly printout, and clamped into an upright position by gluing a series of foam blocks along both sides (Figure 78).

The next step was to attach the stern knee to the lower portion of the stern post, then attach both pieces to the keel. Aligning the stern knee to the stern post was very straightforward, as the bolt used to fasten two pieces remained intact when printed on the

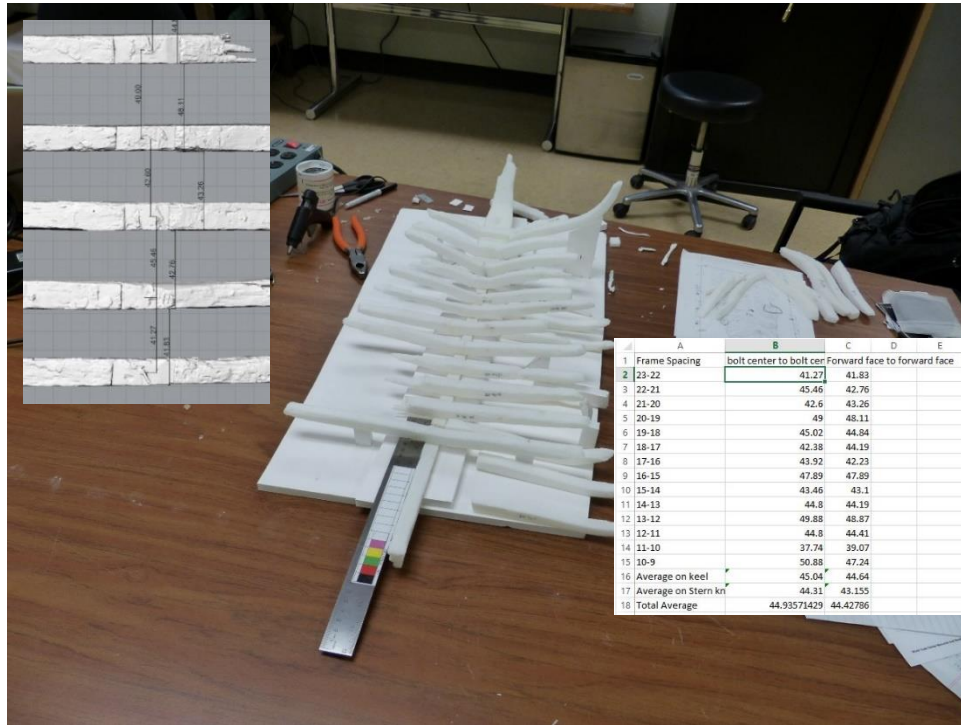


Figure 79: The first attempt at assembling the printed timber models. At floor FN FS 19-0, it became obvious that the spacing calculated was not quite right. Image by the author.

stern knee, and the bolt hole printed on the stern post. Once the bolt was trimmed slightly to accommodate the slightly-shallow bolt hole, the two were dry fitted, checked for accuracy, then glued. After that, both pieces were lined up on the keel based on the paper guide. Both the keel and the stern knee taper in width towards their after ends, and so fitting the stern knee was very straightforward. Once in place, thanks to the subtle variations in depth on the bottom of the knee and the top of the keel from encrustations,

the two pieces ‘clicked’ into place when jostled back and forth. Once that point was found, alignment marks were made on both pieces and they were then glued together. Figure 78 shows these first stages with the aftermost two floors in place. The contact area between the pieces was great enough that when the glue dried, the foam blocks keeping the keel upright was enough to keep the stern knee upright without any need for additional buttressing.

From here things varied between the first and second assemblies. The first go through was too hasty, too cavalier. The progress was so satisfyingly tangible that several entire days in a row were spent carefully placing the floor timbers along the keel and gluing them in place. The placement of the floors was based on the distances between them in the digital model; a chart was made with the distance between each floor in *Rhinoceros 5*, and then a long ruler was placed along the printed keel and each floor was glued at the distances from one another according to the chart, starting from the aftermost floor and working forward (Figure 79). The balance of the floor was done by eye, temporarily shimming them on both the port and starboard side until the glue dried. The reasoning behind this was that hot glue has a small amount of flexibility, especially on such a small contact point, and if need be, the floors could be slightly shifted when the planking was applied later. As the floor assembly came to the forward end of the keel, it became obvious that something was not correct. The placement of the forwardmost floor did not line up with the digital model. Moreover, this run through was done prior to the conceptual realization that frames 10, 14, 18, and 23 were made frames.

The placement of the futtocks was not yet known, and so the plan at the time was to attach them to the forward face of their associated floor.

Once the placement errors were realized, all of the floors were removed, the residual glue cleaned off, and a new tactic was devised. Instead of basing the placement of the floors on the scaled measurements between the digital floors, a new 1:10 top-down view of the model was printed out, this one with the floors in place. The model was then rebuilt by matching the placement of the printed floor pieces with their placement on the printout. Further, instead of relying on the flexibility of the glue to correct any initial errors in the balance of the frames on the keel, a strategy more closely akin to what the original builders must have used was devised. For the three of the four made frames that survived, frames 14, 18, and 23, stanchions were devised in *Rhinoceros 5* and printed out to support both sides of the floor as the glue dried. For the fourth made frame, frame 10, this was not necessary because it fit very snugly into a notch in the forward end of the stern knee. Once the made frames were attached and balanced, a thin wooden batten supplied by ship model maker Glenn Grieco was strung along their outboard face and fastened to the sternpost, and the remaining floors were balanced according to the curve of the battens.

To create the stanchions, the assumption was made that the base of the board that the model was being built on was at the same Z -height as the X -plane in Rhinoceros. The basic concept was to create a solid object in *Rhinoceros 5* that started at the X -plane, extended to the bottom of the floor timber, and then the floor timber was used as a

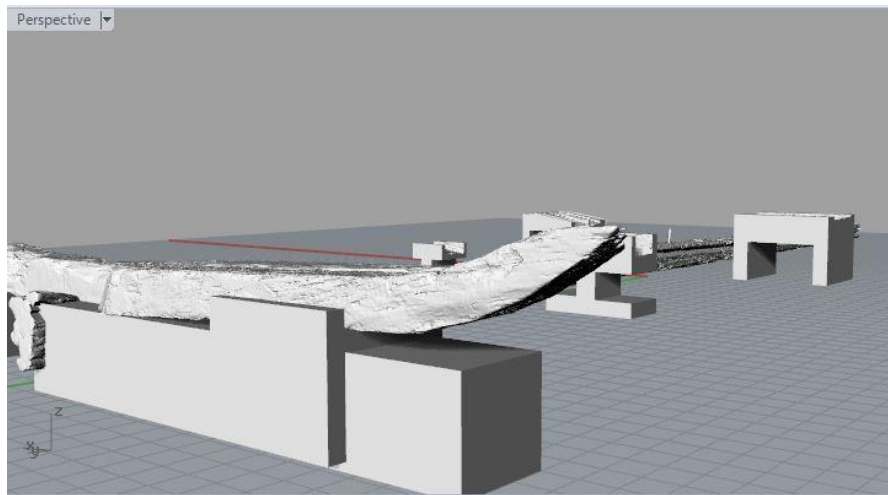


Figure 80: Several early stanchion design attempts. The design to the left was created to hold both the floor and the first futtock. Image by author.

cutting object to trim the top of the solid object. By doing this, the idea was to have a perfect mold of the bottom of the floor as the top surface of the stanchion, allowing for easy placement that would not slip out of place. Though conceptually straightforward, in reality, it took five separate iterations to hone in on a design that worked acceptably well. A few of the early design attempts can be seen in Figure 80.

The different iterations were just variations in the width and length, and experimented with whether or not it was a good idea to have the stanchion wrap up around the sides of the timber. If the stanchion was too thin fore to aft, it did not support

the floor enough to work. If it was too thin outboard to inboard, it was difficult to match up exactly where it should go, and the whole concept of accurate balance was lost. If it wrapped along the sides, it was easier to find the correct position, but the precision of the modeling meant that it fit too tightly, and it was difficult to remove, which was needed to attach the first futtock. If the stanchion was created to hold the first futtock as well, then it was even more difficult to remove, which needed to happen for the model to be planked.

The final stanchion design that was used was a hybrid of the different design iterations; the molded dimension for the stanchions was around 30 cm, and the sided dimension was just slightly greater than that of the timber it was being built for, roughly 15 cm on average. As seen in Figure 81, the stanchion height was brought up to the point

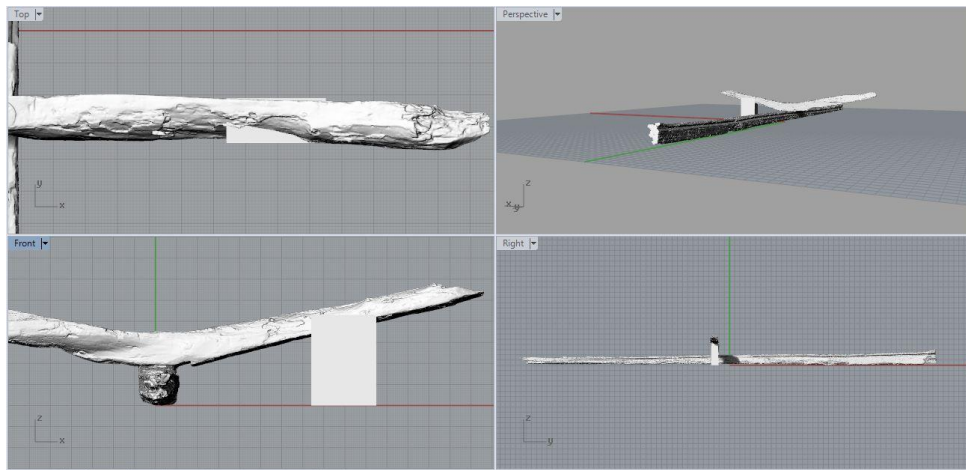


Figure 81: The first step in creating a stanchion that can be printed out and used to balance the physical model on the floor timbers on the keel is to create a solid object between the floor and the timber. Image by the author.

on the floor where it was fully inserted into the mesh without extending beyond the top surface, and then the timber mesh was used to cut the stanchion using the ‘Mesh’ tab, and ‘Mesh Boolean difference’ command. Once the area from the floor was cut away, the stanchion was trimmed to remove the parts of it that would grip the sides of the timber. Further, the bulk of the body of the stanchion was carved down using block objects and mesh Boolean difference commands to make a slimmer object that could be

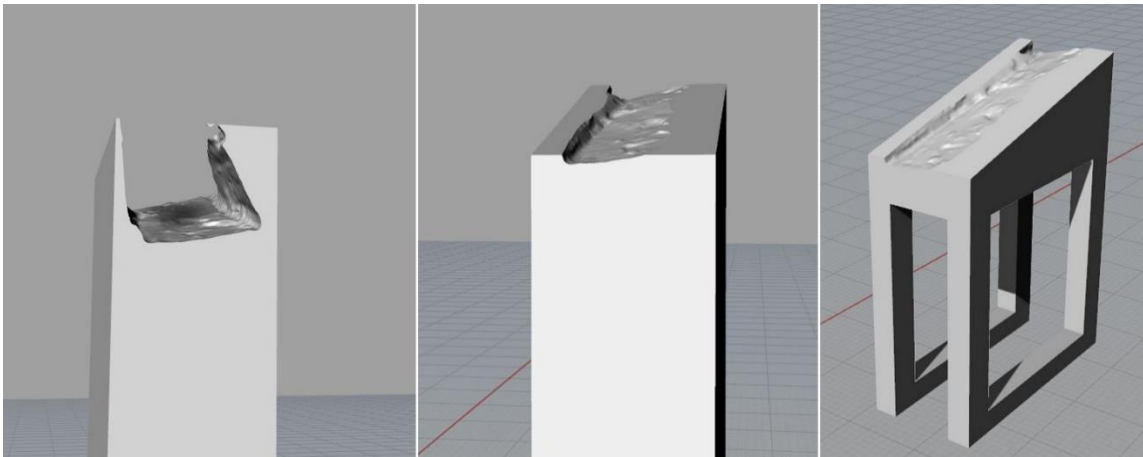


Figure 82: The stanchions are first cut with the Boolean difference between the block and the timber mesh (left). Next they are trimmed down so the model can be set atop it (center). Finally, the body is carved away for a faster print (right). Image by the author.

printed more quickly with less filament (Figure 82).

Once the made floors were balanced and glued into place, the batten was strung along the external face of each one and secured along the stern knee to create a faired curvature for the remaining floors to be put in (Figure 83). The remaining floors were glued into place using the battens in lieu of stanchions, and then the first futtocks for the made frames were attached at the exact point where they fastened to the floors. This only

provided a modicum of hull shape information unfortunately, because the bulk of the hull remains for the made frames was lacking. To further reconstruct the ship, the outer planking will be applied up to the first futtocks for the master frames, then the remaining first futtocks will be glued into place based on the data obtained from the virtual reconstruction and the physical limitations that are realized with the model.



Figure 83: Assembling the physical model. Battens were strung along the master frames and glued in place (left). The author places the remaining floors (center). The model with all floors installed (right). Image by the author.

CHAPTER VII

ALTERNATIVE METHODS OF 3-D DIGITIZATION

As mentioned in Chapter I, there are several alternative methods that are currently utilized for the 3-D digitization of ship timbers. For the purposes of evaluating the efficacy of the high-definition laser scanning process utilized for this project, three of the most common alternative methods for 3-D digitization will be discussed, evaluated, and compared here. The three are computer vision photogrammetry, contact probe digitization utilizing a coordinate measuring machine (CMM) arm, and large-area surveying laser scanners. Each of these methods have been frequently used to capture and convey high-quality archaeological data, and they are routinely utilized by archaeologists around the world (including the author) to aid in the documentation process (see AKRF Inc. 2013, Falck & Fawsitt, 2011, Nayling & Jones, 2014, Watters, et al. n.d., Yamafune 2016).

Computer Vision Photogrammetry

Computer vision photogrammetry uses overlapping photographs to create 3-D models, and of the three methods discussed here, it is by far the least expensive method and requires the least amount of specialized training to begin use. Human beings perceive depth because of binocular vision; our eyes are offset by a fixed distance and our brains can accurately perceive the parallax between them as depth. Using the same principal, photogrammetry uses the parallax between two still images to measure depth.



Figure 84: Early stereoscope image of the Cuyahoga River in Cleveland, OH. Reprinted from the New York Public Library Digital Collection. (The Miriam and Ira D. Wallach Division of Art n.d.)

Photogrammetry, which at its core is simply the ability to make accurate measurements from photographs, originated in 1851, just 12 years after the advent of the camera (Konecny 2014, 143). Early iterations used one pair of pictures at a time, offset by a fixed distance and then viewed with a stereoscope, as seen in Figure 84. With the advance of computer processing power, the ability to utilize more and more photographs of the same area has allowed very complex and detailed 3-D models to be generated of objects using nothing more than photographs. The following is an abbreviated outline of the steps needed to create a computer vision photogrammetric model of an artifact using Agisoft *Photoscan*. For a much more thorough description of the process, please refer to Yamafune (2016).

At its most basic level, computer vision photogrammetry works by comparing pixel values across multiple images. Before discussing photogrammetry though, first it is important to understand the way that a digital camera works. Digital cameras have two main parts: the part that lets photons of light in, and the part that turns that light into an image. The first part consists of a lens to focus the light, and a shutter to control the intensity of light that enters. The second part consists of a sensor that can convert the photons that make it through the lens and shutter into an image. The sensor is a charged coupling device, or CCD. The CCD consists of many tiny light-sensitive pixels, and when photons collide with the CCD, the individual pixel that they interact with converts the photons to a certain number of electrons, depending on the energy of the photon. Because the number of electrons produced corresponds to the energy value of the photon, the energy for each wavelength of color can be interpreted and represented in each pixel for the image produced (The Royal Swedish Academy of Sciences 2009, 12(14)).

The number of pixels that a CCD contains relates directly to the resolution of the photo. CCD pixel counts are measured in megapixels (MP), or one million pixel units. A cellphone might have a CCD with 16MP, meaning that each image produced is theoretically capable of having 16 million pixels. In reality though, the images are typically compressed into a standard format like .jpeg, which groups pixels with similar energy values together to minimize the size of the image files. The process by which a photo is compressed is similar to the way that a program like *Photoscan* can detect the overlap between photos. *Photoscan* looks through an image and groups pixel patterns into

sets of similar values, and then looks for similar patterns in other photos. If enough of the pixel patterns can be matched, the software places a point in the area of overlap, and based on the location of the point, calculates where the camera was located for each photo. This is done over and over with dozens to hundreds of photos, until a point cloud ('sparse cloud') is formed that represents the rough shape of the object.

Once the location of the camera for each photograph is known by the software, the images are re-analyzed for pattern similarities. Knowing the location of the cameras means that the accuracy with which points can be placed to build a point cloud is considerably higher (a 'dense cloud'), and as such many more points are placed. Settings in Agisoft *Photoscan* determine how many points are generated, which is similar to the grid size setting in the LLP settings inasmuch as it directly controls the resolution of the model. Indeed, the resulting point cloud is very reminiscent of the point cloud that is generated via high-definition laser scanning, and like those point clouds, these are used to calculate a mesh. Though the mesh tends to be of a lower resolution than that of a mesh created from a high-definition laser scan, photogrammetry has a major advantage over other methods of 3-D digitization, in that it can create an incredibly true-to-life photographic texture map of the model.

To make a fair comparison between computer vision photogrammetry and high-definition laser scanning, a random timber was chosen from the WTC assemblage and modeled using both methods. Figure 85 shows the stages of processing in Agisoft

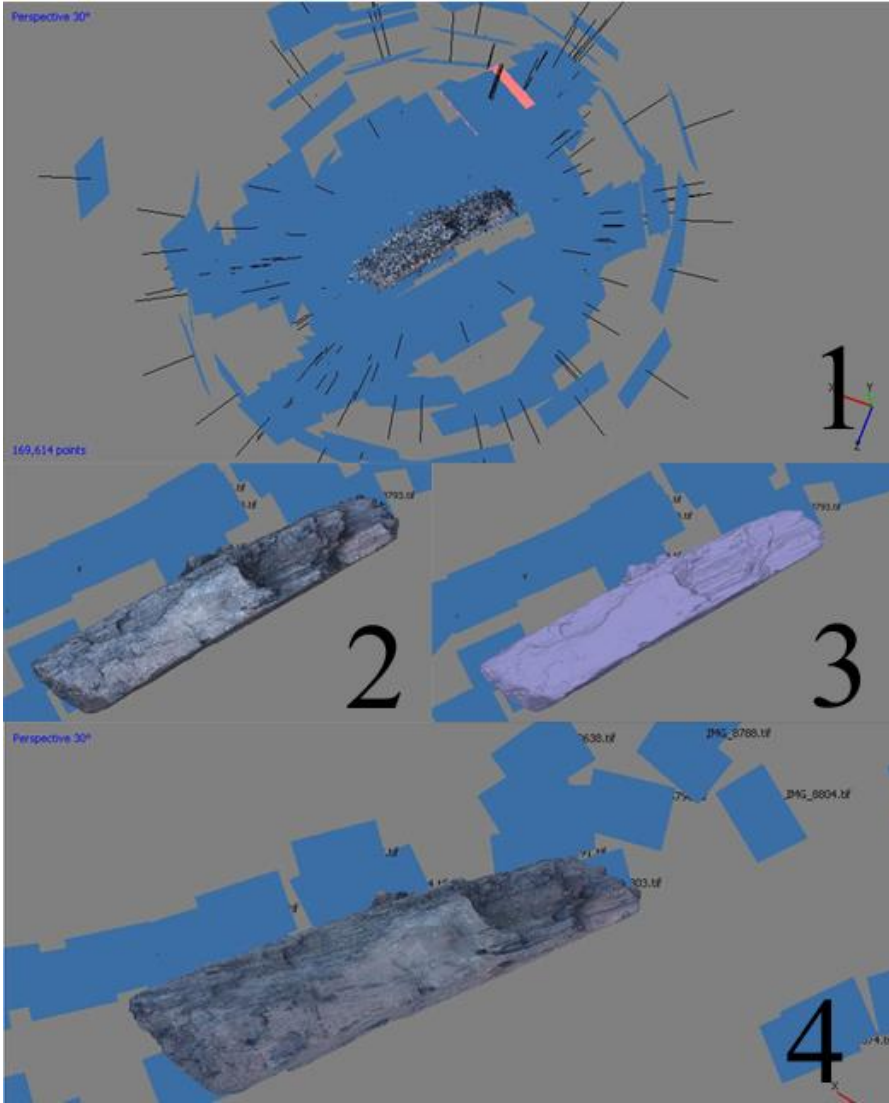


Figure 85: Stages of photogrammetry. 1 - Generate sparse point cloud and calculate camera positions. 2 - Calculate dense point cloud. 3- Calculate mesh. 4- Generate photographic texture map. Image by the author.

Photoscan to develop the photogrammetric model of timber BF 2. Note that this is a fully realized 3-D model, which is not something that *Photoscan* can produce with unprocessed photographs. If a photogrammetric model were made of a shipwreck site, it would only be representative of the parts of the wreck that are visible from the perspective of the camera. Because *Photoscan* uses pixel values to calculate depth, any part of the wreck that is not visible will not be modeled. If you took a particular timber and flipped it upside down, the software would have to try and reconcile the pixel differences for that area of the model, but the pixels for all the material surrounding the

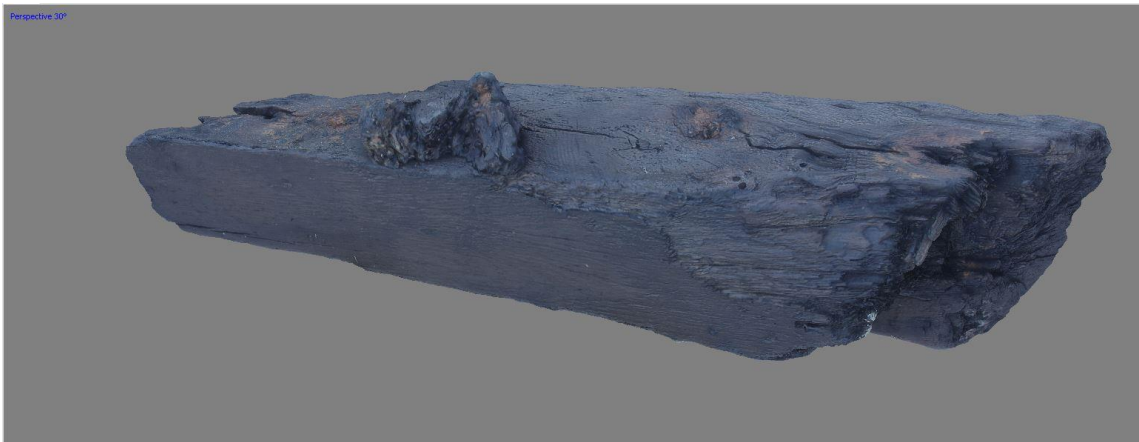


Figure 86: Computer vision photogrammetry model of timber BF 2 generated with Agisoft *Photoscan*.
Image by the author

timber would remain unchanged. It would produce a model, but it would be an inaccurate amalgamation of both sides of the timber. In order to produce the model seen

in Figure 86 it was necessary to go through each photograph individually and mask out everything except the timber. Figure 87 shows an example of what a masked photograph looks like when it is loaded into *Photoscan*. Once all of the photos are masked, the software only has to calculate overlap for the area specified, allowing a fully-realized model accounting for all sides.

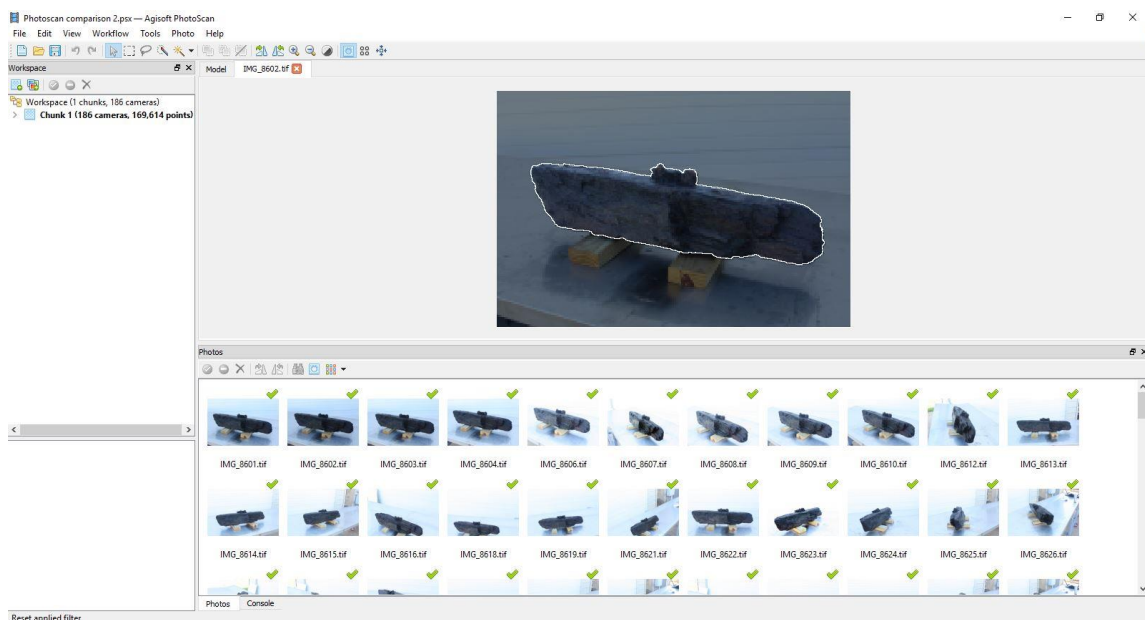


Figure 87: Each photograph of BF-2 was edited in Photoshop and a mask was produced, so that *Photoscan* would not process the background of the image. Image by the author.

In Chapter I, Richard Steffy was quoted as saying that “the parameters of research and reconstruction are defined by the quantity and quality of recorded information from which they are conceived” (Steffy 1994, 191). This concept holds especially true for computer vision photogrammetry. In order to achieve acceptable results for an archaeological photogrammetric model, the source photographs must be consistently excellent. The settings for the camera must be carefully controlled to

produce images that have the same depth of focus, lighting, and white balance. For waterlogged ship timbers, it is often necessary to have photographs that are slightly over-exposed to highlight surface details in the texture mapping phase of the modeling. The technical ability of the photographer and whoever is processing the photos is one of the hurdles that must be overcome to achieve acceptable results. A DSLR in manual mode is recommended for archaeological modeling, as it can be configured to mitigate variations in lighting and white balance.

One of the major advantages of using photogrammetry to document nautical archaeological sites is the versatility of locations where the camera can be used. There is no reason to discuss *in situ* documentation of high-definition laser scanning or contact probing for underwater sites, because at the moment, the instrumentation is not waterproof. Faculty and students from the nautical archaeology program at Texas A&M University have used photogrammetry to document several entire shipwrecks, often with multiple 3-D models to document the various phases of excavation. However, the focus of this dissertation is not *in situ* documentation, it is the documentation of ship timbers after they have been excavated.

Along with the lack of environmental constraints that cameras have over other types of scanners and their ability to create photorealistic texture maps, the equipment and software is much less expensive to use for photogrammetry. The professional version of Agisoft is \$3499, or \$549 for the educational license (Agisoft 2017). This, coupled with a mid-range DSLR and a license for a photo editing program means that high-quality photogrammetry can be achieved with a total investment of less than \$5000.

Compare this to the \$49,900 initially quoted for the FARO Edge CMM arm and \$29,900 for the FARO LLP, and \$5,750 for the initial license of Geomagic *Studio*, with \$2,250 per year for software maintenance (Luza 2017). In 2015, *Studio* was automatically switched over to *Design X* due to a series of acquisitions by its parent company, 3-D Systems (Rapidform 2012). (Note: FARO provided a substantial educational discount of over 30% for this project).

Despite its ease of use, aesthetically-appealing results, and relative affordability, not all of the characteristics of photogrammetry are superior to other methods of digitizing cultural heritage material. For one, the quality of the underlying model is not nearly as consistently accurate as that of high-definition laser scanning. Some sections of a photogrammetric model will often be comparable, but there are almost always ripples in the surface that do not accurately reflect the object being modeled because of subtle inconsistencies in the pixel values of the photographs. These slight blemishes in the model are almost never noticed though, because they are masked by the photographic texture map. Figure 88 shows the difference in quality between the high-definition laser scanned version of WTC timber BF2 and the photogrammetry model with the texture map removed. Note the areas that do not show the same level of detail.

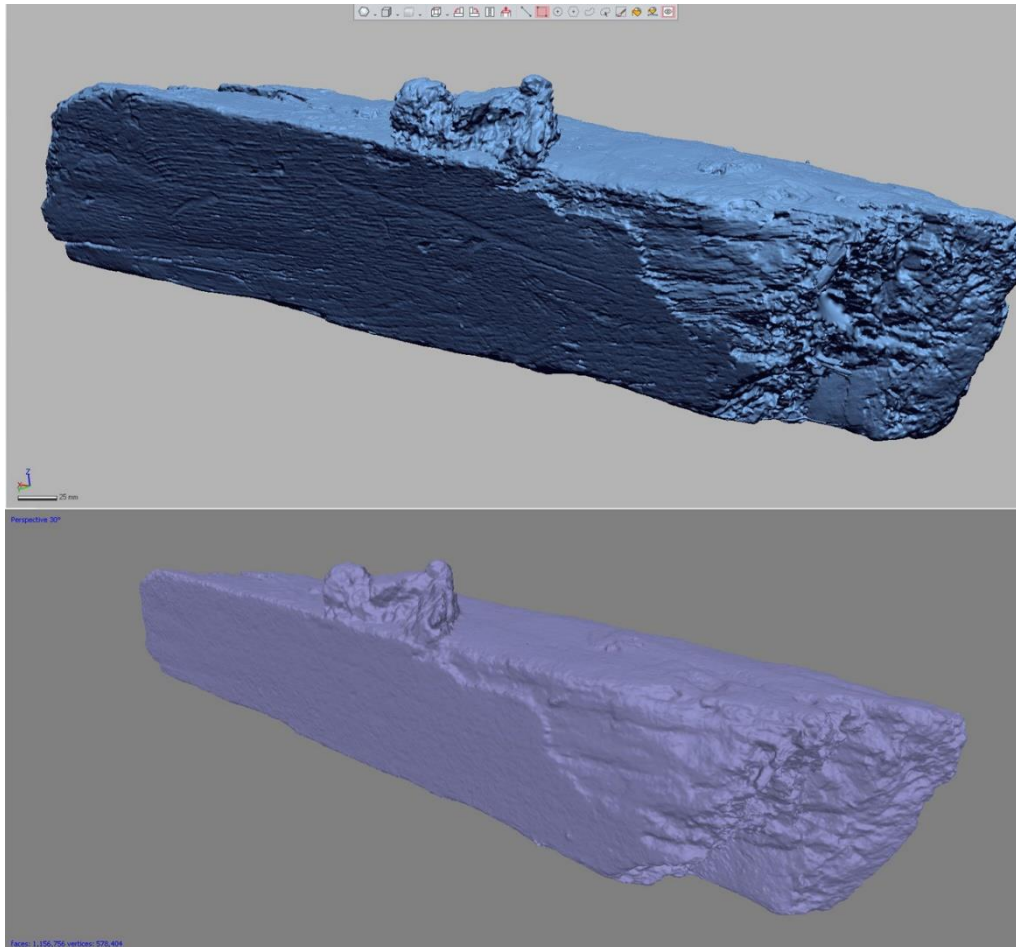


Figure 88: Comparison between high-definition laser scanning (top) and computer vision photogrammetry (bottom). Note the wood grain visible in the top model is interpreted as a grainy flat surface in the bottom. Image by the author.

The argument can be made that the textured photogrammetry model conveys the same information to the archaeologist as the laser-scanned model, or even possibly more information, given the quality of the texture map. It should be kept in mind though, that the texture map is calculated in the same manner as the underlying model, and any inaccuracies that are present on the surface of the model can be easily carried over to the

texture map. The realism of the texture map actually increases the difficulty with which errors can be identified and corrected for. The potential dangers of presenting hyper-realistic facsimiles will be discussed at length in Chapter VIII, but for now, the ability to convey potentially incorrect data very convincingly is something that should give all archaeologists pause, and inspire serious vigilance on the part of both the person making the 3-D models, and the people who are reviewing the work.

Contact Probe Digitization

Another commonly used alternative method for the 3-D digitization of archaeological ship timbers is the use of a contact probe. Contact probe digitization is done with a Coordinate Measuring Machine (CMM) arm. A CMM arm is an articulated arm with a fixed base and a series of internal sensors that measure how the arm is moved. At the end of the arm is a probe, and because the arm tracks its movement, the probe can be positioned anywhere in 3-D space and the location recorded. The location data is typically gathered in the form of a series of points that are used to create a nurbs curve in a program like *Rhinoceros 5*. As mentioned in Chapter V, nurbs models are created with mathematically-defined curves. This is a fundamentally different way to calculate a shape than a polygonal mesh. With a mesh model, the point cloud data that is gathered is used to develop vertices, which are connection points for the small triangles that connect together to create the mesh. The length of the triangle sides define the maximum resolution of the model. Smaller triangles mean a finer resolution, and larger triangles mean a coarser resolution. Because mesh models are built with component

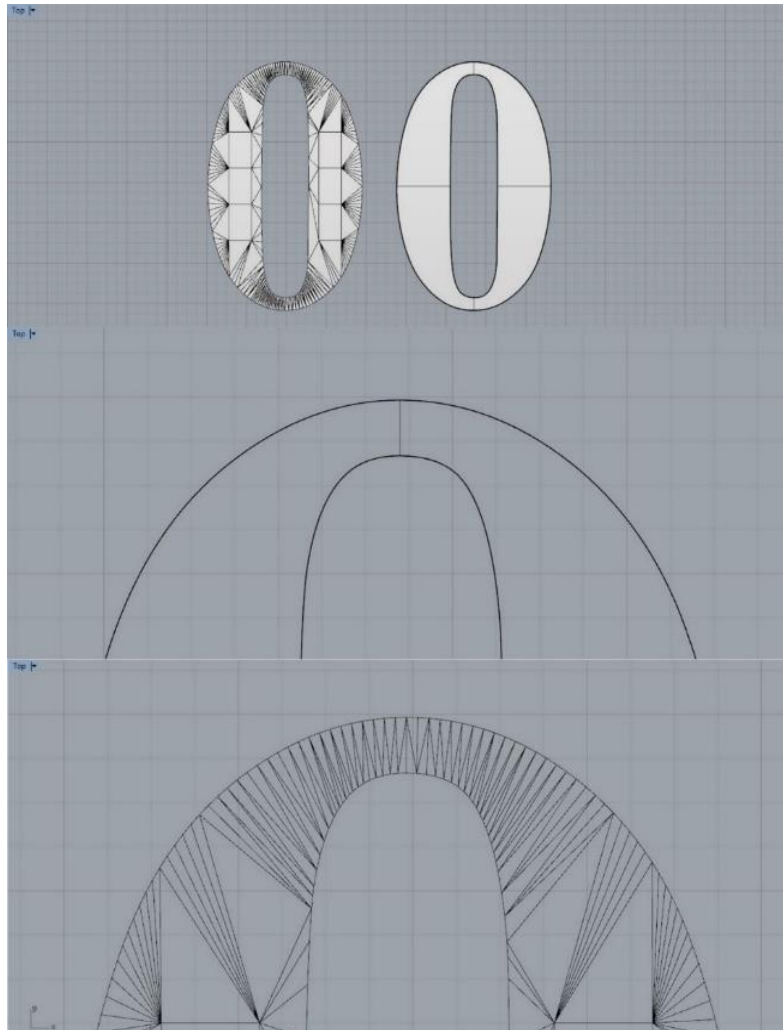


Figure 89: Mesh model of the number zero (top left) vs. a nurbs model of the number zero (top right). The middle is a zoomed in view of the nurbs curve, while the bottom is a zoomed-in view of the mesh curve. Note that the mesh curve is comprised of angled straight lines. Image by the author.

pieces that consist of a series of straight lines, to build a curved surface a mesh needs to use many small straight lines to convey the shape of the curve. On the other hand, a nurbs model uses a mathematical formula to define a curve. When a mesh model is enlarged, the triangle sides become longer, and the curves will look blockier, while with a nurbs model, scaling has no impact on the definition of the curves. Consider the mesh

and nurbs model of the number '0' in Figure 89. At a distance, both models looks like they convey the same shape. When zoomed in on the curve though, the straight line sections that the mesh uses to convey the illusion of a curve become more obvious.

To digitize a timber, the probe tip is dragged along the defining edges of a timber to outline the shape, and then any salient features such as fastener locations or tool marks are also recorded. There are two ways in which data can be gathered using the CMM arm. The first is to use the probe tip to carefully select hundreds of points on the surface of the timber, and then draw a line through these points to define the shape of the timber and any surface details. This is a very accurate way to create a model of a timber, though it is very slow, labor intensive, and there is a high potential for errors to be introduced when the points are used to create lines. A series of points can be interpreted in more than one way when connected to form a curved line, as can be seen in Figure 90. As long as the order is maintained when drawing the curve through the points, this method allows for the very precise placement of data points.

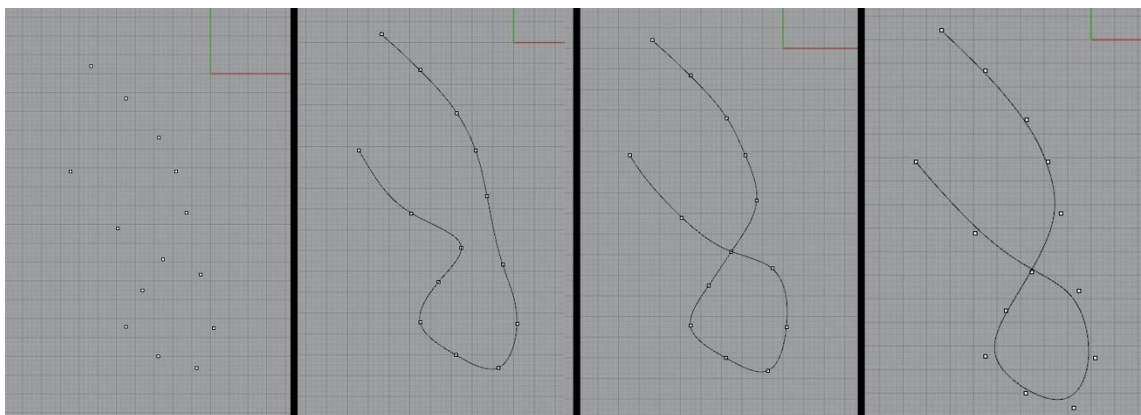


Figure 90: An example of how a series of data points can be interpreted in different ways. The points on the left were used to make the three curves on the right. Image by the author.

The second way is to use the probe to trace the timber in 3-D. The probe is placed on a starting point on the surface of the wood, activated, and while the probe is dragged along the surface, a line is drawn in *Rhinoceros 5* matching the movement of the arm until the process is stopped. Instead of picking a series of points, the arm is used to ‘draw’ the lines in 3-D. The benefit of doing this is that it is substantially faster than picking points, but the drawback is that it makes it easier to make an error while moving



Figure 91: Toby Jones using contact probe digitization to trace a timber from the Newport Ship Project. Reprinted from Friends of the Newport Ship, 2017.

the arm. This was the method used to successfully record the ship timbers for the Newport Medieval Ship, and that recording and subsequent reconstruction was what

inspired the WTC ship recording process (see Jones 2013). To achieve even acceptable results though, the digitization process must be carried out by someone with considerable shipbuilding knowledge to make the decision on which details to include and which to omit.

However the CMM arm is used, the points or curves are obtained manually, and consequently there are less data points used to define each timber than would be obtained with high-definition laser scanning, and therefore there is less information being conveyed in a nurbs model than a mesh model. This is not necessarily a drawback of direct contact digitization though, as the nurbs models produced only have the data present that the archaeologist using the CMM arm considered to be diagnostic; this is similar to the type of interpretation that is done when drawing an artifact by hand. Models created using high-definition laser scanning are not selective about which data is obtained and incorporated, and therefore there is a considerable amount of detail captured that is not necessary to the interpretation of the ship. That said, the potential for data being overlooked or misinterpreted is much higher with only selective data recovery, and there is no way to know what might be missing from the completed models without access to the original material.

Overall, making nurbs models with point data obtained with contact probe digitization is perfectly capable of producing excellent 1:1-scale 3-D models of ships at a fraction of the cost of high-definition laser scanning. The FARO CMM arm used for the WTC ship project is the same price as the laser scanning attachment, and therefore even a brand new CMM arm would be half the cost of a laser scanner with the LLP.

Additionally, the data for direct contact digitization is gathered directly in *Rhinoceros 5*, eliminating the need for the costly *Geomagic Design X* software. On the downside, it takes substantially longer than high-definition laser scanning and can be a rather tedious method to utilize. Along with the tedium, there is the potential for interpretation error, missing data, and erroneous curve construction when using the point-to-point methods.

Large-Area Survey Laser Scanning

Large-area survey laser scanning is a method for rapidly obtaining an accurate point cloud to represent an area that is too large to capture with high-definition laser scanning or contact probe scanning. The instrument itself works on the same laser triangulation principle as the LLP, just on a larger scale. The scanner is mounted on a stable surface, usually a tripod. The laser is projected at a variety of vertical angles using a rotating angled mirror, and the laser light is reflected off of the surrounding surfaces and returned to the scanner. The phase shift between the outgoing laser beam and the beam that is received back is used to measure the distance it travelled. At the same time, the scanner rotates 360° on its base, all the while recording the horizontal angle position while the scanner is running. By combining the distance with the horizontal and vertical angle data, data points are placed in 3-D with their relation to the scanner (Surface and Edge 3D Laser Scanning 2011).

The resulting point cloud is limited to whatever surfaces are within the line of sight of the scanner, and as such multiple scans are typically necessary to record an area. Once the individual scans are complete, the separate scans are registered to one another

to create a 3-D point cloud model. Large-area laser scanning has been used to record the archaeological remains of several ships, including the scanning of disarticulated timbers of the American Revolutionary War schooner *Royal Savage* (Schwarz 2015), as well as three separate in-process excavation scans of the WTC ship, as seen in Figure 92.



Figure 92: Large-area laser scan of the WTC ship during the excavation. The point cloud is made of six individual scans, as can be seen by the dark circles that represent the blind spots of the scanner. Reprinted from AKRF Inc. 2013.

The advantages of a large-area laser scanner are the extreme portability of the scanner and the ability to develop 3-D models of entire archaeological sites. For all intents and purposes, the documentation of an intact waterlogged ship is impossible to do with a LLP or CMM arm. Photogrammetry would be a comparable option, but as mentioned earlier, laser triangulation is more accurate than photogrammetry. The main disadvantage is the resolution of the models. Due to the large size of the scanning area,

the resolution of the point cloud for a large-area scan is lower than it is for a scan generated with a LLP. Analysis of the point cloud in Figure 92 showed the average distance between data points to be around 3-4 mm, or roughly 10% of the resolution of the LLP scans described in Chapter III. Because of the lower resolution, large-area scanning is not ideal for documenting fine details like fastener locations or tool markings on the timbers, but the utility of having a 3-D representation of the ship *in situ* at the excavation site was a great help in the first draft of the virtual reconstruction, and the

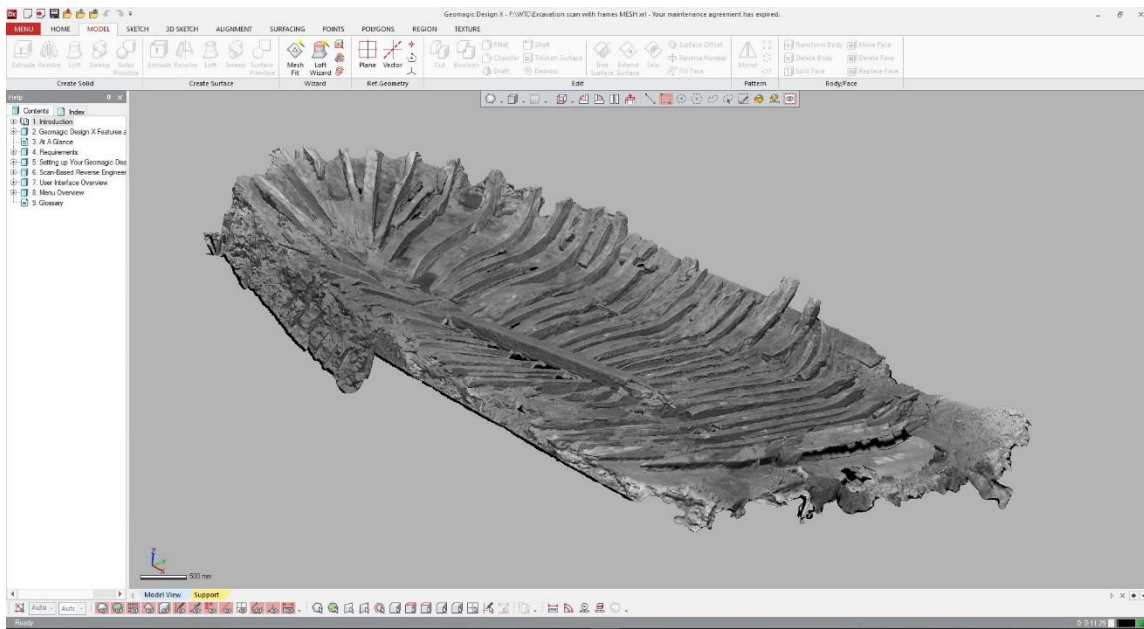


Figure 93: Mesh of the mid-excavation large-area laser scan. The aligned scan data that was included in the AKRF report was imported into *Design X* and meshed. Image by the author.

scans can be used to create accurate and detailed site plans and drawings.

Additionally, the point cloud that is gathered by the large-area scanner can be imported into *Design X* and meshed (Figure 93). This mesh can be compared to the final reconstruction to show the amount of deformation that occurred during the site

formation processes, and can also be used to verify timber orientation and placement.

The WTC ship was scanned this way at three stages during the excavation, for each major layer that was removed. The first scan was of the ship after it had been uncovered but was still intact with the ceiling planking still in place, the second was with the frames in place but the ceiling planking removed, and the third scan was done when only the stern knee and outer planking were still in place.

CHAPTER VIII

ETHICAL AND PHILOSOPHICAL CONSIDERATIONS WITH DIGITAL HERITAGE

What is an Accurate 3-D Model?

With over 42 million points in its point cloud, the plank seen in Figure 94 is among the most well documented 18th-century American ship timbers in the world. But even with 42 million points, the model is only as useful as it is accurate, and its accuracy depends on the equipment used, the people doing the scanning, and the post-processing of the data. Verifying the accuracy of the models was discussed in Chapter III, but considering the overall accuracy of a scan does not end with merely verifying that the data points reflect the object scanned. The plank in Figure 94 is obviously inaccurate in certain regards, most notably that it is blue. Even with this glaringly obvious

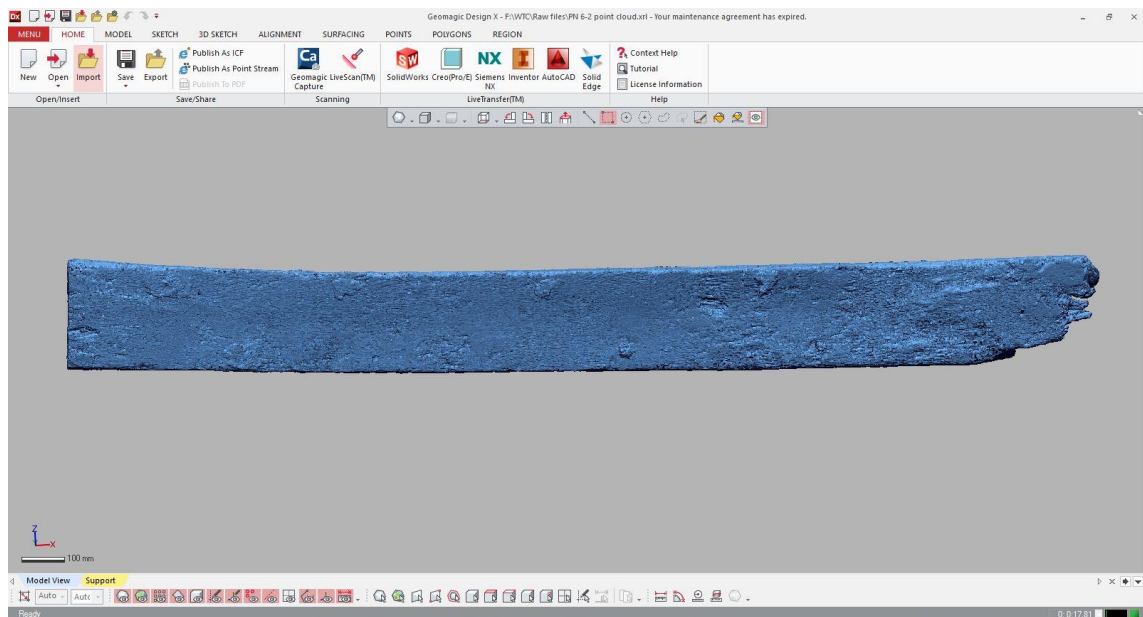


Figure 94: World Trade Center ship outer plank from the sixth strake, starboard side. Image by the author.

inconsistency with reality, at first inspection, it is easy to assume the plank is accurate. It is a highly-detailed model of what does in fact resemble a plank of wood. Given that it is possible to consider something accurate in the face of an obvious flaw is a hurdle that must be overcome when assessing 3-D models; certain aspects of inaccuracy may be ignored, but they need to be done so consciously.

It is important to distinguish between accuracy and precision when it comes to the evaluation of archaeological documentation. Using a dart board as an example, accuracy is the ability to hit the bullseye, while precision is the ability to hit the same spot anywhere on the board over and over. Ideally, archaeological documentation will be both, but while precision is easy to determine, accuracy is sometimes less tangible. Consider the models of planks that were created for this project. A 5 m long by 0.5 m wide plank required six separate scans to capture both sides. Each individual scan was extremely accurate, but when stitched all together, if there were any variations in the curve of the plank that occurred between the scanning of one section and the next, the final aligned model would not accurately reflect the shape of the timber. It is possible for the individual parts of the scan to be very accurate and the overall model to be inaccurate.

If there was no variation in the curvature of the plank and everything aligned perfectly, would that be an accurate model? The real plank can curve and flex, while the digital model of that plank cannot. Additionally, would a perfectly-aligned model be precise? Would someone else scanning that plank choose to mitigate the flexibility of the wood in the same way? Not likely. A second scan, even one that was done with no

variation in the curvature between one side and the other would almost certainly have a slight variation in curvature when compared to the first scan. This knowledge leads to a very interesting question about the nature of our documentation: how do we define accuracy when it comes to documenting flexible materials? Is it better to depict an object in a way that emphasizes all possible information but is not ‘accurate’, or is it better to depict it in a way that is as accurate as possible but perhaps obscures information? For instance, if given the task of making an accurate drawing of a fitted bed sheet, would it be better to draw it flattened out, noting that the corners are bunched from the elastic, or would it be better to draw it with the corners cut and splayed out to allow them to lay flat? With wooden planks, is it better to manipulate the models to ‘flatten’ the planks, or to show them distorted? How can the ability of the wood to flex be taken into account?

The discussion of how to define accuracy extends into photography and texture mapping as well. If a photogrammetric texture map is applied to a 3-D model, or a photograph of an artifact is taken, how important is color temperature, saturation, hue, and white balance to presenting an ‘accurate’ image? Pigment is typically too complex to be reduced to a single wavelength of visible light to define its color, so how can the ‘true’ color of an object be established? Should all shadows be eliminated, or should they be kept in a way that exaggerates surface features? Is an accurate photograph or texture map one that mimics the way the object would be viewed *in situ*?

There is no objectively correct answer to what makes a model truly accurate or not, but these questions are very important to ask, because they help delineate what assumptions are being incorporated into archaeological documentation. When planning

for this project, the assumption was made that the high-definition detail obtained from the LLP would be advantageous for the study of the WTC ship, and that the information would be, at a minimum, as accurate as previous methods used to record ship timbers. The lack of texture mapping and color information was deemed an acceptable loss, as this method was seen as a replacement for drawings or CMM tracing, neither of which include this information, and not photographs, which do.

The Diminishing Returns of Resolution

The resolution of a point cloud refers to the density of the data points that are obtained. The closer the individual data points are to one another, the higher the resolution. As resolution increases, the number of data points also increase. As stated in the configuration settings in Chapter III, the grid resolution for the LLP was set to 0.35 mm. At the time of writing, there were over 150 individual timbers scanned, and with an average of roughly 10 million points per timber, there are over a billion data points for the WTC ship. Over a billion points of data allows for a virtual reconstruction to be done with unprecedented access to the minute details of the timbers, but is this much data necessary? If the ship had been scanned at 0.10 mm instead, there would of course be more data points, and conceivably, smaller and smaller details would be recorded, so would that have resulted in a more accurate reconstruction?

There is a theoretical point at which increasing the resolution of the model no longer delivers any tangible increase in information. In reality, that threshold is impacted by a variety of factors, the most significant being the research questions being asked. If

the focus of the research is to reconstruct the ship, this dissertation shows that not only is the resolution utilized here perfectly acceptable, it actually needs to be reduced to cope with the limits of the computer resources available to manipulate the model. However, if

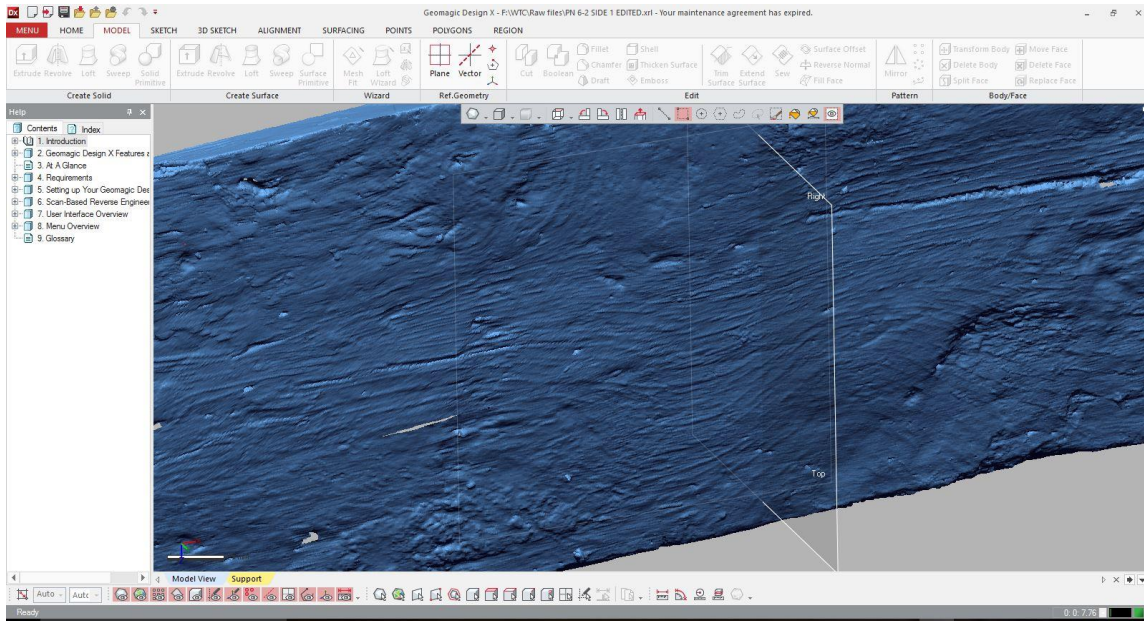


Figure 95: The full resolution point cloud for an outer plank with visible wood grain. Image by the author.

a study is conducted using this scan data in the future, there may well be utility in having maximum-resolution scans. Someone wanting to study the wood grain patterns for the planking could utilize the full-resolution point clouds to easily see that level of detail, as can be seen in Figure 95. The WTC ship data was acquired at a resolution that was not necessary for this study, but will hopefully stand the test of time as an archival-grade model. Robert Warden, the director of the Heritage Conservation Center at Texas A&M University, has proposed that there should be a standard set for ‘research-grade’ 3-D models (Warden 2017). He suggests that all data should be kept in point cloud form, as

this is the rawest form of data and does not introduce the potential interpretive errors that can arise during the meshing process, and that all color data should be rigorously checked for accuracy using color cards. It is an interesting idea, though it would be difficult to enforce as a standard.

A slower, more expensive scanning process today may allow a hypothetical future researcher to utilize higher-quality data, but whether or not that is worth the effort depends on the resources of the project. Deciding on the quality of the scan for 3-D documentation now is not unlike the decisions made by photographers during the shift to digital cameras. Early digital cameras had relatively low-resolution CCD sensors (0.5MP – 2MP, depending on the cost of the camera) and the images produced during the first several years of digital photography would not be acceptable to most researchers today (Rick 1999). There was never any official minimum resolution set by the archaeological community, but research done today based on digital photographs from the late 1990s is much easier if higher-end cameras were used with maximum resolution settings.

It seems intuitive that the higher the resolution of the photo, the better that photo will be, but after a certain threshold is reached, pixel density does not necessarily yield additional information. If the lens of the camera is not able to resolve the light entering beyond a certain pixel density, then increasing that pixel density will achieve nothing. Likewise, the resolution achievable with the LLP depends on the CCD sensor and the wavelength of the laser. After the ant infestation fiasco mentioned in Chapter III, the CRL purchased the newest version of the FARO LLP, and among the technological improvements introduced in the newest model was a CCD sensor that has the ability to

utilize a blue laser, which has a shorter wavelength than the red laser in the older model and can therefore be used to resolve smaller data points. This meant that a higher scanning resolution *could* have been achieved with the timbers scanned with the new LLP, but the configuration settings were kept the same, as a higher resolution was not deemed worth recording. With 3-D scanning, the object being scanned greatly impacts the utility of increased resolution. When scanning something complex like an incised pottery sherd or an astrolabe, higher resolution is prudent to ensure that there are sufficient data points to convey all surface detail. If, on the other hand, a glass beer bottle were being scanned, then the smooth surface can be conveyed just as easily with a low-resolution scan as a high one. For the timbers scanned for the WTC project, the 0.35 mm grid size was determined to be a perfectly acceptable resolution, regardless of the ability of the scanner.

Though there is no blanket statement that can be made for what the ideal resolution settings are for 3-D scanning archaeological material, as a rule, the resolution necessary for achieving the research goal of the project should be determined, and the resolution for the scan should then be set slightly higher. The extra time it takes to scan and process a slightly more resolved model is much less than the time it would take to rescan and reprocess an object if it was determined after the fact that the resolution was too low to provide the relevant data points.

Realism as a Ruse

Once an acceptable level of resolution is set, there is a tendency when viewing a high-resolution 3-D model of an object to assume that it is an accurate depiction. This is not necessarily the case. Figure 96 shows an outer plank that was scanned in four

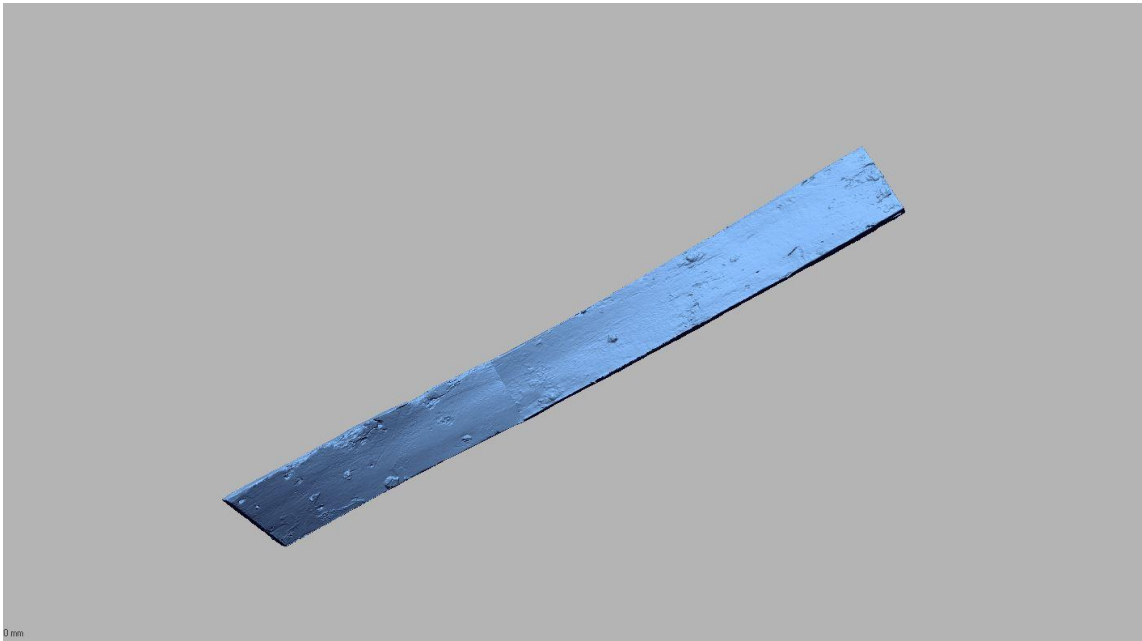


Figure 96: A purposefully misaligned plank. Note the odd seam in the center of the plank. Image by the author.

sections, and then purposefully misaligned and meshed. The final product looks suspiciously shaped for a ship plank, but the model is very convincing without careful examination of the seams between the scan sections. The presentation of 3-D data presents a challenge in that the so-called ‘wow’ factor can tend to overcome healthy skepticism about the veracity of the model.

More than that, it takes a greater degree of skill and effort to create a good 3-D model than it does a bad one. This is not the case with photography, and as such, when a

study is published with photographs, the overall consensus of the archaeological community is that it is reasonable to believe that accompanying photos accurately represent reality. It is possible that an unscrupulous researcher could alter an image to make their argument more convincing, but in reality, this is not a pressing concern. Assuming that there is no diabolical conspiracy in archaeology today to present ‘alternate-fact images’, the technology of digital cameras has reached a point that even with no concept of how cameras work, the average person can take a photograph that will convey detail with perfectly reasonable accuracy. This is not the case when it comes to 3-D modeling, at least not yet. Consider Agisoft’s *Photoscan* software for photogrammetry; it is refined enough that if you put in enough photographs, an impressive 3-D model will be generated, but the chances of that model meeting even the

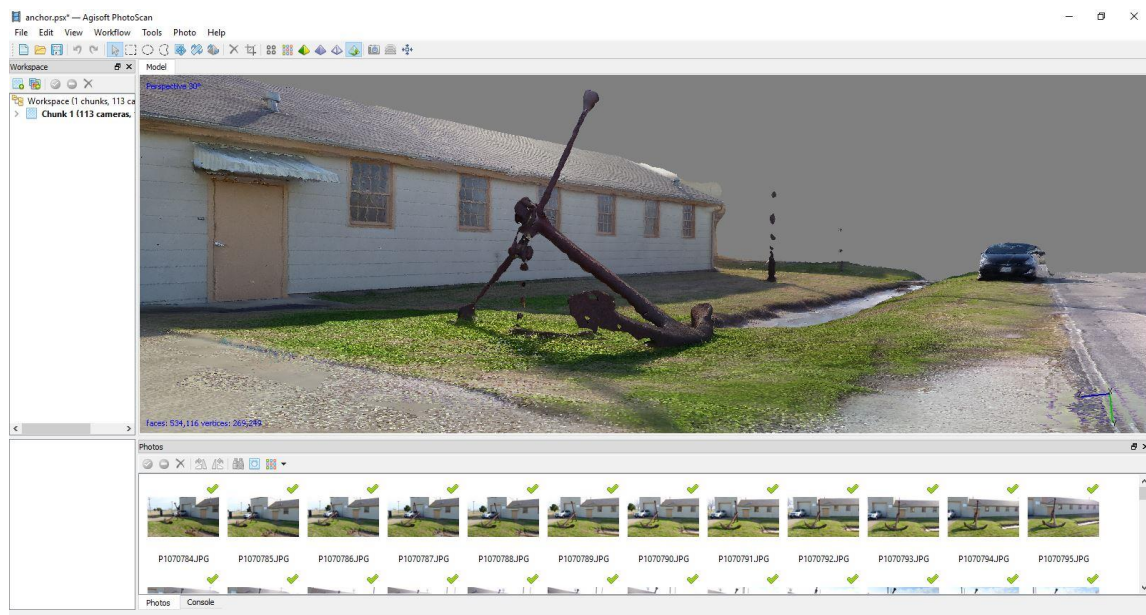


Figure 97: A photogrammetry model of the CRL with obvious errors. Image by the author.

barest standards for archaeological documentation are low.

With \$60 and a smartphone, a student can produce 3-D models with the standard educational version Agisoft *Photoscan* that appear to be detailed enough to fool most casual observers. This is where problems can arise. There are currently no quality control standards by which 3-D models of archaeological sites and artifacts are held, and there are models of archaeological sites currently being published that have obvious incongruences with reality. Figure 97 shows a screen shot of a hastily-made photogrammetry model that was created with photographs taken outside of the CRL at Texas A&M University. Even the most cursory glance reveals a number of glaring errors. The chain for the anchor appears to be a series of blobs. The driveway on the left of the screen has obvious blurry sections. The utility poles to the right appear to be blobs floating from the earth. Most obviously, the sky and background are completely missing, and are represented by a flat gray. Now, looking at the model again, it might seem reasonable to conclude that while the model has its faults, we can safely assume that there is a building with an anchor in front of it, and there is a black car parked down the road. Is there? Is it reasonable to make assumptions about an image that has such obvious faults? Do we assume that the dimensions of the anchor will be correct, even though the chain appears to defy the laws of physics? Where should we draw the line on deciding which areas of the model represent usable data and which are erroneous? What is to stop the next person from drawing it somewhere else?

Because they are so visually impressive, it is easy to approach 3-D models with optimistic cognitive dissonance. Because the models look very realistic, and they

represent such a promising leap forward in the admittedly tedious world of archaeological documentation, it is tempting to overlook strikingly obvious faults and attempt to cherry pick what data is usable and what is not. It is unacceptable to see a portion of a model that obviously cannot exist in reality, and then to simply dismiss that and accept the rest of the model. The algorithmic processes by which *Photoscan* selects common points between overlapping photos are not informed by which parts of an archaeological feature are diagnostic and which are not. The overlap is derived from the photon intensities on a group of adjoining pixels on the CCD sensor. These photons do not enter into the camera lens with any sense of priority, and they are not working to make sure that the models being produced will be the ones that answer research questions. Models that are obviously wrong should not be granted conditional passes based on which parts of the model look convincing enough to stay.

This is not just an issue with photogrammetry; the laser scanning technique used for the WTC project is rife with potential for erroneous data. If there is a part of any timber that was not scanned, that part will not become part of the model. This might seem obvious, but scanning day in and day out for months on end means that sometimes the overlap between scans is not adequate. Further, the editing of the point cloud necessitates some level of intentional deletion to eliminate things like supports, the scanning surface, etc. It is entirely possible for the user to accidentally delete too much data, and once the meshing process fills these gaps in the model to create a watertight mesh, the model moving forward will be truncated in a way that would never be detected without access to the original material. The gap filling is usually presented as a different

texture, but if the resolution is too low, to the untrained eye a spike hole might look like a mere divot in the wood. Even if it were rife with errors, the end-result model of the WTC ship is so compelling that it would be easy for error to be overlooked. (fear not, it is not rife with error; considerable effort was taken to ensure that). The goal of this project was to document the timbers in a way that represents an increase in the quality and quantity of data available for this ship over traditional techniques, but that does not mean that this project should be immune from rigorous assessment and critique. If a model does not look quite right, it must be examined for faults.

Misrepresentation of Data

The rapid adoption of digital means of documentation for cultural heritage materials demands consideration of the consequences of having our collected history stored in a medium that is potentially prone to corruption and distortion. As mentioned in the *Accuracy Verification* section of Chapter III, even subtle manipulation of digital data can lead to entirely different archaeological conclusions. In a field where the difference of a centimeter might represent a century of data, the validity of digital data is frightfully fragile and prone to manipulation. Add to that a ‘publish or perish’ academic environment (Rawat and Meena 2014, 87-89), and the pressure to ensure that data is complying with the expected results instead of the other way around leaves serious potential for abuse.

The reconstruction of the WTC ship remains outlined in this document was done with the overt objective of understanding as much as possible about the ship from the

data that could be obtained from the timbers. Whatever the outcome, there were no financial or professional consequences at stake if an initial assumption was proven incorrect. There was nothing that could have been found in the data that would have adversely impacted the CRL or anyone working there. This was a rare and ideal situation for producing reliable data that accurately represented the physical remains of this particular ship, but by no means does an ideal situation prevent erroneous data. Chapter III and IV describe in detail the substantial data optimization and model manipulation that takes place even when the intention is to present the data as accurate to real life as possible, and every step of the way introduces new potential for error.

What if the situation were different? What if funding or job security were on the line, or if the initial assumptions about the wreck were proved to be incorrect there would be serious consequences? Without giving over too much to conjecture and hypothesizing about what type of scenario and what type of scholar might be prone to intentionally misrepresent data, the fact is that it does happen with regularity across scientific fields, and 3-D models are particularly vulnerable to falsification (Haug 2015). The ease with which someone can falsify digital data to prove their point in this medium is something that needs to be taken into consideration when reviewing and publishing papers that utilize this data to make their case. How one might go about detecting and verifying digital fraud is still unknown territory. Without access to the primary materials, it can be incredibly difficult to identify alteration made to the virtual model.

There are three main ways that a digital model can be altered: distortion, deletion, and addition. Each can be justifiable and necessary for an ethical representation

of digital cultural materials, and each can also be abused to misrepresent the source data. When writing about 3-D modeling, it is important for authors to be explicit about the alterations that were made with the data they are representing. Distortion of data describes changing the shape or scale of a model to better fit the context it is in. Deletion of data is when parts of a model are deleted. As seen in Chapter III, a fair amount of intentional deletion was necessary for the processing of each and every model in this project. Deleting spurious noise, scanned information that is not part of the object being scanned, and excessive overlap is all vital to producing accurate models. Deletion can be intentional or accidental during processing, but once something is deleted from a digital model, there are no traces of that part of the model left. It is important to maintain separate files for all stages of data manipulation to prevent permanent data loss in the case of accidental deletion. Deletion can also be done intentionally to change the model in a way that changes the intellectual impact of a study, for example if an owners or a makers mark on an object were deleted, the provenance or date might be lost.

The addition of data is the type of data manipulation most fraught with ethical peril. Anyone who has seen a big-budget film in the last decade can attest to the incredible realism that computer-generated graphics have achieved. Using the same techniques, the virtual reconstruction of digital objects can be done convincingly enough that the interpretations of the digital artist can be easily mistaken for primary data. Recent projects like the digital reconstruction of the Massalian Treasury in Delphi based on large-area scans, and the Richmond Caligula sculpture reconstruction (Figure 98) that used a FARO LLP similar to the one used for the WTC ship project show the incredible



Figure 98: Digital Sculpture Project: Caligula. The original Roman sculpture Richmond Caligula (left). The 3-D scan (center) The digital restoration (right). The model was made Matthew Brennan at the Virtual World Heritage Laboratory. Reprinted from http://www.digitalsculpture.org/papers/frischer/frischer_paper.html

potential for reconstructing historical objects (Mulliez, Jockey, & Vincitore, 2013; Frisher, 2013). These reconstructions were informed by historical research and the input of several scholars, and they offer a way to make cultural heritage exciting, dynamic, and more accessible to the public than ever before. In doing so, they also present an ethical dilemma in that they present a very convincing interpretation that may not represent reality.

There are three major criticisms leveled at virtual recreation in archaeology. The first, which was made by Paul Miller and Julian Richard of the University of York, is that a virtual reconstruction suggests a sense of reality that either has not been

documented or did not exist (Miller and Richards 1995). If a reconstruction is convincing, most people will accept the reconstruction as reality, when at best, it is merely an educated guess. A very well-researched digital reconstruction presented by established and respected scholars can be even more misleading than intentionally-distorted models, because of the proclivity of academic scholarship to build on accepted theories and interpretations. If the reconstruction of Caligula in Figure 98 becomes widely accepted, it can be very difficult for future researchers to even formulate research questions that might contradict the model. Jeffery Clark of North Dakota State University warns that reconstruction “conveys a false sense of knowledge. This in turn makes it unduly difficult for new interpretations that stand in contrast to the conventional reconstruction to get a fair hearing, thereby impeding advances in our understanding” (Clark 2010, 66).

The second criticism is that digital reconstructions are inconsistent with how they differentiate between the reconstructed portions of a model and the original data. Reconstruction can be beneficial to explaining a theory or to make education more exciting, but it should be done in such a way that the reconstruction is obviously offset from the primary data. This can be done via differential coloration, wireframe, semitransparent representation of reconstructed areas, or perhaps an augmented reality application where the reconstruction appears over the original material when viewed through a tablet or phone screen. If reconstruction must be done, it is essential that it is done in such a way so as to make interpretation obvious.

The third criticism aimed at reconstructions is the omission of a temporal range. This does not apply to something like a statue of Caligula, which is intentionally frozen in a moment of time, but when we begin to try and reconstruct a ship or an archaeological site, these are things that do not represent a specific slice of time; they are the result of long periods of use and occupation. Any model would have to not only account for that, but it would have to justify why a particular moment in history was chosen to be depicted. This can be conveyed by animations that suggest the passage of time, but it is always highly interpretive and therefore fraught with the possibility of inaccuracies.

Who Owns the Past?

In October of 2015, two German artists, Nora al-Badri and Jan Nikolai Nelles claimed that they hid a modified Microsoft Kinect motion sensor in their coats and surreptitiously scanned the bust of Egyptian Queen Nefertiti at the Neues Museum in Berlin (Wilder 2016). In December of 2015, they released the scan data for free to the world, in effect liberating the sculpture from the museum (Nelles and Al-Badri 2015). With the scan data, anyone could download and print a copy of the bust, and several full-sized copies were printed and delivered to Egypt, where it originated from. Their motive was social justice, saying, “For the first time since the sculpture was excavated and stolen over 100 years ago, the iconic artefact will be shown in Cairo” (Nelles and Al-Badri 2015). Though the truth behind the claim that they scanned the bust has been called into question (the Kinect does not have near the resolution seen in the model, and

the model is suspiciously identical to the 3-D scan in the museum archives), the question about the ownership of digital versions of cultural heritage materials that was raised is an important one to consider.

With the Mona Lisa in Paris, the Parthenon in London, and the bust of Nefertiti in Berlin, there is a long and unfortunate history of military powers appropriating cultural material from disadvantaged peoples and displaying them in their museums. These museums are notoriously protective of their collections, and until very recently, the only way for citizens to see these collections was to either visit the museum or to look at photographs. With the advent of 3-D scanning, especially computer vision photogrammetry, it is now possible to create a detailed 3-D model of artifacts and share them with anyone, either digitally or printed in 3-D. For objects that are stored away from their place of origin, this could serve as a way to mitigate the tension between the



Figure 99: Replica of the human-headed winged bull from Nimrud, Iraq on display in the Colosseum in Rome. Reprinted from NPR, credited to Andreas Solaro, AFP Photos.

conflicted cultures and increase access to heritage materials.

The ability to create models of cultural heritage materials is not limited to items in museums. In October of last year an exhibit opened in the Colosseum in Rome featuring full-scale 3-D printed replicas of cultural artifacts from Syria that were destroyed by the so-called Islamic State (Figure 99). The researchers who created the models used photographs from many sources to build photogrammetric models. They may have ‘saved’ these priceless historical artifacts, but they did so in a way that resurrected them far from the people who originally owned them. What about things that are sacred to people? Statues of gods or holy places can also be easily scanned and reproduced, and once the data is released online, there is no redacting it. The consequences of the digitization of the sacred is something that will have to be considered on a case-by-case basis with care and respect, working with cultural groups to ensure that the dissemination of information does not turn into exploitation.

CHAPTER IX

DISSEMINATION OF DATA

The most important part of archaeology, like any other academic pursuit, is the open distribution of information. The means by which archaeological data is shared is typically through peer-reviewed research papers, academic publications such as this dissertation, books, popular magazine articles, documentaries, and museum displays. Ideally, the distribution of the 3-D data generated from this and other digitization projects will be done in a way that takes full advantage of the format without sacrificing compatibility with legacy data, or palatability to the archaeological community and the public. To ensure legacy compatibility, the 2-D timber drawings described in Chapter V were created to allow direct comparison between the WTC ship timbers and those of contemporary ships that were documented with traditional 1:1 tracings. To ensure palatability, a lesson can be taken from the engineers at Apple or Google: the data must be presented in a way that feels intuitive and does not require technical expertise to utilize. Nobody would use an iPhone if they had to laboriously program in each command, no matter how powerful and portable a computer it may be. In the same way, the 3-D models of the ship timbers for this project should be distributed in a way that makes them dynamic and informative without being confusing or burdensome.

There are two main methods of sharing 3-D models. They can be presented in a way that is interactive, or in a way that provides a guided tour of the model without user input. For interactive presentation, there are two principle ways in which 3-D models can

be shared: online or offline. An easy way to conceptualize the difference between these two distribution methods is the difference between streaming a movie on Netflix versus having a physical copy of the movie. For the online sharing model, the data is hosted on a server, and users can access the rendered file via the internet. This allows people without access to modeling software or who do not have powerful enough computing resources to still access and study the data. For data that is shared offline, the data files are physically on the computer of the user, and the software and hardware requirements to open and manipulate the model are the responsibility of the user.

Online Distribution of Interactive Models

There are a number of outlets for online distribution of 3-D data, separated into two main types of hosting options. First, there are companies that provide a hosting service, in which a user-generated 3-D model is uploaded to the company's server, and the company provides access to a viewer by which others can access the model. The second type of online hosting differs only in who does the hosting of the models. Instead of sending the model to an offsite server, the models are hosted on a local server, and then access is provided to outside users via a viewer.

Of the first option, one of the more popular options on the market right now is Sketchfab. With a free account, users can upload files up to 50MB, and annotate the model at five different locations. With a paid 'Pro' account, the model size limit is increased to 200MB, and 20 annotations per scene are allowed (Sketchfab 2017). Sketchfab is popular because it is easy to use, and the viewer is easily embeddable into

social media platforms like Twitter or Facebook. Not having to maintain the server and website makes the sharing process nearly painless, but as with all things, there are drawbacks to using a service like this as well. The largest drawback to using a service like Sketchfab is the licensing of the models. According to their terms of services, using Sketchfab grants the company “worldwide, non-exclusive, royalty-free, perpetual, irrevocable, sub-licensable (through multiple tiers) right and license to use and adapt the User Content for the purposes of developing, distributing, providing, improving, and promoting the Services” (Sketchfab 2017). This may or may not be acceptable for the use of academic data, depending on the funding source and ownership of the cultural heritage material, and the preference of the archaeologist.

The licensing problems are ameliorated with the second option, which is where the institution that creates the 3-D models also hosts the data files and provides access

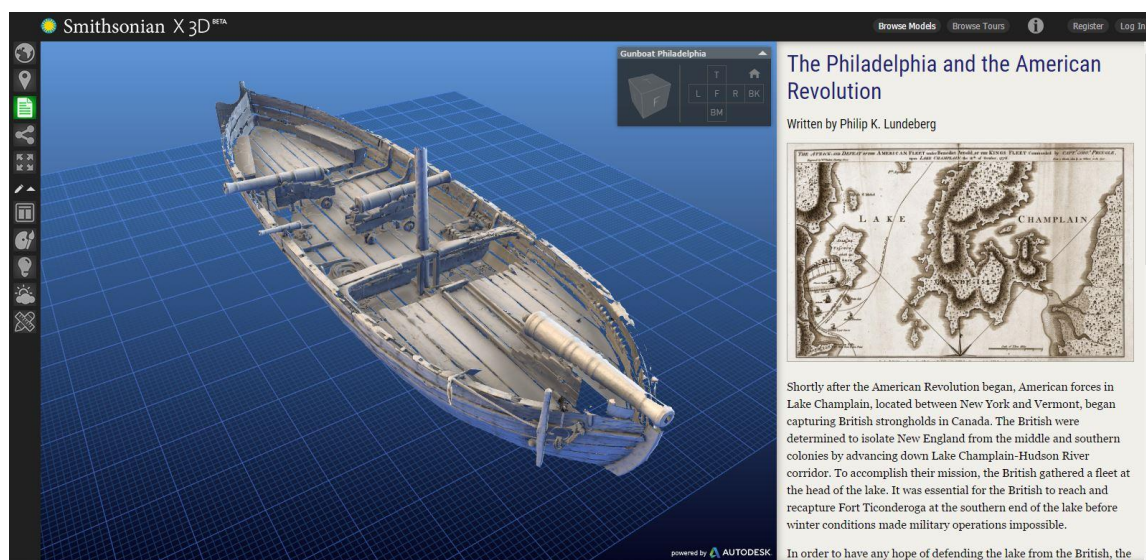


Figure 100: Screenshot of the Smithsonian X 3D website, with a fully interactive model of the Benedict Arnold's gunboat *Philadelphia*. Reprinted from Smithsonian Institution 2017.

via a third-party viewer so the models can be studied. The resources and technical know-how required to do this mean that this type of hosting is typically relegated to large institutions with the financial resources to do so. An excellent example of this method is the Smithsonian X 3D program, seen in Figure 100, which utilizes an Autodesk-powered viewer to embed digitized museum artifacts into the Smithsonian website (Smithsonian Institution 2017). The benefit of this option is that the legal control of how the 3-D models are used is not sacrificed to an outside institution, and full curatorial control is maintained by the institution hosting the files. The drawback of hosting and displaying the data is the cost of creating and maintaining the website and servers, as well as the time and technical skill it takes to do so.

Offline Distribution of Interactive Models

The other major way to share interactive 3-D models is to share the 3-D file directly with whomever wants to use it or study it. This can be done either in a way that allows a user to alter the source data of a model, or in a way that only allows viewing and interaction with the model. Either way, this data is still digital, and therefore is still often shared via the internet. The ‘offline’ designation refers to the fact that the model file must be downloaded to the physical hard drive of the user, and does not reflect the method by which the file is delivered.

If the desire in sharing the 3-D model is for the user to be able to edit the source data, i.e. delete parts of the point cloud, alter the alignment between scans, etc, then the entire source file is shared. This is typically done in one of the two more universal file

types, .stl or .obj, as mentioned in the *Mechanics* section of Chapter IV. Depending on the access to computing resources that the end user has, the format that the data was captured in can be sent without re-formatting the file. Because of the large size of many of these files, they can be difficult to email, so if they need to be shared privately, a cloud storage service like Dropbox or Google Drive is needed to share files to a remote site. If access to the files is intended to be open to the public, 3-D file sharing sites like Makerbot's Thingiverse.com and Autodesk's 123Dapp.com offer free file hosting and downloads.

If the desire is to limit the ability of the end user to alter the model, an excellent option for sharing is an Adobe 3-D PDF. Adobe's PDF reader is ubiquitous on computers and free for download, and it has the ability to view, manipulate, and measure 3-D models. Several 3-D modeling programs have built in 3-D PDF exporting abilities, including *Design X* and *Photoscan*. This is an effective way to share 3-D models with a non-tech-savvy audience, and 3-D PDF's can be protected against editing. Larger PDF files will still tend to bog down most personal computers, so a decimated version of a high-definition laser scan model is typically the best practice for sharing.

Non-Interactive Distribution: Animating the Model

If the information being shared about a 3-D model would be better conveyed with a non-interactive guided tour than a manipulatable model, setting up a basic animation may be the best way to share it. *Rhinoceros 5* has modest animation capabilities, and Adobe *Photoshop* can animate 3-D models as well. A well thought out

animation can take the viewer around or through the model, highlighting the salient details, and narrating the whole tour with on-screen text or audio. Short animations are an excellent way to convey specific parts of the model during presentations of the data, and they can easily be shared without any concerns about compromising the source data of the 3-D model. For a step-by-step guide to animating a 3-D model, please see Chapter V of Yamafune (2016).

Curation

No matter how the data obtained during a 3-D digitization project is shared, long-term curation of that data is a consideration that must be made. Two complete copies of the WTC ship project data were stored on three separate computers, and an additional backup copy was kept on a 2TB external hard drive. Having two complete copies on each computer allowed for a staggered backup procedure; the data acquired each week was updated to one of the back-ups on each computer one week, and the following week the other back-up was updated. For long-term storage, an additional external hard drive will be used, and the data will also be copied over to the CRL master server maintained by Texas A&M University's Information Technology department.

There are concerns for the long-term preservation of digital media. Hard drives are prone to eventual failure, and the amount of data produced by this project would require over 100 archival quality DVDs to store. The external hard drives that hold the master back-ups for the data will have to be checked annually to verify the data is still intact and to prevent the bearing oil in the drive from drying out and causing the disc to

seize (Henry 2015). Along with the physical preservation of the data, another issue that could interfere with long-term longevity is the stability of file formats. The raw, highest-quality data for this project was saved in the Design X proprietary .xrl file format, which is a holdover file format that was used for the previous iteration of the software before acquisition by Geomagic, *Rapidform XOR*. It is possible that this file format will eventually become obsolete, and therefore it is imperative that file format compatibility is maintained on an annual basis. If the time comes when a new format is implemented to replace .xrl files, the data should be copied into the new format, preserving both formats.

With a rare paper document, long-term curation demands strict care and very limited handling and manipulation. Digital data is the opposite; it is at its most reliable and stable when it is regularly interacted with and copied. Taking all of the data from the WTC ship project, copying it to a hard drive, and then locking that hard drive away in a safety deposit box will almost certainly result in the eventual obsolescence of the data. As technology evolves, so do storage mediums and file formats, and because of that the best practice for maintaining digital archaeological archives is vigilance and continued interaction.

CHAPTER X

ASSESSMENT AND CONCLUSION

Before a new documentation methodology like high-definition laser scanning can be widely adopted and become a standard tool for archaeologists, it has two criteria to be met. One, it should fulfill the three requirements outlined in Chapter I: it should be cheaper, faster, and more accurate than the methods of documentation currently employed by archaeologists. If not all three, it must be evaluated on how well it exceeds in one or two of these criteria and determined if the performance is enough to overlook the shortcomings. Two, it should adhere to the four standards set forth by the United States' Secretary of the Interior for the documentation of heritage materials. Standard I states that documentation should adequately explicate and illustrate what is significant or valuable about the object being documented. Standard II states that the documentation should be prepared accurately from reliable sources with the limitations clearly delineated, allowing for independent verification. Standard III states that documentation should be prepared on materials that are readily reproducible, durable, and adhere to the appropriate standards. Finally, section IV states that documentation should be clearly and concisely produced (Interior 1990, 4-8).

Beginning with the first criteria, high-definition laser scanning does not fare well in a side-by-side comparison of costs associated with other methods of archaeological documentation. The up-front cost of the FARO Arm with LLP was substantially higher than any of the equipment needed for traditional 1:1 drawings, photographs,

photogrammetry, or even contact probe digitization. It would be fair to say that the hardware cost is among the most costly for any archaeological documentation technique. Additionally, the software is also expensive; with education discounts, *Design X* is still roughly ten times the cost of Agisoft *Photoscan*, and nearly 20 times more than *Rhinoceros 5*. Almost every aspect of ownership is more costly than alternative methods, with one notable exclusion: labor. The number of hours needed to pay someone to operate the arm and to process the scans using the technique outlined in this dissertation is far less than it would take to draw each timber by hand or to produce a model with contact probe digitization. Depending on the project, photogrammetry might be comparable in labor costs, but for something akin to the WTC ship project, producing fully-realized 3-D models with photogrammetry would mean hundreds of photos taken of each side of each timber, each photo painstakingly masked, and then waiting for the lengthy processing stage. The long-term labor cost of a FARO Arm is less than other methods, but whether or not there is enough constant use for this to offset the upfront cost of equipment is questionable. At the least, it is a question that must be asked on a case-by-case basis.

This leads very naturally into assessing how high-definition laser scanning compares to the other methods in the time it takes to complete high-quality documentation. Without a doubt, no other method of documentation other than simple photography is nearly as fast as high-definition laser scanning. When batch processing was carried out as described in Chapter III, the average time for a model to be put through all of the post-processing steps was down to approximately 45 minutes. The

scanning of 1 m or longer timbers took an average of 1-2 hours with the older FARO Arm, and approximately 30 minutes with the newer one. With the new FARO Arm and the batch processing, the start-to-finish time for all stages of documentation was slightly over an hour per timber.

Finally, the question of accuracy. Issues with true accuracy as mentioned in Chapter VIII aside, this technique has proven itself to produce among the most consistently accurate, fully realized 3-D timber models in the field today. The level of detail achieved allowed for precise measurements to be made on every nail, bolt, spike, and tool mark on each timber. Some issues did arise, like unwanted gap filling during the meshing process, or difficulties with aligning long planks that would flex slightly when moved to a new position. Additionally, the realism of the scans meant that it was easy to get complacent about verifying their accuracy, but other than these minor drawbacks, the accuracy of the data far exceeded the expectations of the author.

Of the first three criteria, the only area where high-definition laser scanning under-performs compared to other methods of archaeological documentation is cost. The cost of a CMM arm with a LLP attachment and the associated software is simply too high for most institutions to adopt. However, the high cost of this equipment should be viewed as a temporary set-back. History has shown time and again that as technology develops, hardware costs eventually drop. The state-of-the-art V5 LLP used for this project will not be state-of-the-art in five years, and when it is not, the prices will drop on used equipment.

With the obvious criteria assessed, the more bureaucratically-verbose guidelines put forth by the Department of the Interior must be addressed. The first question is whether or not the documentation process adequately explicates and illustrates what is significant about the object being documented. In the case of high-definition laser scanning, it does meet this criteria, but not in a way that is immediately evident. Unlike sketches or contact probe digitization, this type of scanning does not parse data based on any interpretive input to determine what is significant, it just displays everything that it records. These scanned models are not particularly useful without intelligent interpretation, though the data can be gathered without it. Once the data is interpreted and contextualized as a means of documentation, high-definition laser scanning more than meets these criteria.

The second question is whether or not the method of documentation is from accurate and reliable sources, and whether or not the weaknesses inherent in the methodology are clearly delineated. This is a more complicated criteria to meet, because as mentioned in Chapter VIII, the scan data looks so impressive that it is easy to accept it as accurate without due criticism. The key to adhering to this guideline is to ensure that all processes of data interpretation are clearly stated, and that the raw data be available to anyone who wishes to verify the accuracy of the scans.

The third Secretary of the Interior standard to be met is whether or not high-definition laser scanning is in a format that is readily reproducible for ease of access, durable for long storage, and in standard sizes for ease of handling. Arguably, the digital data produced by high-definition laser scanning is much more readily reproducible than

most other methods of documentation. The files do demand a program to view the models, but there are many open source, cost-free options for viewing the formats in which this project was saved. Even so, the substantial computing power needed to view and manipulate the model in its entirety is substantial, and it is probable that the average viewer will not have access to such computing resources. To this end, the traditional timber catalog that was produced, as well as the lines that were lofted from the digital model should adequately satisfy anyone who would like to study and verify the documentation from this project. Photogrammetry would produce models with the same restrictions of computing power. CMM measurement models are substantially smaller files that are easier to manipulate, but they are typically stored in *Rhinoceros*' proprietary format, which requires the *Rhinoceros 5* software or their viewing software.

The final criteria to assess the method is whether or not the documentation is clearly and concisely produced. The models that were created with high-definition laser scanning showcase neat, orderly data that is easy to understand and manipulate. Moreover, the data is visually dynamic and easily understood, and offers every conceivable point of view of the timbers. In this regard, high-definition laser scanning easily meets this standard.

This study demonstrates that high-definition laser scanning is an ideal tool for the documentation of excavated ship timbers. The data is accurate and easy to obtain, and the finished models convey all of the points needed to study and understand a ship. As a bonus, the 3-D files allow for dynamic presentation of data, with interactive models, animations, and 3-D printouts of the ship. The speed of the documentation is

unprecedented. In the span of one year, the methodology was devised, every structural timber was scanned, processed, and printed, the virtual model was assembled, ships lines were lofted, and this entire dissertation was written and edited, and all this while working on numerous other projects. Even if the quality of the data was merely on par with traditional drawings, this would have been a spectacular pace. Given that the data is substantially richer than a standard drawing, the overall assessment of high-definition laser scanning as a means to document *ex situ* ship timbers is overwhelmingly positive.

REFERENCES

- 3D Systems, Inc. n.d. "3D Scanners: A Guide to 3D Scanner Technology." Accessed September 3, 2016. <http://www.rapidform.com/3d-scanners/>.
- Agisoft. 2017. *Online Store*. Accessed 27, 2017. <http://www.agisoft.com/buy/online-store/>.
- AKRF Inc. . 2013. *World Trade Center Memorial and Development Plan: Data Recovery and Analysis of WTC Ship*. New York: AKRF Inc. .
- Anderson, Richard K. 1988. *Guidelines for Recording Historic Ships*. Washington D.C.: U.S. Department of Interior National Parks Service.
- Apple Inc. . 2016. *OS X: Cross-Platform Filename Best Practices and Conventions*. August 22. Accessed November 17, 2016. <https://support.apple.com/en-us/HT202808>.
- Bass, George. 2005. *Beneath the Seven Seas: Adventures with the Institute of Nautical Archaeology*. London: Thames and Hudson Ltd.
- Castro, F. 2006. "The Arade 1 Shipwreck: A Small Ship at the Mouth of the Arade River, Portugal." In *Connected By the Sea: Proceedings of the 10th Symposium on Boat and Ship Archaeology*, by F. Hocker and A. Englert, 300-305. Oxford: Oxbow Books.
- Castro, F. 2005. "Archaeology and Dredges: The Arade River Archaeological Complex." *International Journal of Nautical Archaeology* 34 (1): 72-83.

- Central Intelligence Agency. 2017. "Appendix G: Weights and Measures." *World Fact Book*. Accessed February 10, 2017. <https://www.cia.gov/library/publications/the-world-factbook/appendix/appendix-g.html>.
- Church, Jason. 2012. "3D Technology and the H.I. Hunley: Beyond Documentation - Christopher Watters." *National Center for Preservation Technology and Training*. October 18. Accessed February 22, 2017. <https://www.ncptt.nps.gov/blog/3d-technology-and-the-hunley/>.
- Clark, J. 2010. "The Fallacy of Reconstruction." In *Cyber-Archaeology*, by Maurizio Forte, 63-73. Oxford: Archaeopress.
- Crisman, Kevin J. 1993. "An Archaeological Approach." In *Boats: A Manual for Their Documentation*, by P, Spectre, P, Fuller, B Lipke, 304-320. Nashville, TN: American Association for State and Local History.
- Crisman, Kevin J. 2014. "US Schooner *Ticonderoga*." In *Coffins of the Brave: Lake Shipwrecks of the War of 1812*, by Kevin J Crisman, 247-270. College Station, TX: Texas A&M University Press.
- Dillion, D.W. 1993. "Drawing and Lofting from Field Notes." In *Boats: A Manual for Their Documentation*, by Paul Lipke, 223-301. Nashville: American Association for State and Local History.
- Falck, Tori, and Sarah Fawsitt. 2011. *Documenting Archaeological Boat Finds Digitally in 3D*. April 12. Accessed December 13, 2016. <http://www.marmuseum.no/no/arkeologi/dokumentasjonslaboratoriet/Documenting+archaeological+boat+finds+digitally+in+3D.d25-SwJvMWa.ips>.

- FARO. 2017. *Faro Scan Arm Overview*. Accessed February 13, 2017.
<http://www.faro.com/products/metrology/faro-scanarm/overview>.
- . n.d. *Maintenance - Certification*. Accessed 11 29, 2016. www.faro.com/support-en/maintenance.
- FARO. 2012. *Scanning FAQ*. Technical Guide, FARO.
- Fix, Peter. 2015. "Archaeological Watercraft: A Review and Critical Analysis of the Practice (Doctoral Dissertation)." College Station, TX: Texas A&M University, May.
- . 2017. "Personal Correspondence." College Station, TX, February 28.
- Fontenoy, Paul E. 1994. *The Sloops of the Hudson River*. Mystic, CT: Mystic Seaport Museum.
- Friends of the Newport Ship. 2017. *Project Support*. Accessed February 22, 2017.
<http://newportship.org/project-support.aspx>.
- Frischer, Bernard. 2013. "Digital Sculpture Project: Caligula." *The Digital Sculpture Project*. March 22. Accessed February 12, 2017.
http://www.digitalsculpture.org/papers/frischer/frischer_paper.html.
- Geomagic. n.d. *Geomagic Design X Landing Page*. Accessed December 7, 2016.
<http://www.geomagic.com/en/products-landing-pages/designx>.
- Geomagic Support. 2016. "Re: RESOLUTION QUESTION." *e-mail*. 12 2.
- Goldenberg, Joseph. 1976. *Shipbuilding in Colonial America*. Charlottesville, VA: University Press of Virginia.

- Grieco, Gelnn. 2003. "Modeling La Belle: A Reconstruction of a Seventeenth-Century Light Frigate." College Station, TX: Texas A&M University, May.
- Hamilton, Donny L. 1996. *Basic Methods of Conserving Underwater Archaeological Material Culture*. Washington D.C. : U.S. Department of Defense.
- Haug, C. 2015. "Peer-Review Fraud - Hacking the Scientific Publication Process." *New England Journal of Medicine* (373): 2393-2395.
- Henry, Alan. 2015. *How Long Will My Hard Drives Really Last?* April 27. Accessed February 19, 2017. <http://lifehacker.com/how-long-will-my-hard-drives-really-last-1700405627>.
- Hodgson, Gary. n.d. *Slic3r Manual: Speed*. Accessed February 22, 2017. <http://manual.slic3r.org/expert-mode/speed>.
- Interior, US Department of. 1990. *Secretary of the Interior's Standards and Guidelines for Architectural and Engineering Documentation*. Washington D.C.: US Department of the Interior, National Parks Service. <https://www.nps.gov/hdp/standards/standards.pdf>.
- Jones, Toby. 2013. *The Newport Medieval Ship: Timber Recording Manual*. York: Newport Medieval Ship Archive.
- Konecny, Gottfried. 2014. *Konecny, Gottfried. 2014. Geoinformation : remote sensing, photogrammetry, and geographic information systems. Second edition*. Boca Raton, FL: CRC Press.
- Lebrun, E, N Jones, and L Gilbert. 2014. "Chemical Warfare Among Invaders: A Detoxification Interaction Facilitates an Ant Invasion." *Science* 1014-1017.

- Loureiro, Vanessa, and Joao Gachet Alves. 2008. "The Arade 1 Shipwreck: Preliminary Results of the 2004 and 2005 Field Seasons." *International Journal of Nautical Archaeology* 37 (2): 273-282.
- Luza, Rebekah. 2017. "Geomagic Software Quote." College Station, TX, February 7.
- Makerbot. 2017. *Custom Settings*. Accessed February 22, 2017.
https://support.makerbot.com/learn/makerbot-desktop-software/print-settings/custom-settings_11912.
2007. *MarineWiki*. November 22. Accessed February 2, 2017.
http://www.marinewiki.org/index.php?title=File:Lines_plan.jpg.
- McHenry, Kenton, and Peter Bajcsy. 2008. *An Overview of 3D Data Content, File Formats, and Viewers*. Technical, Urbana, IL: National Center for Supercomputing Applications.
- Miller, Paul, and Julian Richards. 1995. "The Good, the Bad, and the Downright Misleading: Archaeological Adoption of Computer Visualization." *Computer Applications and Quantitative Methods in Archaeology*. Oxford: Tempus Reparatum. 19-22.
- Mueller, S, S Im, S Gurevich, A Tiebrich, L Pfisterer, F Guimbretiere, and P Baudisch. 2014. "WirePrint: 3D Printed Previews for Fast Prototyping." *UIST '14 October 5-8 2014*. Honolulu: UIST. 273-280.
- Mulliez, Maud, Philippe Jockey, and Mauro Vincitore. 2013. "Virtual Reconstruction and Experimental Attempt in Archaeology: The Massalian Treasury in Delphi." October 28. <http://ieeexplore.ieee.org/document/6743799/>.

2016. *National 9/11 Memorial*. Accessed October 11, 2016.
<http://www.911memorial.org/faq-about-911>.
- Nayling, Nigel, and Toby Jones. 2014. "The Newport Medieval Ship, Wales, United Kingdom." *The International Journal of Nautical Archaeology* 43 (2): 239-278.
- Nelles, Jan Nikolai, and Nora Al-Badri. 2015. *Nefertiti Hack*. December. Accessed February 12, 2017. <http://nefertitihack.alloversky.com/>.
- Parkoff, Justin. 2016. "A Formidable Looking Pile of Iron Boilers and Machinery": Reconstructing the Civil War Gunboat USS *Westfield* (Dostoral dissertation)." Texas A&M University, December.
- Pearson, Colin. 1987. *Conservation of Marine Archaeological Objects*. London: Butterworths.
- Pulak, Cemal, Rebecca Ingram, and Michael Jones. 2014. "Eight Byzantine Shipwrecks from the Theodosian Harbour Excavations at Yenikapı in Istanbul, Turkey: an Introduction." *International Journal of Nautical Archaeology* 44 (1): 39-73.
- Rapidform. 2012. *3D Systems Buys Rapidform*. October 9. Accessed 11 9, 2016.
<http://www.rapidform.com/about-us/press-news/3d-systems-buys-rapidform/>.
- Rawat, S, and S Meena. 2014. "Publish or Perish: Where are We Heading?" *Journal of Research in Medical Sciences: The Official Journal of Isfahan University of Medical Sciences* 19 (2): 87-89.
- Renfrew, C, and P Bahn. 2012. *Archaeology: Theories, Methods, and Practice*. London: Thames and Hudson.

- Rick, John. 1999. *Digital Still Cameras and Archaeology*. Society for American Archaeology Bulletin, Washington D.C.: Society for American Archaeology.
<http://www.saa.org/Portals/0/SAA/publications/SAAbulletin/17-3/saa18.html>.
- Sabick, Christopher. 2014. "'A Perfect Masterpiece of Workmanship': His Majesty's Hired Transport Schooner *Nancy*." In *Coffins of the Brave: Lake Shipwrecks of the War of 1812*, by Kevin Crisman, 71-85. College Station, TX: Texas A&M University Press.
- Schwarz, George. 2015. "Reconstructing Naval History: The 3D Scanning of *Royal Savage*." *The Sextant: Taxing a Fix on the History and Heritage of Today's U.S. Navy*. December 23. Accessed February 18, 2017.
<http://usnhistory.navylive.dodlive.mil/2015/12/23/reconstructing-naval-history-the-3d-scanning-of-royal-savage/>.
- Sketchfab. 2017. *Sketchfab Plans*. Accessed February 19, 2017.
<https://sketchfab.com/plans>.
- . 2017. *Terms of Use*. Accessed February 19, 2017. <https://sketchfab.com/terms>.
- Smithsonian Institution . 2017. *Smithsonian X 3D* . Accessed February 19, 2017.
<https://3d.si.edu/>.
- Sørensen, Anne C. 2001. *Ladby: A Danish Ship-Grave from the Viking Age*. Roskilde: The Viking Ship Museum.
- Steffy, J. Richard. 1994. *Wooden Ship Building and the Interpretation of Shipwrecks*. College Station, TX: Texas A&M University Press.

Surface and Edge 3D Laser Scanning. 2011. *How the Laser Scanner Works*. Accessed February 18, 2017. <http://www.surfaceandedge.com/technology/how-the-laser-scanner-works>.

Taggart, Rachel. 2013. *3D Systems to Acquire Geomagic*. January 3. Accessed 11 9, 2016. <http://www.geomagic.com/en/community/press-releases/3d-systems-to-acquire-geomagic/>.

The Miriam and Ira D. Wallach Division of Art, Prints, and Photographs. n.d. *Cuyahoga River From R.R. Bridge*. . Stereograph. New York Public Library Digital Collections. Accessed February 22, 2017. <http://digitalcollections.nypl.org/items/510d47e0-9ac6-a3d9-e040-e00a18064a99>.

The Royal Swedish Academy of Sciences. 2009. *Two Revolutionary Optical Technologies*. Scientific Background on the Nobel Prize in Physics 2009, Class for Physics, Stockholm: The Royal Swedish Academy of Sciences, 12 (14).

Warden, Robert. 2017. "Personal Communication." Austin, TX, January 24.

Watters, Christopher, Michael Scafuri, Benjamin Rennison, and Vincent Blouin. n.d. "3D Technology and the H.L. Hunley: Beyond Documentation."

Weather Underground. 2016. *Weather History for KCLL*. August. Accessed November 17, 2016. https://www.wunderground.com/history/airport/KCLL/2016/8/9/WeeklyHistory.html?req_city=&req_state=&req_statename=&reqdb.zip=&reqdb.magic=&reqdb.wmo=.

Wilder, Charly. 2016. "Swiping a Priceless Antiquity... With a Scanner and a 3-D Printer." *New York Times*. New York, New York, March 1. Accessed February 12, 2017. <https://www.nytimes.com/2016/03/02/arts/design/other-nefertiti-3d-printer.html>.

Yamafune, Kotaro. 2016. "Using Computer Vision Photogrammetry (Agisoft Photoscan) to Record and Analyze Underwater Shipwreck Sites." May.

Zortrax. 2016. *Z-Suite Manual*. Accessed December 8, 2016.
<http://support.zortrax.com/z-suite-manual/>.

APPENDIX I
HARDWARE SPECIFICATIONS

Laser Scanner

FARO Fusion CMM Arm with V2 Laser Line Probe

Arm Length: 6ft (12ft diameter reach)

Accuracy: 50 μ m

Repeatability: \pm 50 μ m

Points per line: 640

Scan rate: 30FPS

FARO Edge CMM Arm with V5 Laser Line Probe

Arm Length: 4.5ft (12ft diameter reach)

Accuracy: 25 μ m

Single Point Repeatability: 0.029mm

Points per line: 2000

Scan rate: 280FPS

Scanning Laptop

HP Envy

Intel Core i7-6700HQ CPU @ 2.60GHz

8-core

16.0 GB Ram

Nvidia GeForce GTX 950M graphics card

Windows 10 64-bit

Processing computer

Alienware Aurora

Intel Core i7-4930K CPU @ 4.1GHz

6-core

32.0 GB Ram

Nvidia GeForce GTX 780 graphics card

APPENDIX II

PROCEDURE FOR EDITING AND ALIGNING POINT CLOUD DATA PRIOR TO MESHING

1. Open the *Design X* point cloud for the first section of the scan
2. Using the selection tools, select and delete the unwanted scan data, such as the table or supports.
3. Filter for noise. In the 'Points' tab, click the 'Filter Noise' icon. This is the same process that is used in the Mesh Buildup Wizard described in the Post-Processing section of Chapter III. For most models, 100 is an appropriate setpoint for the noisy cluster selection.
4. Combine the separate point clouds. As mentioned in the Scanning Procedure section of Chapter III, each time the LLP was paused during the scan, *Design X* saves the data collected prior to the pause as a separate section of the scan. Each of these sections remains aligned, but they must be combined to a single point cloud before being aligned with the scans of the other sides of the timber. In the 'Points' tab, select 'Combine', then select all scan sections and click the checkmark to combine.

5. Repeat the first four steps with each scan of the timber until all sides are edited, combined point clouds. Remember to save these edits as separate files. The original data files must never be overwritten.

6. Open one of the scan sections, then import the next section it should be aligned to. In the 'Alignment' tab, select 'Align Between Scan Data'. The alignment procedure is the same as it was described in the *Post-Processing* section of Chapter III.

7. Once the two scans are aligned, combine them using the steps in step 4.

8. Repeat steps 6 and 7 until all portions of the model are aligned and combined.

APPENDIX III

ABBREVIATED SCANTLING LIST FOR THE WTC SHIP.

Timber Designation	Dimensions
Keel length	796.05 cm
Keel width	fowardmost 17.5 cm, aftmost 11.93 cm
Keel height	fowardmost 22.3 cm, aftmost 12.87 cm
Keelson length	340.33 cm
Keelson width	fowardmost 28.37 cm, aftmost 19.97 cm
Keelson height	fowardmost 16.83 cm, aftmost 10.45 cm
Floor timbers (average)	sided: 14.39 cm molded: 13.70 cm
First futtocks (average)	sided: 13.19 cm molded: 13.14 cm
Stern knee length	213.34 cm at base, 19.17 cm at top
Stern knee width	forwardmost 49.0 cm, aftmost 30.52 cm
Stern knee height	forwardmost 11.69 cm, aftmost 94.19 cm
Ceiling planking (average thickness)	26.01 mm (likely 1 inch)
Outer planking (average thickness)	37.79 mm (likely 1.5 inch)